Simulating *Ips* ~~*Typographus*~~*typographus* *(L.)*, ~~Outbreak Dynamics~~outbreak dynamics and their ~~Influence on Carbon Balance Estimates~~influence on carbon balance estimates with ORCHIDEE ~~r7791~~r8627

Guillaume Marie[1]*, Jina Jeong[2]*, Hervé Jactel[3], Gunnar Petter[4], Maxime Cailleret[5], Matthew J. McGrath[1], Vladislav Bastrikov[6], Josefine Ghattas[7], Bertrand Guenet[8], Anne Sofie Lansø[9], Kim Naudts[11], Aude Valade[10], Chao Yue[12], Sebastiaan Luyssaert[2]

[1] Laboratoire des Sciences du Climat et de l'Environnement, CEA CNRS UVSQ UP Saclay, 91191 Orme des Merisiers, Gif-sur-Yvette, France

[2] Faculty of Science, A-LIFE, Vrije Universiteit Amsterdam, 1081 BT Amsterdam, the Netherlands

[3] INRAE, University of Bordeaux, ~~umr~~UMR Biogeco, 33612 Cestas, France

[4] ETH Zürich, Department of Environmental Systems Science, Forest Ecology, 8092 Zürich, Switzerland

[5] INRAE, Aix-Marseille Univ, UMR RECOVER, 13182 Aix-en-Provence, France

[6] Science Partner, France

[7] Institut Pierre-Simon Laplace – Sciences du climat (IPSL), 75105 Jussieu, France

[8] Laboratoire de Géologie, Ecole Normale Supérieure, CNRS, PSL Research University, IPSL, 75005 Paris, France

[9] Department of Environmental Science, Aarhus Universitet, Frederiksborgvej 399, 4000 Roskilde, Denmark

[10] Eco & Sols, Univ Montpellier, CIRAD, INRAE, 34060 Institut Agro, IRD, Montpellier, France

[11] Department of Earth Sciences, Vrije Universiteit Amsterdam, 1081 HV Amsterdam, the Netherlands

[12] State Key Laboratory of Soil Erosion and Dryland Farming on the Loess Plateau, Northwest A & F University, Yangling, Shaanxi, China

* These authors contributed equally to this study

Corresponding author: Guillaume Marie, guillaume.marie@lsce.ipsl.fr, Jina Jeong, j.jeong@vu.nl, Sebastiaan Luyssaert, s.luyssaert@vu.nl

Abstract : New (a)biotic conditions resulting from climate change are expected to change disturbance dynamics, such as ~~wind throw~~windthrow, forest fires, droughts, and insect outbreaks, and their interactions. These unprecedented natural disturbance dynamics might alter the capability of forest ecosystems to buffer atmospheric CO_2 increases, potentially leading forests to transform from sinks into sources of CO_2. This study aims to enhance the ORCHIDEE land surface model to study the impacts of climate change on the dynamics of the bark beetle ***Ips***

typographus ~~dynamics~~ and subsequent effects on forest functioning. The ~~bark beetle (~~***Ips typographus***~~)~~ outbreak model is inspired by previous work from Temperli et al. 2013 for the LandClim landscape model. The new implementation of this model in ORCHIDEE ~~r7791~~r8627 accounts for key differences between ORCHIDEE and LandClim: (1) the coarser spatial resolution of ORCHIDEE, (2) the higher temporal resolution of ORCHIDEE, and (3) the pre-existing process representation of windthrow, drought, and forest structure in ORCHIDEE. Simulation experiments demonstrated the ~~model's capacity~~capability of ORCHIDEE to simulate a ~~broad spectrum~~variety of post-disturbance forest dynamics observed in empirical studies. Through an array of simulation experiments across various climatic conditions and ~~disturbance~~windthrow intensities, the ~~enhanced~~ model was ~~rigorously~~ tested for ~~sensitivity. The results indicated that by using different sets~~its sensitivity to climate, initial disturbance, and selected parameter values. The results of these tests indicated that with a single set of parameters, ~~model~~ORCHIDEE outputs spanned the range of observed dynamics~~, highlighting the significant~~. Additional tests highlighted the substantial impact of incorporating ~~beetle~~*Ips typographus* outbreaks on carbon dynamics. Notably, the study revealed that modeling abrupt mortality events, as opposed to a continuous mortality framework, provides ~~valuable~~new insights into the short-term carbon sequestration potential of forests under disturbance regimes by showing that the continuous mortality framework tends to overestimate the carbon sink capacity of forests in the 20 to 50 year range in ecosystems under high disturbance pressure, compared to scenarios with abrupt mortality events. This model enhancement underscores the critical need to include disturbance dynamics in land surface models to refine predictions of forest carbon dynamics in a changing climate.

1. Introduction

Future climate will likely bring new abiotic constraints through the co-occurrence of multiple connected hazards, e.g., "hotter droughts", which are droughts combined with heat waves (Allen et al., 2015; Zscheischler et al., 2018), but also new biotic conditions from interacting natural and anthropogenic disturbances, e.g., insect outbreaks following windthrow or forest fires (Seidl et al., 2017). Unprecedented natural disturbance dynamics might alter biogeochemical cycles specifically the capability of forest ecosystems to buffer the CO_2 increase in the atmosphere (Hicke et al., 2012; Seidl et al., 2014) and the risk that forests are transformed from sinks into sources of CO_2 (Kurz et al., 2008a). The magnitude of such alteration, however, remains uncertain principally due to the lack of impact studies that include disturbance regime shifts at global scale (Seidl et al., 2011).

Land surface models are used to study the relationships between climate change and the biogeochemical cycles of carbon, water, and nitrogen (~~Cox~~Ciais et al., ~~2000; Ciais~~2005; Cox et al., ~~2005~~2000; Friedlingstein et al., 2006; ~~Zaehle and Dalmonech, 2011; Luyssaert et al., 2018~~Luyssaert et al., 2018; Zaehle and Dalmonech, 2011). Many of these models use background mortality to obtain an equilibrium in their biomass pools. This classic approach towards forest dynamics, which assumes steady-state conditions over long periods of time, may not be suitable for assessing the impacts of disturbances on shorter time scales under a fast changing climate. This could be considered a shortcoming in the land surface models because disturbances can have significant impacts on ecosystem services, such as water regulation, carbon sequestration, and biodiversity (Quillet et al., 2010). Mechanistic approaches that

account for a variety of mortality causes, such as age, size, competition, climate, and disturbances, are now being considered and tested to simulate forest dynamics more accurately (Migliavacca et al., 2021). For example, the land surface model ORCHIDEE accounts for mortality from interspecific competition for light in addition to background mortality (Naudts et al., 2015). Implementing a more mechanistic view on mortality is thought to be essential for improving our understanding of the impacts of climate change on forest dynamics and the provision of ecosystem services.

Land surface models also face the challenge of better describing mortality particularly when it comes to ecosystem responses to "cascading disturbances", where legacy effects from one disturbance affect the next (Buma, 2015; Zscheischler et al., 2018~~; Buma, 2015~~). Biotic disturbances, such as bark beetle outbreaks, strongly depend on previous disturbances as their infestation capabilities are higher when tree vitality is low, for example following drought or storm events (Seidl et al., 2018). This illustrates how interactions between biotic and abiotic disturbances can have substantial effects on ecosystem dynamics and must be accounted for in land surface models to improve our understanding of the impacts of climate change on forest dynamics (~~Temperli~~Seidl et al., ~~2013; Seidl~~2011; Temperli et al., ~~2011~~2013a). While progress has been made towards including abrupt mortality from individual disturbance types such as wildfire (~~Yue et al., 2014;~~ Lasslop et al., 2014; Migliavacca et al., 2013~~;~~ Yue et al., 2014), windthrow (Chen et al., 2018) and drought (Yao et al., 2022), the interaction of biotic and abiotic disturbances remains both a knowledge and modeling gap (Kautz et al., 2018).

Bark beetle infestations are increasingly recognized as disturbance events of regional to global importance (~~Kurz~~Bentz et al., ~~2008b; Bentz~~2010; Kurz et al., ~~2010~~2008b; Seidl et al., 2018). Notably, a bark beetle outbreak ravaged over 90% of Engelmann spruce trees across approximately 325,000 hectares in the Canadian and American Rocky Mountains between 2005 and 2017 (Andrus et al., 2020). In Europe, the ~~spruce~~ bark beetle~~,~~ *Ips typographus*~~,~~ has been involved in up to 8% of total tree mortality due to natural disturbances from 1850 to 2000 (Hlásny et al., 2021a). A recent increase in beetle activity, particularly following mild winters (~~Kurz~~Andrus et al., ~~2008b; Andrus~~2020; Kurz et al., ~~2020~~2008c), windthrow (Mezei et al., 2017), and droughts (Nardi et al., 2023) have been well-documented (Hlásny et al., 2021a; Pasztor et al., 2014), underscoring the need to integrate bark beetle ~~(*Ips typographus*)~~ dynamics into land surface modeling.

Past studies used a variety of approaches to model the impacts of bark beetles on forests. While some ~~model~~models treated bark beetle outbreaks as background mortality (~~Naudts~~Luyssaert et al., ~~2016; Luyssaert~~2018; Naudts et al., ~~2018~~2016), others dynamically modeled these outbreaks within ecosystems (~~Temperli~~Jönsson et al., ~~2013~~2012; Seidl and Rammer, 2016; ~~Jönsson~~Temperli et al., ~~2012~~2013b). Studies with prescribed beetle outbreaks tend to focus on the direct effects of the outbreak on forest conditions and carbon fluxes, but are likely to overlook more complex feedback processes, such as interactions with other disturbances and longer-term impacts. Conversely, dynamic modeling of beetle outbreaks, provides a more comprehensive view by incorporating the lifecycle of bark beetles, tree defense mechanisms, and ensuing alterations in forest composition and functionality.

Simulation experiments for *Ips typographus* outbreaks using the LPJ-GUESS vegetation model highlighted regional variations in outbreak frequencies, pinpointing climate change as a key exacerbating factor (Jönsson et al., 2012). Simulation experiments with the iLand landscape model suggested that almost 65% of ~~the bark beetle (~~*Ips typographus*~~)~~ outbreaks are aggravated by other environmental drivers (Seidl and Rammer, 2016). A 4°C temperature increase could result in a 265% increase in disturbed ~~areas~~area and a 1800% growth in the average patch size of the disturbance (Siedl and Rammer 2016). Disturbance interactions were ten times more sensitive to temperature changes, boosting the disturbance regime's climate sensitivity. The results of these studies justify the inclusion of interacting disturbances in land surface models, such as ORCHIDEE, which are used in future climate predictions and impact studies (Boucher et al., 2020).

The objectives of this study are: (1) to develop and implement a spatially implicit ~~bark beetle (*Ips Typographus*) outbreak model~~outbreak model for *Ips typographus* in the land surface model ORCHIDEE inspired by the work from Temperli et al. (2013), and (2) use simulation experiments to characterize the behavior of this newly added model functionality.

2. Model description

2.1. The land surface model ORCHIDEE

ORCHIDEE is the land surface model of the IPSL (Institut Pierre Simon Laplace) Earth system model (~~Krinner~~Boucher et al., ~~2005; Boucher~~2020; Krinner et al., ~~2020~~2005). ORCHIDEE can, however, also be run uncoupled as a stand-alone land surface model forced by temperature, humidity, pressure, precipitation, and wind ~~conditions~~fields. Unlike the coupled setup, which needs to run on the global scale, the stand-alone configuration can cover any area ranging from a single grid point to the global domain. In this study ~~we decide to run ORCHIDEE uncoupled~~ORCHIDEE was run as a stand-alone land surface model.

ORCHIDEE does not enforce any particular spatial resolution. The spatial resolution is an implicit user setting that is determined by the resolution of the climate forcing (or the resolution of the atmospheric model in a coupled configuration). ORCHIDEE can run on any temporal resolution. This apparent flexibility is somewhat restricted as processes are formalized at given time steps: half-hourly (e.g., photosynthesis and energy budget), daily (i.e., net primary production), and annual (i.e. vegetation demographic processes). With the current model architecture meaningful simulations should have a temporal resolution of one minute to one hour for the calculation of energy balance, water balance, and photosynthesis.

ORCHIDEE utilizes meta-classes to ~~describe different types of~~discretize the global diversity in vegetation. The model includes 13 meta-classes by default, including one class for bare soil, eight classes for various combinations of leaf-type and climate zones of forests, two classes for grasslands, and two classes for croplands. Each meta-class can be further subdivided into an unlimited number of plant functional types (PFTs). The current default setting of

ORCHIDEE distinguishes 15 PFTs where the ~~C3 grasslands have now a separate PFT in the~~meta-class of C3 grasslands have been separated into a boreal, temperate and tropical ~~zone~~C3 grassland PFT.

At the beginning of a simulation, each forest PFT in ORCHIDEE contains a monospecific forest stand that is ~~defined~~structured by a user-defined but fixed number of diameter classes (three by default). Throughout the simulation, the boundaries of the diameter classes are adjusted to accommodate changes in the stand structure, while the number of classes remains constant. Flexible class boundaries provide a computationally efficient approach to simulate different forest structures. For instance, an even-aged forest is simulated by using a small diameter range between the smallest and largest trees, resulting in all trees belonging to the same stratum. Conversely, an uneven-aged forest is simulated by applying a wide range between diameter classes, such that different classes represent different canopy strata.

The model uses allometric relationships to link tree height and crown diameter to stem diameter. Individual tree canopies are not explicitly represented, instead a canopy structure model based on simple geometric forms (Haverd et al. 2012) has been included in ORCHIDEE (Naudts et al., 2015). Diameter classes represent trees with different mean diameter and height, which informs the user about the social position of trees within the canopy. Intra-stand competition is based on the basal area of individual trees, which accounts for the fact that trees with a higher basal area occupy dominant positions in the canopy and are therefore more likely to intercept light and thus contribute more to stand-level photosynthesis and biomass growth compared to suppressed trees (Deleuze et al., 2004). If recruitment occurs, diameter classes evolve into cohorts. However, in the absence of recruitment, all diameter classes contain trees of the same age.

Individual tree mortality from self-thinning, wind storms, and forest management is explicitly simulated. Other sources of mortality are implicitly accounted for through a so-called constant background mortality rate. Furthermore, age classes (four by default) can be used after land cover change, forest management, and disturbance events to explicitly simulate the regrowth of the forest. Following a land cover change, biomass and soil carbon pools (but not soil water columns) are either merged or split to represent the various outcomes of a land cover change. The ability of ORCHIDEE to simulate dynamic canopy structures (~~Naudts~~Chen et al., ~~2015; Ryder~~2016; Naudts et al., ~~2016; Chen~~2015b; Ryder et al., 2016), a feature essential to simulate both the biogeochemical and biophysical effects of natural and anthropogenic disturbances, is exploited in other parts of the model, i.e., precipitation interception, transpiration, energy budget calculations, the radiation scheme, and the calculation of the absorbed light for photosynthesis.

Since revision 7791, mortality ~~from bark beetle (~~*Ips*from*Ips typographus*~~)~~ outbreaks is ~~now~~ explicitly accounted for and thus conceptually excluded from the so-called environmental background mortality. Subsequently, changes in canopy structure resulting from growth, forest management, land cover changes, wind storms, and ~~bark beetle (~~*Ips typographus*~~)~~ outbreaks are accounted for in the calculations of the carbon, water, and energy exchanges between

the land surface~~. ORCHIDEE's functionality~~ and the atmosphere. For details on the functionality of the ORCHIDEE model that is not of direct relevance for this study, e.g., energy budget calculations, soil hydrology, snow phenology, albedo, roughness, photosynthesis, respiration, phenology, carbon and nitrogen allocation, land cover changes, product use, and the nitrogen cycle are ~~detailed in (~~readers are referred to Krinner et al., 2005; Zaehle and Friend, 2010; Naudts et al., 2015; Vuichard et al., 2019~~)~~.

2.2. Origin of the bark beetle (*Ips typographus*) ~~module~~model: the LANDCLIM legacy

Although mortality from windthrow (Yi-Ying et al., 2018) and forest management (~~Naudts~~Luyssaert et al., ~~2016; Luyssaert~~2018; Naudts et al., ~~2018~~2016) were already accounted for in ORCHIDEE prior to ~~r7791~~r8627, insect outbreaks and their interaction with other disturbances were not. The LandClim model (Schumacher, 2004) and more specifically the ~~bark beetle (*Ips typographus*) module~~*Ips typographus* model developed by Temperli et al. (2013) has been used as basis to develop the ~~bark beetle module~~*Ips typographus* model in ORCHIDEE ~~r7791~~r8627.

LandClim is a spatially explicit stochastic landscape model in which forest dynamics are simulated at a yearly time step for 10–100 km^2 landscapes consisting of 25 m × 25 m patches. Within a patch recruitment, growth, mortality and competition among age cohorts of different tree species are simulated with a gap model (Bugmann, 1996) in response to monthly mean temperature, climatic drought, and light availability. LandClim, for which a detailed description can be found in (Schumacher, 2004; Temperli et al., 2013), includes the functionality to simulate the decadal dynamics and consequences of ~~bark beetle~~*Ips typographus* outbreaks at the landscape-scale (Temperli et al., 2013). In the LandClim approach, the extent, occurrence and severity of beetle-induced tree mortality are driven by the landscape susceptibility, beetle pressure, and infested tree biomass. While the LandClim beetle ~~module~~model was designed and structured to be generally applicable for northern hemisphere climate-sensitive bark beetle-host systems, it was ~~originally~~ parameterized to represent disturbances by the ~~European spruce bark beetle (~~*Ips typographus*~~)~~ in Norway spruce (*Picea abies* Karst.; Temperli et al. 2013).

As LandClim and ORCHIDEE are developed for different purposes, their temporal and spatial scales differ. These differences in model resolution justify developing a new model while ~~still~~ following the principles embedded in the LandClim approach. LandClim assesses bark beetle damage at 25 m x 25 m patches and to do so it uses information from other nearby patches as well as landscape characteristics such as slope, aspect and altitude. The susceptibility of a landscape to bark beetle infestations is calculated using multiple factors such as drought-induced tree resistance, age of the oldest spruce cohort, proportion of spruce in the patch's basal area, and spruce biomass damaged by windthrow. These ~~factors,~~drivers are presented as sigmoidal relationships~~,~~ ranging from 0 to 1 (denoting none to maximum susceptibility respectively) that are combined in a susceptibility index for each Norway spruce cohort in a patch. Bark beetle pressure is quantified as the potential number of beetles that can infest a patch, and its calculation considers, among others, previous beetle activity, maximum possible spruce biomass that beetles could kill, and temperature-dependent bark beetle phenology. Finally, the susceptibility index and beetle pressure are used to estimate the total infested tree biomass and total biomass killed by bark beetles for each cohort within a patch.

In ORCHIDEE, however, the simulation unit is about six orders of magnitude larger, i.e. 25 km x 25 km. Hence, a single ~~pixel~~gridcell in ORCHIDEE exceeds the size of an entire landscape in LandClim. Where landscape characteristics in LandClim can be represented by ~~a~~ statistical ~~distribution~~distributions, the same characteristics in ORCHIDEE are ~~summarized in a single value~~represented by single values. These differences between LandClim and ORCHIDEE imply that the original bark beetle ~~module~~model cannot be implemented in ORCHIDEE without ~~deep adjustments. We develop a pixel-level model that does not require spatial information and statistical distributions of landscape characteristics.~~

~~In the newly developed module of ORCHIDEE, the foundational concept is retained from LANDCLIM, yet the variables influencing susceptibility calculations have largely been modified, with the exception of the phenology model, which continues to follow the framework established by Temperli et al. in 2013. Given the extensive and significant alterations, a direct comparison between ORCHIDEE and LANDCLIM may no longer be pertinent. However, we have developed a flowchart (Fig. 2) to provide an overarching perspective of our advancements, facilitating an understanding of how it diverges from the initial methodology.~~

~~**bark beetle (*Ips typographus*)**~~substantial adjustments; the model at the ORCHIDEE gridcell should work without requiring spatial information and statistical distributions of landscape characteristics because those are not available in ORCHIDEE.

2.3. Bark beetle outbreak development stages

~~bark~~Bark beetle ~~(*Ips typographus*) outbreak development stages~~outbreak development stages (Fig. 1) are useful to understand the dynamics of an outbreak ~~((Fig. 1) and have been described in numerous studies (Wermelinger, 2004; Edburg et al., 2012; Hlásny et al., 2021a). Nonetheless, in ORCHIDEE r7791, we design a model framework which~~Edburg et al., 2012; Hlásny et al., 2021a; Wermelinger, 2004). Nonetheless, the outbreak model in ORCHIDEE r8627 **simulates the dynamic of** ~~bark beetle~~the Ips *typographus* outbreak as a continuous process. Hence, endemic, epidemic, build-up and post-epidemic stages are not explicitly simulated ~~and these~~. In this study, outbreak development stages were only introduced to structure the model description. If needed, these stages could be distinguished while post-processing the simulation results if (arbitrary) thresholds are set for specific variables such as ~~$i_{beetles\ pressure}$, $i_{beetles\ mass\ attack}$, or $B_{beetles\ kill}$ (these variables are defined further below).~~ $DR_{beetles}$.

7

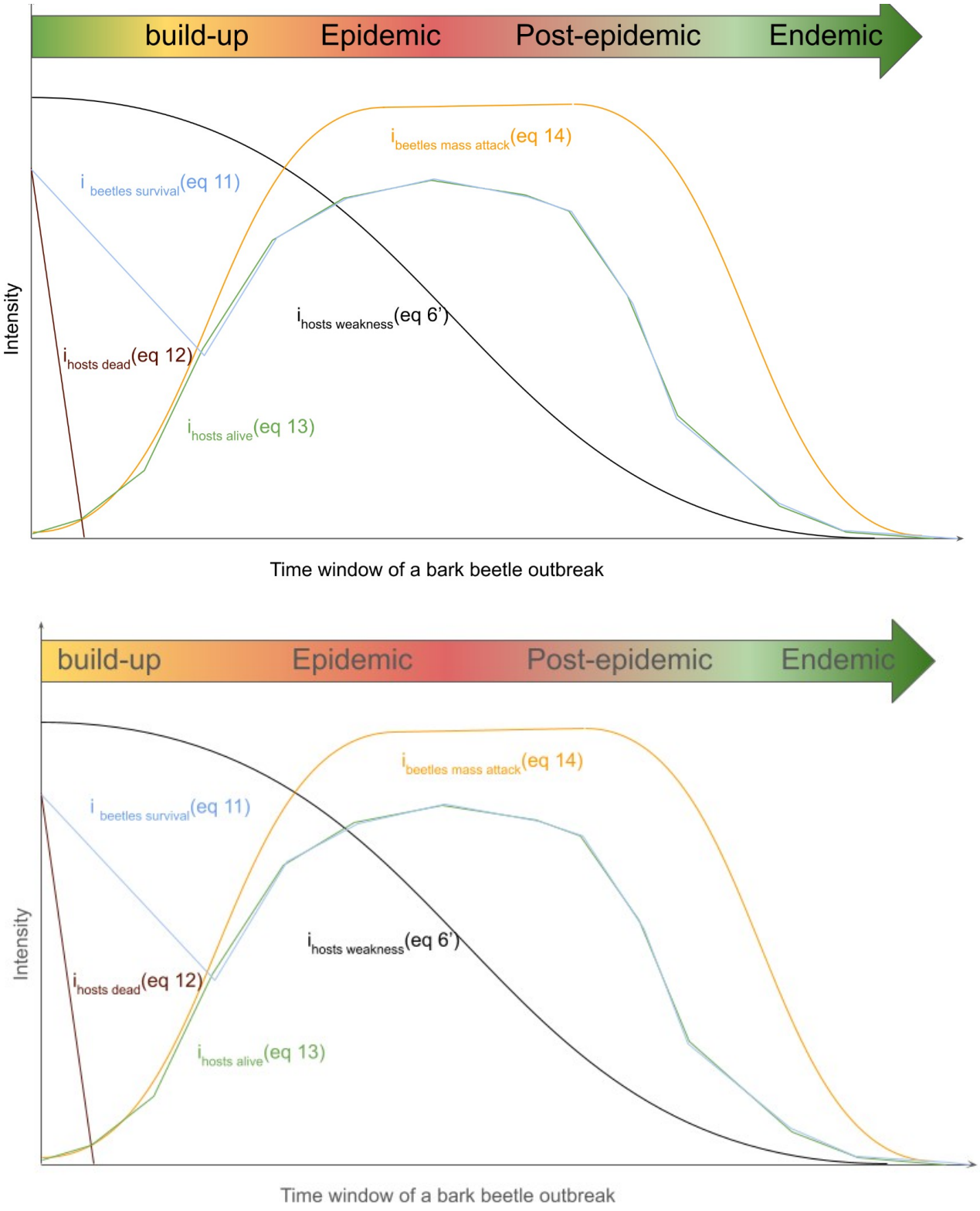

build-up
Epidemic
Post-epidemic
Endemic
i beetles mass attack (eq 14)
i beetles survival (eq 11)
Intensity
i hosts weakness (eq 6')
i hosts dead (eq 12)
i hosts alive (eq 13)
Time window of a bark beetle outbreak

Figure 1 : ~~This figure illustrates the dynamic interplay of factors during a bark beetle (*Ips typographus*) outbreak. It depicts the intensity and timeline of key variables such as beetle survival, beetles mass attack, and host weakness (section 2.4). The time window spans four outbreak development stages: build-up, epidemic, post-epidemic, and endemic. The curves represent key~~

8

~~variables, showing the escalation of beetle attacks and subsequent decline in host population, which eventually leads to a stabilization of the system in the endemic~~Dynamic interplay of the different host and beetle characteristics during a bark beetle (*Ips typographus*) outbreak. The time window spans four outbreak development stages: build-up, epidemic, post-epidemic, and endemic. The curves represent key characteristics, showing the growth in beetle population and subsequent decline in host population. $I_{hosts\ dead}$ characterizes the presence of defenseless uprooted or cut spruce trees; $i_{hosts\ alive}$, characterizes living spruce trees that could become hosts for the bark beetles; $i_{hosts\ susceptibility}$, susceptibility of spruce trees to bark beetle attack; $i_{beetles\ mass\ attack}$, quantifies the capability of the bark beetles to mass attack; $i_{beetles\ survival}$, characterizes the survival of bark beetles. Host and bark beetle characteristics are detailed in the subsequent text. When the density of the host trees is declining due to an increased host mortality from the bark beetle outbreak itself, the competition between trees for light and nutrients declines as well. As a consequence, the host susceptibility decreases which in ORCHIDEE is the main pathway for an outbreak to move back to the endemic phase. After 1 year the wood from a storm is not fresh enough for bark beetles to breed in. In ORCHIDEE, the bark beetle population needs to be capable of mass attacking living trees within a year to make the transition from the build-up to the epidemic **phase.**

2.4. bark beetle (*Ips typographus*) damage in ORCHIDEE

~~**Table 1: List of symbols**~~

~~**Symbol**~~	~~**Description**~~	~~**Units**~~
~~α~~	~~Alpha parameter from the self thinning relationship~~	~~unitless~~
~~β~~	~~Beta parameter from the self thinning relationship~~	~~unitless~~
~~act_{limit}~~	~~B_{kill}/B_{total} at which $i_{beetles\ activity}$ = 0.5~~	~~$gC.m^{-2}$~~
~~$B_{beetles\ kill}$~~	~~Biomass of spruce killed by bark beetle annually~~	~~$gC.m^{-2}$~~
~~$B_{windthrow\ kill}$~~	~~Biomass of spruce killed by windthrow event~~	~~$gC.m^{-2}$~~
~~$B_{beetles\ attacked}$~~	~~Biomass of spruce attacked by bark beetle annually~~	~~$gC.m^{-2}$~~
~~B_{total}~~	~~Total living spruce stand biomass~~	~~$gC.m^{-2}$~~
~~B_{wood}~~	~~Spruce woody biomass~~	~~$gC.m^{-2}$~~
~~BP_{limit}~~	~~$i_{beetle\ pressure}$ at which $i_{beetles\ mass\ attack}$ = 0.5~~	~~unitless~~
~~D_{max}~~	~~Maximum Tree stand density~~	~~$tree.ha^{-1}$~~
~~$D_{age\ class}$~~	~~Spuce age classes stand density~~	~~$tree.ha^{-1}$~~
~~DD_{eff}~~	~~Cumulative effective Degrees Day~~	~~$°C.Day^{-1}$~~
~~DD_{ref}~~	~~Reference Degrees Day to fulfill one beetle generation~~	~~$°C.Day^{-1}$~~
~~$Dia_{quadratic}$~~	~~Mean quadratic diameter~~	~~meters~~
~~$DR_{beetles}$~~	~~$B_{beetles\ kill}/B_{total}$ * 100~~	~~%~~

9

$DR_{windthrow}$	$B_{windtrow\ kill}/B_{total} * 100$	%
F_{spruce}	Spruce stand area fraction	unitless
$F_{age\ class}$	Spruce age classes area fraction	unitless
$F_{non\text{-}spruce}$	Non-spruce area fraction	unitless
G_{limit}	Beetles generation number at which $i_{beetle\ generation} = 0.5$	Generation
$i_{hosts\_competition}$	Spruce trees under competition pressure	unitless
$i_{hosts\_weakness}$	Spruce trees weakness to bark beetle attack	unitless
$i_{hosts\_attractivity}$	Spruce attractiveness for bark beetles	unitless
i_{hosts_dead}	defenseless spruce trees uprooted or cutted	unitless
i_{hosts_alive}	Potential living spruce hosts for bark beetle	unitless
$i_{hosts\_defence}$	Spruce trees capacity to resist a bark beetle attack	unitless
i_{hosts_share}	Spruces hidden by other species to bark beetle detection	unitless
$i_{hosts\_competition,\ age\_class}$	Spruce age class under competition pressure	unitless
$i_{hosts\_defence,\ age\ class}$	Spruce age class capacity to resist a bark beetle attack	unitless
$i_{hosts\_health,\ age\_class}$	Spruce age class health condition	unitless
$i_{beetles\_pressure}$	Proxy of bark beetle population level	unitless
$i_{beetles\_survival}$	Bark beetle survival index	unitless
$i_{beetles\_generation}$	Bark beetle generation index	unitless
$i_{beetles\_activity}$	Previous bark beetles activity index	unitless
$i_{beetles\_mass\_attack}$	Bark beetles mass attack capability	unitless
max_{Nwood}	Value of N_{wood} at which $i_{hosts\ dead} = 1.0$	unitless
N_{wood}	Spruce wood necromass	$gC.m^{-2}$
$P_{success,\ age\ class}$	Probability of successful attack per age class	unitless
P_{attack}	Probability of beetles attack	unitless
PWS_{max}	Maximum long term Spruce water stress	unitless
PWS_{spruce}	Spruce water stress	unitless
$PWS_{age\ class}$	Spruce age classes water stress	unitless
PWS_{limit}	Spruce water stress at which $i_{hosts\ defense} = 0.5$	unitless
RDi_{limit}	Relative density index at which $i_{hosts\ competition} = 0.5$	unitless
$RDi_{weakness}$	Relative density index at which $i_{host\ weakness} = 0.5$	unitless
RDi_{spruce}	Spruce stand relative density index [0,1]	unitless
$RDi_{age\ class}$	Spruce age classes relative density index [0,1]	unitless
$S_{competition}$	Shape parameter in the calculation of $i_{hosts\ competition}$	unitless
$S_{weakness}$	Shape parameter in the calculation of $i_{hosts\ weakness}$	unitless
$S_{drought}$	Shape parameter in the calculation of $i_{hosts\ defense}$	unitless
S_{share}	Shape parameter in the calculation of $i_{hosts\ share}$	unitless

~~$S_{activity}$~~	~~Shape parameter in the calculation of $i_{beetle\ activity,\ y-1}$~~	~~unitless~~
~~$S_{generation}$~~	~~Shape parameter in the calculation of $i_{beetle\ generation}$~~	~~unitless~~
~~Sh_{spruce}~~	~~Share fraction of Spruce~~	~~unitless~~
~~Sh_{limit}~~	~~Share fraction at which $i_{hosts\ share}$ = 0.5~~	~~unitless~~
~~T_{air}~~	~~Air Temperature~~	~~°C~~

260 **2.5.**

Table 1: List of symbols

Symbol	Description	Units
α	Intercept of the self thinning relationship	unitless
β	Exponent of the self thinning relationship	unitless
act_{limit}	B_{kill}/B_{total} at which $i_{beetles\ activity}$ = 0.5	$gC.m^{-2}$
$B_{beetles\ kill}$	Biomass of spruce killed by bark beetle annually	$gC.m^{-2}$
$B_{windthrow\ kill}$	Biomass of spruce killed by windthrow event	$gC.m^{-2}$
$B_{beetles\ attacked}$	Biomass of spruce attacked by bark beetle annually	$gC.m^{-2}$
B_{total}	Total living biomass of spruce stand	$gC.m^{-2}$
B_{wood}	Woody biomass of spruce stand	$gC.m^{-2}$
BP_{limit}	$i_{beetle\ pressure}$ at which $i_{beetles\ mass\ attack}$ = 0.5	unitless
D_{max}	Maximum stand density	$tree.ha^{-1}$
$D_{age\ class}$	Stand tree density of spruce age classes	$tree.ha^{-1}$
D_{spruce}	Stand tree density of spruce	$tree.ha^{-1}$
DD_{eff}	Cumulative effective degrees days	$°C.Day^{-1}$
DD_{ref}	Reference degrees days to complete one beetle generation	$°C.Day^{-1}$
$Dia_{quadratic}$	Mean quadratic diameter	meters
$DR_{beetles}$	$B_{beetles\ kill}/B_{total}$ * 100	%
$DR_{windthrow}$	$B_{windtrow\ kill}/B_{total}$ * 100	%
F_{spruce}	Area fraction of spruce within gridcell	unitless
$F_{age\ class}$	Area fraction of spruce age classes	unitless
$F_{non\text{-}spruce}$	Non-spruce area fraction	unitless
G_{limit}	Beetles generation number at which $i_{beetle\ generation}$ = 0.5	Generation
$I_{hosts\ competition}$	Spruce trees under competition pressure	unitless
$I_{hosts\ susceptibility}$	Spruce trees susceptibility to bark beetle attack	unitless
$I_{hosts\ attractivity}$	Spruce attractivity for bark beetles	unitless
$I_{hosts\ dead}$	Defenseless spruce trees uprooted or cut	unitless
$I_{hosts\ alive}$	Potential living hosts for bark beetle	unitless
$I_{hosts\ defense}$	Spruce trees capability to resist a bark beetle attack	unitless
$I_{hosts\ share}$	Spruces hidden by other species to bark beetle detection	unitless

$I_{hosts\ competition,\ age\ class}$	Spruce age class under competition pressure	unitless
$I_{hosts\ defense,\ age\ class}$	Spruce age class capability to resist a bark beetle attack	unitless
$I_{hosts\ health,\ age\_class}$	Spruce age class health condition	unitless
$I_{beetles\ pressure}$	Proxy of bark beetle population level	unitless
$I_{beetles\ survival}$	Bark beetle survival index	unitless
$I_{beetles\ generation}$	Bark beetle generation index	unitless
$i_{beetles\_activity}$	Previous bark beetles activity index	unitless
$i_{beetles\_mass\_attack}$	Bark beetles mass attack capability	unitless
max_{Nwood}	Value of N_{wood} at which $i_{hosts\ dead} = 1.0$	unitless
N_{wood}	Spruce woody necromass	$gC.m^{-2}$
$P_{success,\ age\_class}$	Probability of successful attack per age class	unitless
P_{attack}	Probability of beetles attack	unitless
PWS_{max}	Maximum long term spruce water stress	unitless
PWS_{spruce}	Spruce water stress	unitless
PWS_{age_class}	Spruce age classes water stress	unitless
PWS_{limit}	Spruce water stress at which $i_{hosts\ defense} = 0.5$	unitless
i_{rd_limit}	Relative density index at which $i_{hosts\ competition} = 0.5$	unitless
$i_{rd\_susceptibility}$	Relative density index at which $i_{host\ susceptibility} = 0.5$	unitless
i_{rd_spruce}	Spruce stand relative density index [0,1]	unitless
$I_{rd,\ age\ class}$	Spruce age classes relative density index [0,1]	unitless
$S_{competition}$	Shape parameter in the calculation of $i_{hosts\ competition}$	unitless
$S_{susceptibility}$	Shape parameter in the calculation of $i_{hosts\ susceptibility}$	unitless
$S_{drought}$	Shape parameter in the calculation of $i_{hosts\ defense}$	unitless
S_{share}	Shape parameter in the calculation of $i_{hosts\ share}$	unitless
$S_{activity}$	Shape parameter in the calculation of $i_{beetle\ activity,\ y-1}$	unitless
$S_{generation}$	Shape parameter in the calculation of $i_{beetle\ generation}$	unitless
Sh_{spruce}	Share fraction of spruce against non-spruce in gridcell	unitless
Sh_{limit}	Share fraction at which $i_{hosts\ share} = 0.5$	unitless
T_{air}	Air temperature	°C
T_{max}	Temperature above which beetles developpement stop	°C
T_{min}	Temperature below which beetles developpement stop	°C
T_{bark}	Bark temperature	°C
T_{opt}	Optimal bark temperature for beetles development	°C

The biomass of trees killed by bark beetles in one year and one ~~pixel~~gridcell ($B_{beetles\ kill}$) is calculated as the product of the biomass of trees attacked by bark ~~beetle~~beetles ($B_{beetles\ attacked}$) and the probability of a successful ~~attacks~~attack

($P_{success,\ age\ class}$) averaged over the number of spruce age classes and weighted by their actual fraction ($F_{age\ class}$) ~~for a given tree species (/ F_{spruce}~~). The approach assumes that a successful beetle colonization always results in the death of the attacked tree which is a simplification from reality (A. Leufvén et al. 1986).

$$B_{beetles\ kill} = \sum_{nb\ age\ classes}^{age\ class=1} P_{success,\ age\ class} \times B_{beetles\ attacked} \times \frac{F_{age\ class}}{F_{spruce}} \quad (1)$$

During the endemic stage, $B_{beetles\ attacked}$ and $B_{beetles\ kill}$ are at their lowest values and the damage from bark beetles has little impact on the structure and function of the forest. Losses from $B_{beetles\ kill}$ can be considered to contribute to the background mortality.

The biomass of trees attacked by bark beetles ($B_{beetles\ attacked}$) is ~~defined as an attempt from the bark beetles to overcome~~the outcome of bark beetles that successfully overcame the tree defenses and ~~thus succeeding~~succeeded in boring holes in the bark in order to reach the sapwood. $B_{beetles\ attacked}$ is calculated at the ~~pixel level~~gridcell by multiplying the actual stand biomass of spruce (B_{total}) and the probability that bark beetles attack spruce trees in the ~~pixel~~gridcell ($P_{attacked}$).

$$B_{beetles\ attacked} = B_{total} \times P_{attacked} \quad (2)$$

$P_{attacked}$ represent the ability of the bark beetles to spread and to locate new suitable spruce trees as hosts for breeding. $P_{attacked}$ is calculated by the product of two indexes (all indexes in this study are denoted i and are analogue the ~~the~~ susceptibility indexes from Temperli et al. 2013): (1) the beetle pressure index ($i_{beetles\ pressure}$) which a proxy of the bark beetle population and (2) the stand ~~attractiveness~~attractivity index ($i_{hosts\ attractivity}$) ~~which is a proxy of the overall stand health. Health was here defined as~~is related to its health and reflects the ability of the forest to resist an external stressor such as bark beetle attacks.

$$P_{attacked} = i_{hosts\ attractivity} \times i_{beetles\ pressure} \quad (3)$$

2.6. ~~Stand attractiveness~~Host attractivity

The stand ~~attractiveness~~attractivity index ($i_{hosts\ attractivity}$) ~~varies between 0.5 and 1~~represents how interesting a stand is for a new bark beetle colony. When $i_{hosts\ attractivity}$ tends to ~~0.5~~0, the stand is constituted mainly by healthy trees which are less attractive for beetles whereas an $i_{hosts\ attractivity}$ approaching 1 represents a highly stressed ~~forest~~spruce stand suitable for colonization by bark beetles. Factors that contribute to the stress of a forest ~~in ORCHIDEE~~ are: nitrogen limitation, limited carbohydrate reserves, and monospecific spruce forest. Trees experiencing extended periods of environmental stress are expected to have less carbon and nitrogen reserves available for defense compounds, making them vulnerable for bark beetle attacks even at relatively low beetle population densities (Raffa et al., 2008). Nonetheless, reserves pools in ORCHIDEE ~~r7791~~r8627 have not yet been evaluated so, instead proxies were used

such as long term drought (***PWS***$_{max}$) and relative density index (~~RDi~~i_{rd}) which were already simulated in ORCHIDEE ~~r7791~~r8627.

$$i_{hosts\ attractivity} = max\left(i_{hosts\ competition}, i_{hosts\ defense}\right) \times i_{hosts\ share} \quad (4)$$

Where $i_{hosts\ competition}$ and $i_{hosts\ defense}$ both represent proxies for the reduction of the nitrogen and carbohydrate reserve due to strong competition for light and soil resources, and ~~repetitive~~ consecutive years that are drier than average. For this study, the ~~average~~max drought intensity during the last three years (PWS_{max}) is considered, as a proxy of spruce stand healthiness:

$$\square_{hosts\ defense}\square^{S\square_{drought}\cdot\left(1-PWS\square_{max}-PWS\square_{limit}\right)} \quad \square_{hosts\ defense}\square^{S\square_{drought}\cdot\left(1-PW\square_{max}-PW\square_{limit}\right)} \quad (5a)$$

~~Where,~~

$$\square_{max}\sum_{\square}^{age\ class=1}\square_{spruce}\square_{spruce,n-3}\square_{max}\sum_{\square}^{age\ class=1}\square_{spruce,n}\square_{spruce,n-1}\square_{spruce,n-2}\quad \frac{\square_{age\ class\square}}{F\square_{spruce\square}}\frac{\square_{spruce\ class}}{\square_{spruce}} \quad (5b)$$

Where ~~PWS~~$_{max}$$PWS_{spruce}$ is the ~~maximum~~average daily plant water stress index ~~during the last 3 years, PWS$_{limit}$ is the plant water stress below which the healthiness of the stand will strongly be affected~~over the growing season for the spruce stand and is equal to 0 when plants are highly stressed. PWS_{limit} is the plant water stress below which the healthiness of the stand will strongly be affected. *Nb age class* is the numbers age class within the stand and is equal to 3 in this study. In addition to drought, overstocked forest may also decrease the overall healthiness of a spruce stand (***i***$_{hosts\ competition}$).

$$\square_{hosts\ competition}\square^{S\square_{competition}\cdot\left(RDi\square_{spruce}-RDi\square_{limit}\right)} \quad \square_{hosts\ competition}\square^{S\square_{competition}\cdot\left(i\square_{rd\ spruce}-i\square_{rdlimit}\right)} \quad (6a)$$

In ORCHIDEE, the relative density index (~~RDi~~i_{rd}) is used to quantify the competition between trees at the stand level. At an ~~RDi~~i_{rd} of 1, the forest is expected to be at its maximum density given the carrying capacity of the site, implying the highest level of competition between trees. ~~RDi$_{limit}$~~$i_{rd\ limit}$ represents the limit at which the bark beetle outbreak starts to decline because of lack of suitable host trees. ~~At the spatial scale of the ORCHIDEE model, RDi$_{limit}$ could be considered as a parameter for spatial upscaling since it describes how many trees survive after an outbreak which is very dependent on the size of the pixel. When a pixel represents a single stand (~1 ha) all trees may be killed during an outbreak so RDi$_{limit}$ will be setup close to 0. When an ORCHIDEE pixel is used to represent an area of~~The severity of bark beetle-caused tree mortality decreases when we increase the spatial resolution from the stand to the landscape scale. At the landscape scale, which can cover areas up to 2500 km², the duration of

mortality may be longer and the severity lower because beetles disperse across the landscape and cause mortality at different times. This distinction is important for interpreting model results, particularly when considering parameters like $i_{rd\ limit}$ in the ORCHIDEE model. $i_{rd\ limit}$ describes the proportion of trees surviving after an outbreak and should therefore be adjusted for the spatial scale of a gridcell in ORCHIDEE. In model set-up where a gridcell represents a single stand (~1 ha), $i_{rd\ limit}$ should be close to 0, indicating that nearly all trees may be killed. However, in a simulation with gridcells representing 2500 km², not all trees will be killed, which is reflected in setting ~~RDi_{limit}~~ $= i_{rd\ limit}$ to 0.4.

~~RDi_{spruce}~~$i_{rd\ spruce}$ is computed as follows:

$$i_{spruce}\, i_{rd\ spruce} \sum_{age\ class=1}^{} \left(\sum_{age\ class=1}^{} \frac{D_{age\ class}}{D_{max}} \times \frac{F_{age\ class}}{F_{spruce}} \right) \quad (6b)$$

Where $D_{age\ class}$ is the current tree density of an age class and $F_{age\ class}$ is the fraction of spruce in the ~~pixel~~gridcell that resides in this age class. D_{max} represents the maximum stand density of a stand given its diameter. In ORCHIDEE D_{max} is calculated based on the ~~mean quadratic~~quadratic mean diameter (cm) of the age class and two species specific parameters, α and β:

$$D_{max} = \left(Dia_{quadratic,\ age\ class} / \alpha \right)^{(1/\beta)} \quad (6c)$$

The index $i_{hosts\ share}$ (used in eq. 4) takes into account that in a mixed tree species landscape, even a few non-host trees may chemically hinder bark beetles in finding their host trees (Zhang and Schlyter, 2004) explaining why insect pests, including *Ips typographus* outbreaks, often cause more damage in pure compared to mixed stands (Nardi et al., 2023). ORCHIDEE ~~r7791~~r8627 does not simulate multi-species stands but does account for landscape-level heterogeneity of forests with different plant functional types. The bark beetle ~~module~~model in ORCHIDEE assumes that within a ~~pixel~~gridcell, the fraction of spruce over other tree species is a proxy for the degree of mixture:

$$i_{hosts\ share}^{S_{share} \cdot (sh_{spruce} - sh_{limit})}\, i_{hosts\ share}^{i_{share} \cdot (S_{spruce} - S_{limit})} \quad (7a)$$

Where,

$$i_{spruce}\, i_{¿¿}\, i_{sp\ ruce}\, i_{non-spruce}\, i_{spruce} \quad (7b)$$

2.7. Implicit representation of bark beetle populations

The bark beetle pressure Index ($i_{beetles\ pressure}$) is now formulated based on two components: (1) the bark beetle breeding index of the current year ($i_{beetles\ generation}$), and (2) an index of the loss of tree biomass in the previous year due

15

to bark beetle infestation (~~$i_{beetles\ activity}$~~ $i_{beetles\ activity}$). ~~$i_{beetles\ activity}$~~ $i_{beetles\ activity}$ is thus a proxy of the previous year's bark beetle activity. The expression accounts for the legacy effect of bark beetle activities by averaging activities over the current and previous years. In this approach, the susceptibility index ($i_{beetles\ survival}$) serves as an indicator for increased bark beetle survival which could result from favorable conditions for beetle demography (see next section).

$$i_{beetles\ pressure} = i_{beetles\ survival} \times \frac{\left(i_{beetles\ generation} + i_{beetles\ activity}\right)}{2} \quad (8)$$

The model calculates $i_{beetles\ generation}$ from a logistic function, which depends on the number of generations a bark beetle population can sustain within a single year:

$$i_{beetles\ generation} = 1/\left(1 + e^{-S_{generation} \cdot \left(\frac{DD_{eff}}{DD_{ref}} - G_{limit}\right)}\right) \quad (9)$$

Where $S_{generation}$ and G_{limit} are tuning parameters for the logistic function, DD_{eff} represents the sum of effective ~~temperatures~~temperature for bark beetle reproduction in $^{-1}$°C.Day^{-1}, while DD_{ref} denotes the thermal sum of degree days for one bark beetle generation in $^{-1}$°C.Day^{-1}. Saturation of $i_{beetles\ generation}$ represents the lack of available breeding substrate when many generations develop over a short period.

DD_{eff} is calculated from January 1st until the diapause of the first generation. In ORCHIDEE, diapause is triggered when daylength exceeds 14.5 hours (e.g., April 27th for France). Each day before the diapause with a daily average temperature around the bark above ~~8~~8.3°C ~~is accounted for in sum~~T_{eff}(T_{min}) and below 38.4°C (T_{max}) is accounted for in the summation of DD_{eff} (eq.10). This approach simulates the phenology of bark beetles, which tend to breed earlier when winter and spring were warmer, thus allowing for multiple generations in the same year (Hlásny et al., 2021a). ~~More details on the phenology model are available in~~

$$_{eff} = \sum_{diapause}^{i=1} {}_{opt}\ {}_{min}\ ^{(0.0288 * {}_{bark,i})}\ ^{(0.0288 * {}_{eff} - (40.99 - {}_{bark,i})/3.59)} \quad (10)$$

Where i is a day, $n_{diapause}$ is the number of days between the 1st of january and the day of the diapause. T_{opt} *(30.3°C)* is the optimal bark temperature for beetles development and T_{min} *(8.3°C)* is the temperature below which the beetles developpement stop. $T_{bark,\ i}$ is the average daily bark temperature. $T_{bark,\ i}$ is calculated as the daily average air temperature minus 2°C. All parameters values are taken from Temperli et al. 2013.

The bark beetle activity of the previous year ($i_{beetles\ activity}$) is calculated as:

$$_{beetles\ activity}\ ^{-S_{activity}\left(\frac{_{kill,\ y-1}}{B_{total}} - act_{limit}\right)}\ _{beetles\ activity}\ ^{-_{activity}\left(\frac{_{kill,\ y-1}}{_{total}} - ac_{limit}\right)}) \quad (~~10~~11)$$

Where $i_{beetles\ activity}$ denotes the biomass of the stand damaged by bark beetles in the previous year, B_{total} is the total biomass of the stand, and $S_{activity}$ and act_{limit} are parameters that drive the intensity of this negative feedback.

During the build-up stage ~~(Fig. 1)~~ the population of bark beetles can either return to its endemic stage ~~(Fig. 1)~~ if tree defense mechanisms are preventing bark beetles from successfully attacking healthy trees, or evolve into an epidemic stage (Fig. 1) if the tree defense mechanisms fail. During ~~this stage, tree canopies remain green, therefore, this stage is also known as the green stage (Fig. 1). During~~ the post-epidemic stage, the forest is still subject to higher mortality than usual but signs of recovery appear (Hlásny et al., 2021a). Recovery may help the forest ecosystem to return to its original state or switch to a new state (different species, change in the forest structure) depending on the intensity and the frequency of the disturbance (Van Meerbeek et al., 2021).

2.8. Bark beetle survival

The ~~capacity~~capability of the bark beetles to survive the winter in between two breeding seasons is ~~a crucial mechanism explaining massive tree mortality due to an outbreak~~critical in simulating epidemic outbreaks. During regular winters, winter mortality for bark beetles is around 40% for the adults and 100% for the juveniles (Jönsson et al. 2012). In our scheme, this mortality rate is implicitly accounted for in the calculation of the bark beetle survival index ($i_{beetles\ survival}$). A lack of data linking bark beetle survival to anomalous winter temperatures ~~prevented us from,~~ justifies the implicit approach and prevented including this information as a modulator of $i_{beetles\ survival}$. The latter explains why winter temperatures do not appear in eq. 11. Instead the model simulates the ~~excess of survival due to~~survival as a function of the abundance of suitable tree hosts which decreases the competition for shelter and food:

$$i_{beetles\,survival} = max\left(i_{hosts\,dead}, i_{hosts\,alive}\right) \quad (~~11~~12)$$

The availability of wood necromass from trees that died recently, particularly following windstorms, plays a critical role in bark beetle survival and proliferation. In the year following a windstorm, uprooted and broken trees may offer an ideal breeding substrate for bark beetles, facilitating their population growth.

In Temperli et al. (2013) an empirical correlation between windthrow events and bark beetle susceptibility was established. ORCHIDEE enhances realism by considering the actual suitable hosts (living or recently dead trees) as the primary driver of bark beetle survival. To avoid overestimating bark beetle population growth, max_{Nwood} has been introduced. ~~This ensures that an excess of breeding substrate does not artificially inflate beetle numbers, acknowledging that recent dead trees lose their freshness and thus suitability for breeding after a year. Any addition of dead trees beyond max_{Nwood} is considered ineffective in affecting the bark beetle population.~~

Any addition of dead trees beyond max_{Nwood} is considered ineffective in affecting the bark beetle population. This ensures that an excess of breeding substrate does not artificially inflate beetle numbers.

This relationship is quantitatively represented in ORCHIDEE through the dead host index, $i_{hosts\ dead}$, which is driven by the availability of recent dead trees. The formulation of $i_{hosts\ dead}$ is as follows:

$$i_{hosts\,dead} = min\left(\frac{N\,\square_{wood}}{B\,\square_{wood}} / max\,\square_{Nwood}, 1\right) \qquad (\sout{12}13)$$

Here, N_{wood} represents the quantity of woody necromass from the current year, B_{wood} is the total living woody biomass in the stand, and max_{Nwood} is the threshold of the ratio N_{wood}/B_{wood} signifying the maximum level. This index captures the immediate increase in dead trees ~~post-windthrow, which may drive bark beetle breeding. However, after a year, this substrate becomes unsuitable for breeding and is excluded~~ suitable for bark beetle breeding following a windthrow event. However, it takes about a year for dead wood to lose its freshness and suitability for bark beetle breeding. This is accounted for by excluding woody necromass that is older than 1 year from the $i_{hosts\ dead}$ calculation.

~~Finally,~~ max_{Nwood} can also be considered as a parameter that depends on the spatial scale of the simulation. The mortality rate of trees ($DR_{windtrow}$) that will trigger an outbreak is very different across spatial scales. Where a relatively high share of dead wood is needed to trigger an outbreak at the patch-scale, a much lower share of dead wood suffices at the landscape-scale to trigger a widespread bark beetle outbreak. So these parameters must be set ~~up~~ according to the spatial resolution of the simulation experiment.

$i_{hosts\ alive}$ denotes the survival of bark beetles which is facilitated by the abundance of suitable trees which reduces the competition among bark beetles for breeding substrates and therefore increases their survival.

$$\square_{hosts\,alive}\,\square_{beetles\,mass\,attack}\,\square_{hosts\,weakness}\,\square_{hosts\,alive}\,\square_{beetles\,mass\,attack}\,\square_{hosts\,susceptibility}$$

(~~13~~14)

The amount of suitable tree hosts $i_{hosts\ alive}$ is driven by two factors: (1) the abundance of weak trees which can be more easily infected by bark beetles. ORCHIDEE does not explicitly represent weak trees, but tree health is thought to decrease with an increasing density given the stand diameter. The index for host suitability is thus calculated by making use of the relative density index (~~RDi$_{spruce}$~~ $i_{rd\ spruce}$).

$$\square_{hosts\,weakness}\,\square^{S\,\square_{weakness}\cdot\left(RDi\,\square_{spruce}-RDi\,\square_{weakness}\right)}\,\square_{hosts\,susceptibility}\,\square^{S\,\square_{susceptibility}\cdot\left(i\,\square_{rd\,spruce}-i\,\square_{rd\,susceptibility}\right)} \qquad (6a')$$

Equation 6a' is close to equation 6a but the parameter ~~$S_{weakness}$~~ $S_{susceptibility}$ has been reduced by a factor of two in order to reflect that $i_{hosts\ weakness}$ ~~are~~ $_{susceptibility}$ is more sensitive to ~~RDi~~$i_{rd\ spruce}$ than $i_{hosts\ competition}$. (2) $i_{hosts\ mass\ attack}$ which represent

the ability of bark beetles to attack healthy trees when the number of bark beetles is large enough. This index only depends on the size of the bark beetle population ($i_{beetles\ pressure}$ see eq. 8)

$$i_{hosts\ mass\ attack} = 1/\left(1+e^{S_{mass\ attack}\cdot\left(i_{beetles\ pressure}-BP_{limit}\right)}\right) \quad (14\,15)$$

Where $S_{hosts\ mass\ attack}$ and BP_{limit} are parameters. $S_{mass\ attack}$ controls the steepness of the relationship while BP_{limit} is the bark beetle pressure index at which the population is moving from endemic to epidemic stage where mass attacks are possible.

The epidemic stage corresponds to the capability of bark beetles to mass attack healthy trees and overrule tree defenses (Biedermann et al., 2019). At this point in the outbreak, all trees are potential targets irrespective of their health. ~~Owing to the widespread mortality of individual trees, the forest dies resulting in a stage also known as the red stage (Fig. S2, stage 3). Three causes may~~Three causes have been suggested to explain the end of ~~an~~the epidemic phase: (1) the most likely cause is a high interspecific competition among beetles for tree host when the density is decreasing (decreasing $i_{hosts\ alive}$) (~~Pineau~~Komonen et al., ~~2017; Komonen~~2011; Pineau et al., ~~2011~~2017), (2) a series of very cold years will decrease their ability to reproduce (decreasing $i_{beetles\ generation}$), and (3) a rarely demonstrated increasing population of beetle predators (Berryman, 2002). In ORCHIDEE ~~r7791~~r8627, the first two causes are represented but the last, i.e.~~,~~ the predators are not ~~represented~~.

2.9. Tree mortality from bark beetle infestation

When bark beetles attack a tree, the success of their attack will likely depend on the ~~capacity~~capability of the tree to defend itself from the attack. Trees defend themselves against beetle attacks by producing secondary metabolites (Huang et al., 2020). The high carbon and nitrogen costs of these compounds limit their production to periods with environmental conditions favorable for growth (Lieutier, 2002). The probability of a successful bark beetle attack is driven by the size of the bark beetle population (~~i~~~~beetle~~$i_{beetles\ pressure}$) and the ~~weakness~~health of each tree. ORCHIDEE, however, is not simulating individual trees but rather diameter classes within an age class. An index of tree ~~weakness~~health for each age class ($i_{hosts\ health,\ age\ class}$) was calculated as:

$$P_{success,\ age\ class} = i_{hosts\ health,\ age\ class} \times i_{beetles\ pressure} \quad (15\,16)$$

A tree rarely dies solely from bark beetle damage (except during mass attacks) as female beetles often carry blue-stain fungi, which colonizes the phloem and sapwood, blocking the water-conducting vessels of the tree (Ballard et al., 1982). This results in tree death from carbon starvation or desiccation. As ORCHIDEE ~~r7791~~r8627 does not simulate the effects of changes in sapwood conductivity on photosynthesis and the resultant probability of tree mortality, the index of weakened trees index ($i_{hosts\ health,\ age\ class}$) makes use of two proxies similarly to equation 5 and 6 but simplified to be calculated only for one age class at ~~the~~a time:

$$i_{hosts\ health,\ age\ class} = \frac{\left(i_{hosts\ competition,\ age\ class} + i_{hostsdefense,\ age\ class}\right)}{2} \qquad (\text{~~16~~}17)$$

$$i_{hosts\ defense,\ age\ class} = 1/\left(1+e^{S_{drought}\cdot\left(1-PWS_{age\ class}-PWS_{limit}\right)}\right) \qquad (5a')$$

Contrary to equation 5a, $\boldsymbol{PWS_{age\ class}}$ is the plant water stress from the current year.

$$_{hosts\ competition,\ age\ class}^{S_{competition}\cdot\left(RDi_{age\ class}-RDi_{limit}\right)}{}_{hosts\ competition,\ age\ class}^{S_{competition}\cdot\left(i_{rdage\ class}-i_{rd\ limit}\right)} \qquad (6a'')$$

$$_{age\ class}{}_{rd\ age\ class}\frac{D_{age\ class}}{D_{max}} \qquad (6b'')$$

To access the ~~Bark~~bark beetle damage rate ($\boldsymbol{DR_{bettles}}$), ~~we simply divide $B_{beetles\ kill}$~~ $B_{beetles\ kill}$ has to be divided by $\boldsymbol{B_{total}}$.

2.10. Flow of the calculations

~~As the~~The equations presented above contain feedback loops ~~the flow of the calculation is shown in Fig. 2~~which have been visualized in Fig. 2. In ORCHIDEE these feedback loops are accounted for in subsequent time steps rather than the same time step.

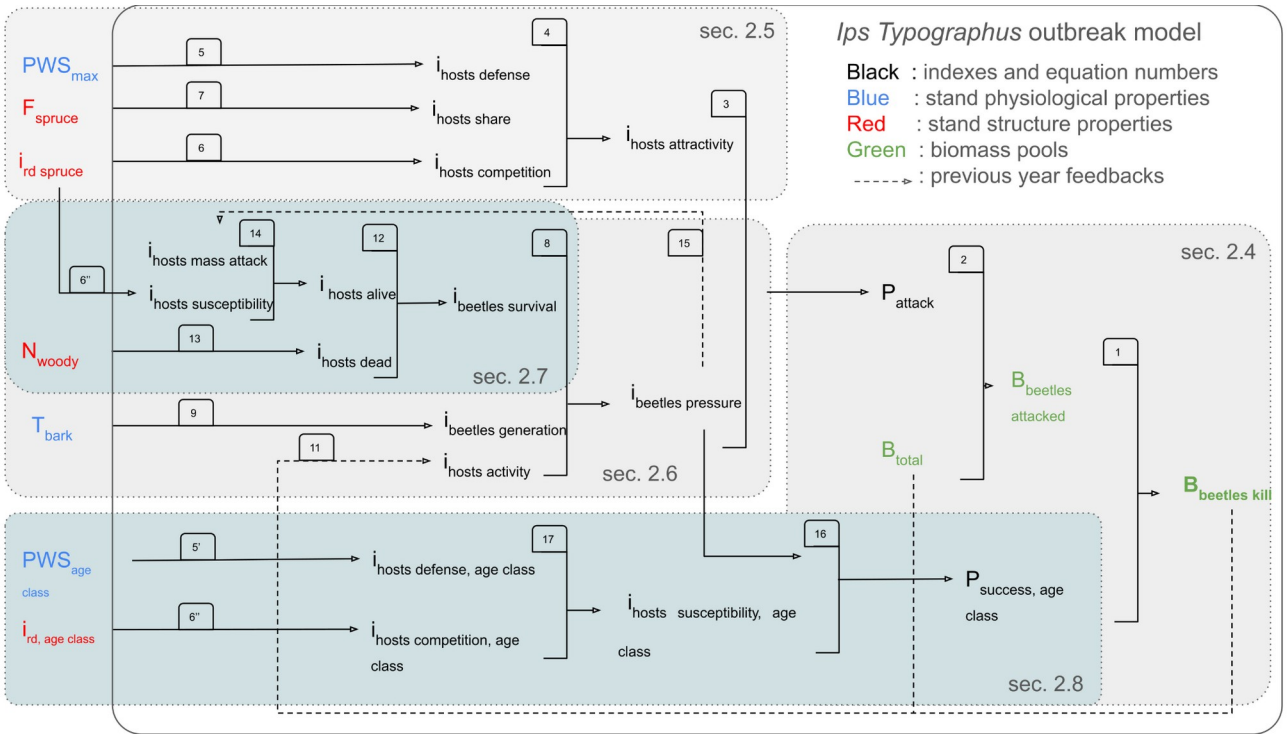

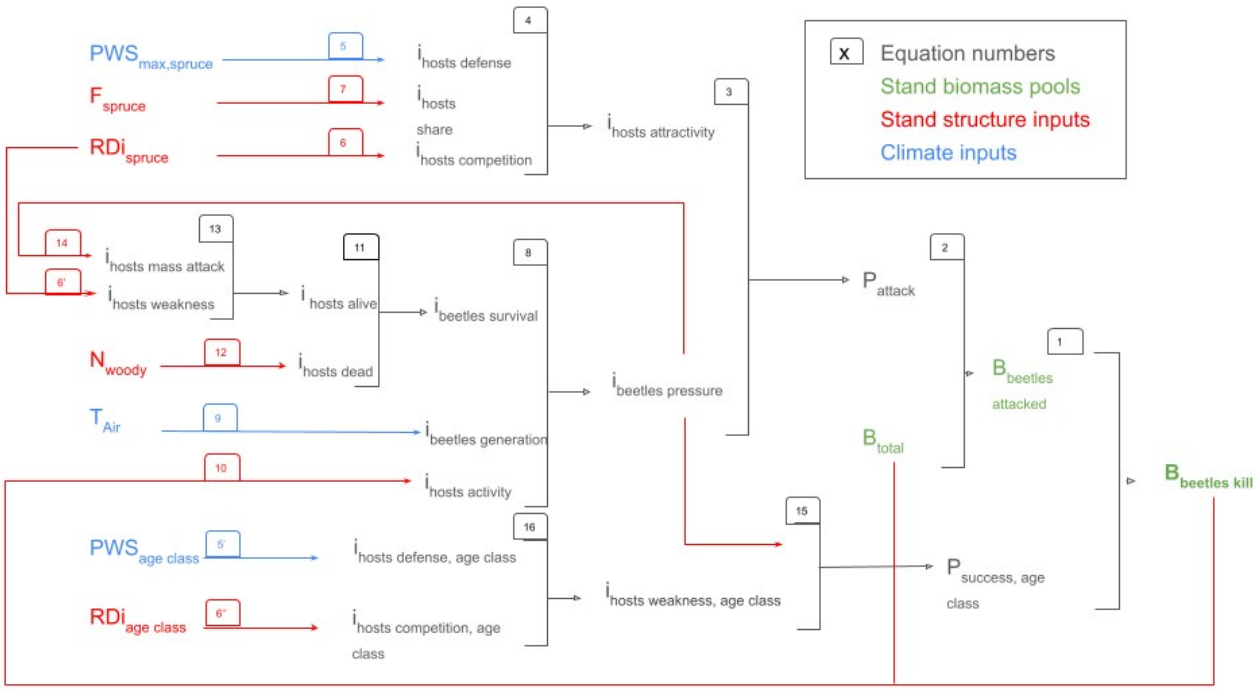

Figure 2: ~~Flow~~Order of the calculations ~~in the bark beetle outbreak module developed in this study~~and feedback in the *Ips typographus* outbreak model of ORCHIDEE. The numbers correspond to the equation numbers ~~provided~~ in this study. The dotted line boxes represent 5 main concepts of the outbreak model described in section 2.4, 2.5, 2.6, 2.7, 2.8.

3. Methods and material

3.1. Model configuration

Given the large-scale nature of the ORCHIDEE ~~we carried out,~~ a sensitivity experiment of the bark beetle outbreak functionality was carried out rather than focusing the model evaluation on matching observed damage volumes at specific case studies. ~~Such an approach~~Focussing on model sensitivity for a range of environmental conditions is thought to reduce the risk of overfitting the model to specific site conditions (Abramowitz et al., 2008).

ORCHIDEE ~~r7791~~r8627 including the bark beetle ~~module~~model was run ~~for 8~~at the location of eight FLUXNET sites, selected to simulate a credible temperature and precipitation gradient for spruce (see ~~further~~ below). For each location, the half-hourly meteorological data from the flux tower were gap filled and reformatted so that they could be used as climate forcing by the ORCHIDEE. Boundary conditions for ORCHIDEE, such as soil texture, pH and soil color were retrieved from the USDA map, for the corresponding ~~pixel~~gridcell. The observed land cover and land use for the ~~pixel~~gridcell were ignored and set to pure spruce because this study did not investigate the effect of species mixture in the simulation experiments. The resolution of the ~~pixel~~gridcell chosen for this analysis is 2500 km². ~~It~~Although this corresponds to a ~~fine~~high resolution for ~~ORCHIDEE~~ large-scale simulations ~~but~~ with ORCHIDEE it is a coarse resolution for studying bark beetle outbreaks.

21

The climate forcings were looped over as much as needed to bring the carbon, nitrogen, and water pools to equilibrium during a 340 years long spinup ~~followed by a windthrow event and a 100-years simulation~~. Following the spinup, a 100-years simulation was run starting with a windthrow event on the first day of the first year. The results presented in this study come from the 100-years long ~~site~~ simulations. Given the focus on even-aged monospecific spruce forests in regions where spruce growth is not constrained by precipitation, variables such as $i_{hosts\ share}$ and $i_{hosts\ defense}$ were omitted from this study. Note that ORCHIDEE ~~do~~does not account for possible acclimation ~~of the bark beetle population to each location.~~

~~**Site selection**~~e.g., temporal changes in bark beetle behavior or bark beetle resistance to external stressor such as winter temperature.

3.2. Selection of locations

Bark beetle populations are known to be sensitive to temperature as they are more likely to survive a mild winter (Lombardero et al., 2000) and tend to breed earlier when winter and spring are warmer than usual, allowing for multiple generations in the same year (Hlásny et al., 2021a, also see eq. 10 from section 2.6). In order to assess the temperature effect of the bark beetle outbreak ~~module~~model in ORCHIDEE, eight locations in Europe were selected (Table 2) which represent the range of climatic conditions within the distribution area of Norway spruce (*Picea Abies* Karst L.) ~~which is,~~ the main host plant for *Ips typographus*, the bark beetle species under investigation.

Table 2: Climate characteristics of the eight ~~sites~~locations used in the simulation experiments ~~gradient underlying our experimental setup~~. The ~~site~~ acronyms refer to the site names used in the FLUXNET database (Pastorello et al. 2020).

Site ~~(FLUXNET)~~	**FI-HYY**	**DK-SOR**	**DE-THA**	**CZ-WET**	**FR-HES**	**FR-FON**	**IT-REN**	**IT-COL**
Full name	Hyytiala	Soroe	Tharandt	~~Wetstein~~ Třeboň	Hesse	Fontainebleau	Renon	Collelongo
Country	Finland	~~Danmark~~ Denmark	Germany	~~Germany~~ Czech	France	France	Italy	Italy
Latitude (°N)	~~61.8~~61.84	~~55.5~~55.49	~~50.9~~50.96	~~49.0~~49.02	48.4	~~48.7~~48.48	~~46.5~~46.59	~~41.8~~41.85
Longitude (°E)	~~24.3~~24.29	~~11.6~~11.64	~~13.6~~13.57	~~14.8~~14.77	7.1	~~2.8~~2.78	~~11.4~~11.43	~~13.6~~13.59
MAT (°C)	3.8	8.2	8.2	7.7	9.5	10.2	4.7	6.3
MinAT (°C)	-10.8	2.7	-3.9	-5.2	0.1	-1.1	-6.3	-3.8
MAP ($mm.y^{-1}$)	522	811	734	587	653	989	752	1050
Mean annual net radiation ($w.m^{-2}$)	42.1	49.4	52.5	68.0	53.7	50.3	67.7	68.3

22

For these eight locations, half-hourly weather data from the FLUXNET database (Pastorello et al., 2020) were used to drive ORCHIDEE. Some of these locations (FON, SOR, HES, COL, WET) are in reality not covered by spruce but all sites are, however, located within the distribution of Norway spruce. In this study, ~~site~~ locations were selected to use the observed weather data to simulate a credible temperature and rainfall gradient for spruce. ~~-~~ HES location is no longer part of the FLUXNET network but the previous data are still available are relevant for this analysis.

3.3. Sensitivity to model parameters

The sensitivity assessment evaluates the responsiveness of four key variables ($i_{hosts\ \sout{weakness}susceptibility}$, $i_{beetles\ mass\ attack}$, $i_{beetles\ generation}$, $i_{beetles\ activity}$) of the ~~bark beetle model of~~*Ips typographus* outbreak model implemented in ORCHIDEE. The assessment aims to demonstrate the ability of ORCHIDEE to simulate diverse dynamics of bark beetle infestations. The selection of $i_{hosts\ \sout{weakness}susceptibility}$, $i_{beetles\ activity}$, $i_{beetles\ mass\ attack}$, and $i_{beetles\ generation}$ was based on two criteria: (1) their substantial influence on the dynamics of the ~~bark beetle epidemic~~*Ips typographus* outbreak noted during model development, and (2) their independence from direct measurable data, rendering them less suitable for evaluation through literature review.~~-~~

For each ~~variable~~of the four variables, three distinct values were assigned to two parameters labeled "~~*S*~~*Shape*" and "~~limit~~*Limit*". The ~~*S*~~*Shape* parameter determines the shape of the logistic relationship, with three values tested ~~for each variable~~: (a) ~~*S=-1*~~*Shape*=-1.0, yielding a linear relationship, (b) ~~*-1<S<-100*~~*5.0<Shape<-30.0*, resulting in a logistic curve, and (c) ~~*S>-100*~~*Shape*=-500.0, turning the logistic relationship into a step function. For the logistic curve, the exact *Shape* value between -30.0 and -5.0 is chosen according to each index under study: (1) $S_{susceptibility}$ = -5.0; (2) $S_{activity}$= -20.0; (3) $S_{mass\ attack}$= -30.0; and (4) $S_{generation}$=5.0 . For $S_{mass\ attack}$ and $S_{activity}$, higher values have been chosen because the slope of the logistic curve has a significant impact in order to trigger an outbreak.

The second parameter called "*Limit*" determines the threshold, derived from expert insights, at which the logistic relationship will reach its midpoint value of 0.5 (~~*RDi*~~$_{\sout{weakness}i_{rd\ susceptibility}}$, BP_{limit}, Act_{limit}, *or* G_{limit}). For instance, ~~*RDi*~~$_{\sout{weakness}i_{rd\ susceptibility}}$ is set at 0.55, indicating $i_{hosts\ \sout{weakness}susceptibility}$ midpoint sensitivity (Eq. 6'). Setting BP_{limit} at 0.12 results in an $i_{beetles\ mass\ attack}$ midpoint when $i_{beetles\ pressure}$ is 0.12, selected for its proximity to scenarios where $i_{hosts\ dead}$ equals 1.0 (Eq. 14). Act_{limit}, was positioned at 0.06, ~~signifies~~signifying the $i_{beetles\ activity}$ midpoint at a $DR_{beetles}$ = *6%* from the preceding year, exceeding endemic levels yet not reaching epidemic outbreaks (Eq. 10). Lastly, G_{limit} is fixed at 1.0, denoting ~~$i_{beetles\ generation}$'s midpoint~~the midpoint for $i_{beetles\ generation}$ upon completing one generation annually, underpinning the rarity of bark beetle outbreaks with fewer than one generation per year (Eq. 9). Starting from these reference values, a "*restrictive*" simulation was run in which the "*Limit*" parameter values were reduced by 50%. Likewise a "*permissive*" simulation was run to test 50% higher ~~"*Limit*" parameter values.~~

~~This assessment explores 36 parameters value combinations (3 x 3 parameter values x 4 parameters~~values for "*Limit*".

23

The sensitivity analysis of the model parameters explores 36 (3 shapes x 3 limits x 4 equations) combinations of parameters values named "set", but the full design of the experiment is 8^3=512 sets (8 parameters, 3 values for each). This deliberate choice has been made because of the computation time cost of a single run. In order to reduce the number of runs from 512 to 36, we had to make simplifications: (1) one equation at the time is studied, reducing to 9 the number of sets necessary to realize the sensitivity analysis (2) every other parameters from the remaining equation is set to default value e.g. "Limits" are set to their reference values and "shape" are set to their a priori assumption (table 4). The major drawback of this approach is that interaction effects between equations can not be investigated in the study. Nonetheless, this sensitivity analysis aims to document model behavior, rather than seeking precise parameter values which can be achieved with the main effect of each equation only (see section 3.4).

The simulations were run for the THA site, where they were repeated for two prescribed windthrow events with a different intensity, i.e., a $DR_{windthrow}$ of 0.1 and 10%. The effect of the parameters with a negligible windthrow event, i.e., killing only 0.1% of the trees, was tested to confirm that the selected parameters did ~~not simulates false positives, i.e. ORCHIDEE simulating~~make ORCHIDEE simulate a bark beetle outbreak in the absence of windthrow~~. Note that this sensitivity analysis aims to document model behavior, rather than seeking precise parameter values (see section 3.4).~~

~~3.4. Parameter tuning~~

~~The simulation experiment presented in this section was repeated for all eight sites and those results were used to tune key model parameters. In order to select parameters values for $i_{hosts\ weakness}$ (*score5* in section 3.4).~~

3.5. Parameter tuning and credibility score

The results of the sensitivity experiment were used to select key model parameters. Selecting the values for the *Shape* and *Limit* parameters (see section 3.3) used in the calculation of the variables $i_{hosts\ susceptibility}$, $i_{beetles\ mass\ attack}$, $i_{beetles\ generation}$, and $i_{beetles\ activity}$ ~~that resulted in simulations reproducing observed dynamics of bark beetle outbreaks, the literature was searched~~has been carried out in order to reproduce the observed dynamics of bark beetle outbreaks. Observed dynamics were compiled through a literature search for peer-reviewed papers that reported quantitative characteristics of bark beetle outbreaks (Table 3). Four characteristics could be documented and use to calculate score:

- The delay between the windthrow event and the start of the bark beetle outbreak (*score1*).
- The length of the bark beetle outbreak is defined by the number of years required for a bark beetle population to go back to its endemic level (*score2*).
- The cumulative number of trees per unit area, killed by the bark beetles at the end of an outbreak (*score3*).
- The average tree mortality rate ($DR_{beetles}$) during an endemic stage~~.~~

- ~~As already mentioned in the section 2.4, at landscapes scale we do not expect that the all spruces in the landscape will be killed by an outbreak, so we choose to set RDI_{limit} to 0.4 which mean that an outbreak will not kill more than 60 % of the trees in one pixel irrespective of the outbreak intensity.~~ (*score4*).

Based on Table S1 and the reference range in Table 3, scores are calculated for each parameter set. The Credibility Score (*CS*) is the sum of four scores, indicating that the result falls within the four reference ranges described above and no outbreak is triggered when DRwindthrow = 0.1%. The *CS* is computed as follows: *CS = (score1 + score2 + score3 + score4) x score*5. Only parameter sets achieving a *CS* of 4 will be selected. If multiple parameter values are possible for a given equation, the most frequently selected value will be preferred.

~~**Table 3 : Literature-based summary of characteristics of large-scale bark beetle outbreaks.**~~

~~**Outbreak characteristics**~~	~~**Observations/model outputs from literatures**~~	~~**How to estimate in ORCHIDEE ?**~~
~~Delay before the start of an outbreak~~	~~A notable surge in the population of *I. typographus*, a species of bark beetle, was observed in windthrow areas during the second to third summer following the storm (Wichmann and Ravn, 2001; Wermelinger, 2004; Kärvemo and Schroeder, 2010; Havašová et al., 2017).~~	~~Using the tree mortality rate by bark beetles ($DR_{beetles}$), one can access the number of years since the storm before reaching the maximum mortality rate (epidemic stage).~~
~~Length of an outbreak~~	~~Studies suggest that bark beetle outbreaks in Europe can last anywhere from 11 to 17 years (Hlásny et al., 2021b; Mezei et al., 2014; Bakke, 1989).~~	~~Using the tree mortality rate by bark beetles ($DR_{beetles}$), one can access the number of years since the storm before reaching the minimum mortality rate (endemic stage).~~
~~Severity rate of an outbreak~~	~~A severe bark beetle outbreak resulted in a 52%-60% reduction in tree numbers at large landscape scale (>2000km²) (Pfeifer et al., 2011; Morehouse et al., 2008)~~	~~Count the number of trees killed by bark beetles until the end of the outbreak, then divide by the number of trees just after the storm event.~~
~~Endemic mortality rate~~	~~Total background mortality is around 1.2%/year. Bark beetles are estimated to account for 40% of the total mortality (≈0.5%/year) (Das et al., 2016; Berner et al., 2017; Hlásny et al., 2021b).~~	~~After the end of the outbreak, count the number of trees that die every year. Then average it.~~

Table 3 : Literature-based summary of characteristics of large-scale bark beetle outbreaks. Due to data spacity, the characteristics combine outbreak dynamics of different bark beetle species, different host species, and different locations. The reference range is used to calculate the credibility score (CS) of each set of parameters (but see table s1).

Outbreak characteristics	**Literature findings**	**Reference range**	**How to estimate in ORCHIDEE ?**
Delay before the start of an outbreak (build-up)	A notable surge in the population of *I. typographus* was observed in windthrow areas during the second to third summer following the storm (Havašová et al., 2017; Kärvemo	[2, 3] years, use in the calculation of *score1*	Using the tree mortality rate by bark beetles ($DR_{beetles}$), one can access the number of years since the storm before reaching the maximum mortality rate (epidemic stage).

25

	and Schroeder, 2010; Wermelinger, 2004; Wichmann and Ravn, 2001).		
Length of an outbreak (epidemic)	Studies suggest that *I. typographus* outbreaks in Europe can last anywhere from 11 to 17 years (Bakke, 1989; Hlásny et al., 2021b; Mezei et al., 2014).	[11, 17] years, use in the calculation of *score2*	Using the tree mortality rate by bark beetles ($DR_{beetles}$), one can access the number of years past since the storm before reaching the minimum mortality rate (endemic stage).
Severity rate of an outbreak (severity)	A severe bark *D. Ponderosa* outbreak resulted in a 52%-60% reduction in tree numbers at large landscape scale (>2000km²) (Morehouse et al., 2008; Pfeifer et al., 2011) In Wallonia and East France, *I. Typographus* outbreak resulted in 12.6% reduction of spruce forest area in 6 years (Arthur, G., et al. 2024).	Highly dependent from the size of the forest studied but for a grid cell of 2500km2, ones could expect a [25%, 45%] reduction over the entire course of a massive outbreak. Use in the calculation of *score3*	Count the number of trees killed by bark beetles until the end of the outbreak, then divide by the number of trees just after the storm event.
Endemic mortality rate (endemic)	Total background mortality is around 1.2%.year^{-1}. Bark beetles as a functional group are estimated to account for 40% of the total mortality in the United States (≈0.5%.year^{-1}) (Berner et al., 2017; Das et al., 2016; Hlásny et al., 2021b).	Not enough data was available to estimate a range. Nonetheless we decided to calculate a range including a 10% uncertainty [0.45-0.55] %.year^{-1}. Use in the calculation of *score4*	After the end of the outbreak, count the number of trees that die every year. Then average it.

3.6. ~~Impact of climate and windthrow : simulation experiment~~Sensitivity to climate and windthrow

In this simulation experiment, the ~~amount~~influx of fresh dead tree hosts (N_{wood}) used ~~by the bark beetles to breed~~for bark beetle breeding was controlled by modifying the maximum damage rate of a windthrow event ($DR_{windthrow}$) in ORCHIDEE. Seven $DR_{windthrow}$ were simulated (i.e, 0.1%, 5%, 7.5%, 10%, 15%, 20%, 35%). Given the monotonic nature of the relationships between $DR_{windthrow}$ and $i_{hosts\ dead}$ (Eq. 12), each event triggers a proportional increase in the dead host availability ($i_{hosts\ dead}$) scaling between 0 and 1 (Fig. 3). Through its equations, ORCHIDEE assumes that for damage rates above 20% ~~$i_{hosts\ dead}$~~the variable $i_{hosts\ dead}$ (N_{wood}) will always be equal to 1.0. ~~RDi_{spruce}~~$i_{rd\ spruce}$, however, may further decrease with increasing windthrow damage, which makes the 35% damage rate still interesting to investigate. Although the simulations were run for all $DR_{windthrow}$, only four windthrow damage rates ~~were presented to enhance the readability of the result section~~ including a windstorm resulting in a 35% damage rate (Fig. 3), were presented to enhance the readability of the result section.

660

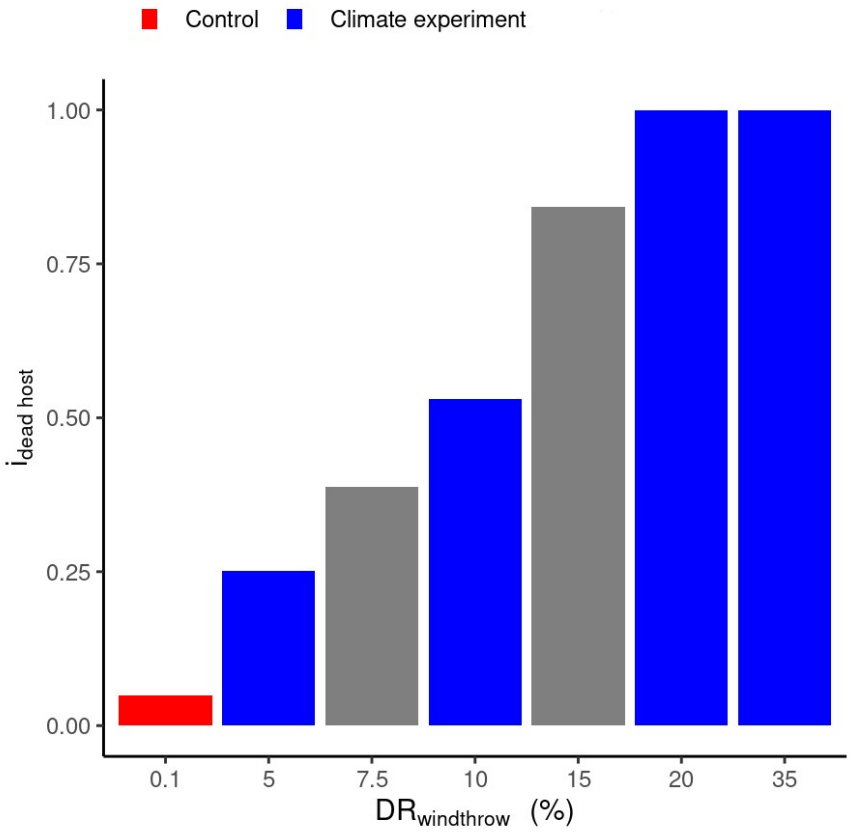
Control
Climate experiment
1.00
0.75
0.50
0.25
0.00
$i_{dead\ host}$
0.1
5
7.5
10
15
20
35
$DR_{windthrow}$ (%)

27

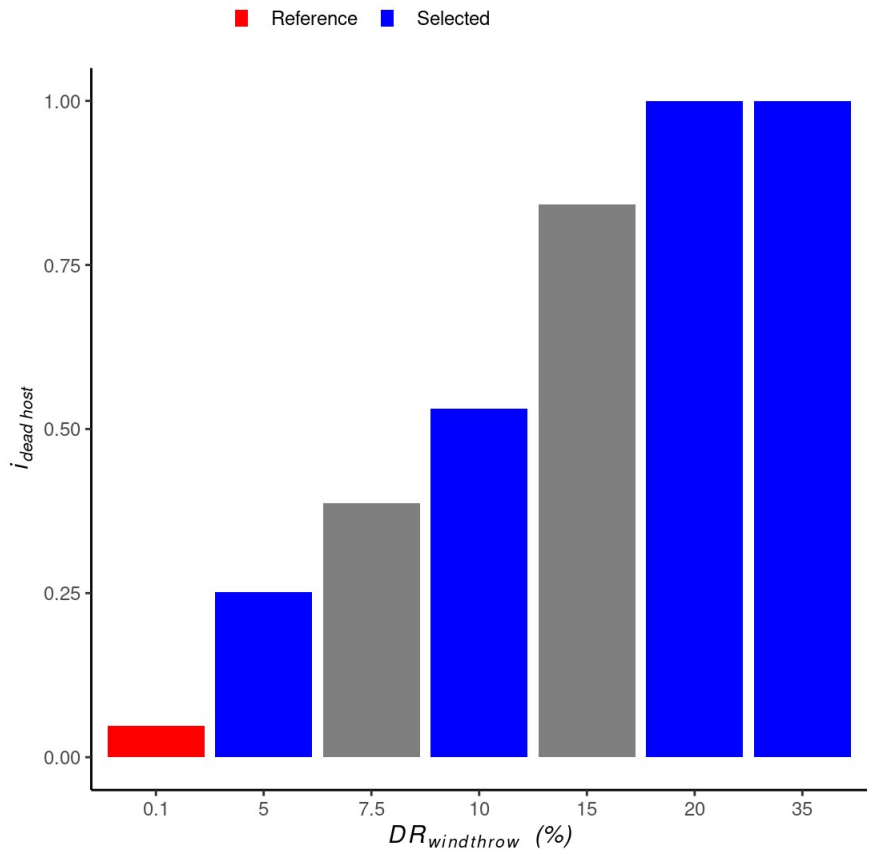

Figure 3: Relationship between windthrow damage rate ($DR_{windthrow}$) and dead host index ($i_{hosts\ dead}$). For each site a $DR_{windtrow}$= *0.1%* was used as the ~~control~~reference simulation because an endemic bark beetle population is expected following such a low intensity windthrow event. ~~Four $DR_{windthrow}$~~The four $DR_{windthrow}$ shown in blue were selected for subsequent presentation of the results because they cover the entire range for the $i_{hosts\ dead}$.

~~Site selection was based on the average numbers of generation a bark beetle population can achieve in one year. As described in Temperli 2013, the main driver of numbers of generation~~The main driver of the number of generations a bark beetle population can achieve in one year is the number of days higher than ~~7.5~~8.3°C during winter time (Temperli et al., 2013) which is the reason why temperature is so important for bark beetle reproduction. By taking REN, THA, WET and HES, ~~we can investigate a range in bark beetle generations between 0.8 and 3.5 (Fig. 4) which is a relevant range already observed in Europe. Restraining our~~the number of bark beetle generations ranged from 0.8 to 3.5 (Fig. 4) which is similar to the number of generations observed across Europe (Faccoli and Stergulc, 2006; Jönsson et al., 2009, 2011). Limiting the analysis to only four sites ~~will simplify~~simplifies the presentation ~~in the results section~~without affecting the range under investigation.

28

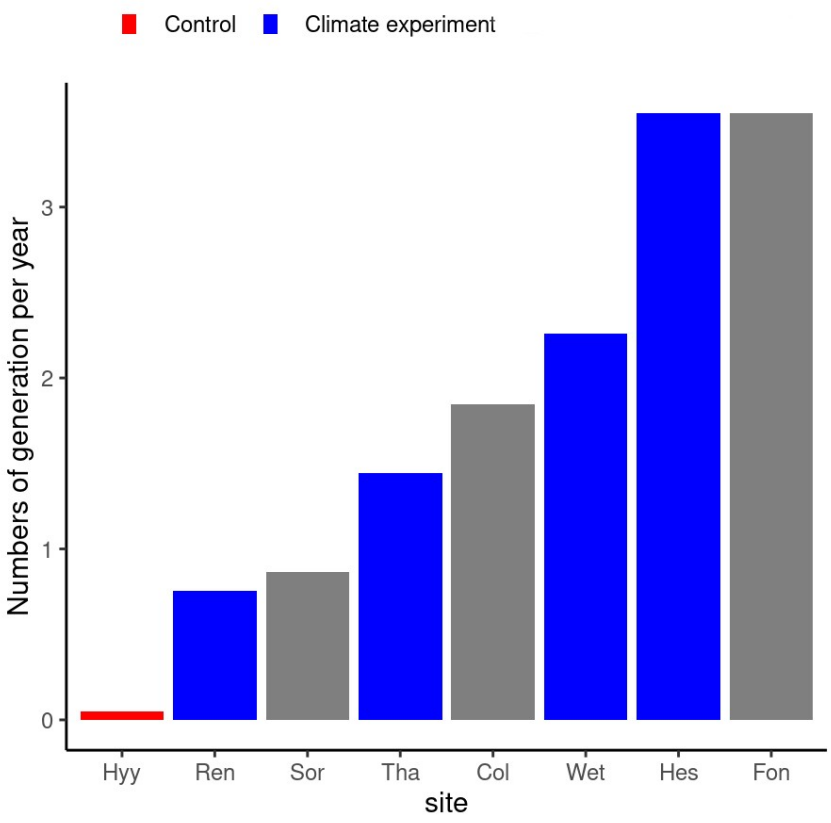
Control
Climate experiment
Numbers of generation per year
0
1
2
3
Hyy
Ren
Sor
Tha
Col
Wet
Hes
Fon
site

29

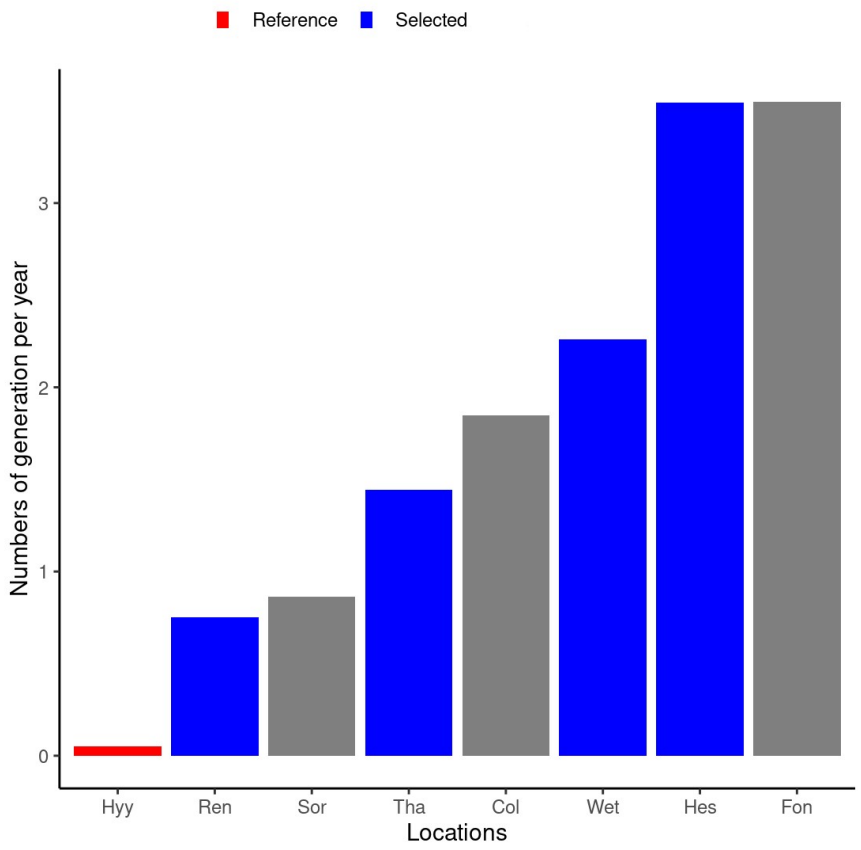

Figure 4: Average number of bark beetle generations during the 5 years following the wind storm for ~~the 8 sites~~at eight locations along a climate gradient. The HYY ~~site~~location in Finland was selected as the ~~control site~~reference for the REN, THA, WET and HES ~~sites~~locations. Only results from the ~~control~~reference and ~~selected sites~~four selected locations (shown in blue) are shown in the results to enhance readability ~~of the figures. Although all simulations were also run for SOR, COL and FON their results were found to be too similar to the results of selected sites to present them as well.~~ .

For the climate gradient, the ~~HYY site was chosen to serve~~simulation for HYY served as a ~~control~~reference since the ~~numbers of generation~~number of generations is lower than 1 for which no outbreak should happen under any circumstances. Under present climate conditions, an outbreak in HYY should be considered ~~as a false positive~~an undesirable model result. Likewise, a $DR_{windthrow}=0.1\%$ ~~—~~ is considered too low to trigger an outbreak and was therefore used as the ~~control~~reference for the wind damage rate tests.

The experiment consisted of ~~25~~40 simulations, i.e., ~~5 selected~~8 sites (including ~~a control~~the reference) x 5 wind damage rates (including ~~a control)~~the reference). Although the simulations were also run for SOR, COL and FON their results were found to be too similar to the results of selected sites to present them as well. Hence, the result section presents only 25 out of the 40 simulations. Three output variables were assessed: bark beetle damage rate

30

($DR_{beetles}$), total biomass (B_{total}), and net primary production (*NPP*). Total biomass was investigated over 100 years whereas $DR_{beetles}$ and ***NPP*** were assessed for the first 20 years following a windthrow.

3.7. Continuous vs abrupt mortality

Where most land surface models use a fixed turnover time to simulate continuous mortality (~~Thurner~~Pugh et al., 2017; ~~Pugh~~Thurner et al., 2017), ecological reality is better described by abrupt mortality events. An idealized simulation experiment was used to qualify the impact of abrupt mortality on net biome productivity by changing from a framework in which mortality is approximated by a constant background mortality to a framework in which mortality occurs in abrupt, discrete events. ~~To test the~~The impact of a change in mortality framework ~~two versions of ORCHIDEE were compared to create an idealized simulation experiment~~was assessed with an idealized simulation experiment that compares three configurations of ORCHIDEE: (1) a ~~version simulating~~configuration that simulates mortality as a continuous process, labeled "the ~~smooth version"~~continuous configuration" which corresponds to previous versions of ORCHIDEE, and (2) ~~the version~~a configuration capable of simulating abrupt mortality from windthrow and subsequent bark beetle outbreaks, labeled "the abrupt ~~version~~configuration" and (3) a ~~version~~configuration in which windthrow is activated but bark beetles outbreak is ~~include in the mortality background~~implicitly accounted for in the background mortality. This third configuration enabled attributing the impact to windthrow. The effect of simulating abrupt mortality was evaluated over 20, 50, and 100 year time horizons.

The ~~effect~~impact of changing the ~~framework of simulating mortality~~mortality framework from continuous to abrupt was ~~qualified~~quantified on the basis of 120 simulations (8 ~~sites~~locations x 7 windthrow damage rates x 2 ~~model versions~~configurations + 8 sites x 1 ~~smooth version~~configuration) of 100 years each.

The simulations with abrupt mortality were run first. Subsequently, the number of trees killed was quantified and used as a reference value for the continuous mortality set-up. This approach resulted in the same quantities of dead trees at the end of the simulation for both frameworks, which then differed only in the timing of the simulated mortality. This precaution is necessary to avoid comparing two different mortality regimes where the result would mainly be explained by the intensity of the mortality rather than by its underlying mechanisms.

Changes in forest functioning were evaluated through the temporal evolution of accumulated net biome productivity (***NBP***) over a 100-years time frame. ***NBP*** is defined as the regional net carbon accumulation after considering losses of carbon from fire, harvest, and other episodic disturbances. ~~NBP is a key variable in the carbon cycle of forest ecosystems) as it integrates photosynthesis, autotrophic, and heterotrophic respiration. In ORCHIDEE, NBP is estimated as proposed in Chapin et al. (2006). Changes in net biome productivity are thus the result of changes in photosynthesis, which in turn is driven by changes in leaf area, autotrophic respiration, and heterotrophic respiration. The latter is influenced by the availability of litter inputs, including litter from trees that died from the bark beetle outbreak~~In ORCHIDEE, *NBP* is calculated following the definition by Chapin et al. (2006) as the carbon remaining

in the biomass, litter and soil after accounting for photosynthesis, and respiration because fire, harvest, leaching and volatile emissions were not accounted for in this simulations experiment.

4. Results

4.1. Sensitivity to model ~~parameters~~parameter sets

The impact of spruce stand competition (i_{hosts} ~~$_{weakness}$~~$_{susceptibility}$) on outbreak dynamics was examined by adjusting the parameters ~~$S_{weakness}$ and $RDi_{weakness}$~~$S_{susceptibility}$ and $i_{rd\ susceptibility}$ in equation 6a'. When ~~$S_{weakness}$~~$S_{susceptibility}$ resulted in a linear relationship (~~$S_{weakness}$~~$S_{susceptibility}$ = ~~-1~~1.0), no peak in bark beetle damage occurred for the three tested values of ~~$RDi_{weakness}$~~$i_{rd\ susceptibility}$ (permissive, reference, restrictive) at a 10% windthrow damage rate (Fig. 5, ~~4th row, 2nd column~~panel h). However, employing a step function (~~$S_{weakness} > -100$~~$S_{susceptibilty} = -500.0$) led to either sporadic peaks of bark beetle damage with a permissive ~~$RDi_{weakness}$~~$i_{rd\ susceptibility}$ or a two-year outbreak with a maximum damage rate of 60% with a restrictive ~~$RDi_{weakness}$~~$i_{rd\ susceptibility}$ (Fig. 5, ~~4th row, 2nd column~~panel h), neither of which aligns with the observations summarized in Table 3.

The ~~most favorable outcome~~closest outcome to observation from table 3 was obtained with a logistic relationship (~~$-1 < S_{weakness} << -100$), where $RDi_{weakness}$ dictated~~$S_{susceptibility} = -5.0$), where $i_{rd\ susceptibility}$ determined the duration of the outbreak: 11, 16, and 25 years for restrictive, reference, and permissive parameter values, respectively (Fig. 5, ~~4th row, 2nd column~~ panel h). Either the restrictive or reference parameter value could be utilized since a range of 11-16 years aligns with the observations (Table 3). To examine ~~false positives~~the occurrence of improbable outbreaks, sensitivity tests were repeated for a 0.1% windthrow damage rate. None of the nine parameter combinations triggered an outbreak (Fig. 5, ~~4th row, 1st column~~ panel g), suggesting that ~~false positives~~ improbable outbreaks due to the calculation of i_{hosts} ~~$_{weakness}$ are improbable.~~

~~The feedback effect~~$_{susceptibility}$ are unlikely.

From the calculation of the credibility score, only one set obtains a score of 4 ($S_{susceptibility} = -5.0$, $i_{rd\ susceptibility}$=0.55, Table s1). The concerning parameters value has been selected and reported in table 4.

The effect of the capability of bark beetle to mass attack ~~capability~~ ($i_{beetles\ mass\ attack}$) when the ~~bark beetle~~ population ~~reaches~~exceeds a ~~certain~~ threshold was evaluated by varying $\boldsymbol{S_{mass\ attack}}$ and $\boldsymbol{BP_{limit}}$ (Eq. 14). Linear relationships ($S_{mass\ attack}$ = ~~-1~~1.0) resulted in similar outbreak dynamics for all $\boldsymbol{BP_{limit}}$ values, with the model settling on a constant endemic damage ~~post-~~following an outbreak, though higher than observed (Table 3, Fig. 5, panel f). Introducing a logistic or step function ~~minimally~~slightly altered outbreak dynamics except when assuming a step function for the restrictive value, which prevented an ~~outbreak.Repeating~~outbreak. Repeating sensitivity tests for a 0.1% windthrow damage rate showed that assuming linear or logistic relationships could trigger an outbreak (Fig. 5, ~~3th row, 1st column~~panel e), indicating that ~~false positives~~improbable outbreaks may arise from the calculation of $i_{hosts\ mass\ attack}$.

From the calculation of the credibility score, three sets obtain a score of 4 but only set 4.6 was chosen because of its intermediate position compared to sets 4.9 and 4.5 (Table s1). The concerning parameter values ($S_{mass\ attack}$ = *-30.0*, BP_{limit}*=0.06*) have been selected and reported in table 4.

The impact of bark beetle activities from the previous year (***$i_{beetles\ activity}$***) on outbreak dynamics was investigated by varying ***$S_{activity}$*** and ***act_{limit}*** (Eq. 10). Linear or logistic relationships resulted in ~~overly prolonged~~excessively long outbreaks (>30 years) compared to observations (Table 3, ~~1st row, 2nd column~~panel b), whereas assuming a step-function relationship simulated a decline in the outbreak after 14 years. Sensitivity tests repeated for a 0.1% windthrow damage rate showed that assuming a linear relationship could trigger an improbable outbreak (Fig. 5, ~~1st row, 1st column), suggesting potential false positives from the calculation of $i_{beetles\ activity}$~~panel a) through the calculation of $i_{beetles\ activity}$.

From the calculation of the credibility score, only one set obtains a score of 4 ($S_{activity}$ *= -500.0*, act_{limit}*=0.12*, Table s1). The concerning parameters value has been selected and reported in table 4.

To explore the effect of the numbers of generation ($i_{beetles\ generation}$) on the outbreak dynamics, ***$S_{generation}$*** and ***G_{limit}*** from equation 9 were varied. Bark beetle damage rate was more sensitive to ***G_{limit}*** than ***$S_{generation}$***, but only a linear relationship with the reference ***G_{limit}*** = 1.0 yielded an intermediate outbreak intensity consistent with the ~~location (~~continental climate at the test location (i.e., THA, Fig. 5, panel d). Other combinations resulted in either too strong or no peak during the outbreak. Repeating sensitivity tests for a 0.1% windthrow damage rate showed that none of the nine parameter combinations triggered an outbreak (Fig. 5 ~~2nd row, 1st column~~panel c), indicating that ~~false positives~~improbable outbreaks from the calculation of ***$i_{beetles\ generation}$*** are unlikely.

From the calculation of the credibility score, three sets obtain a score of 4 but only set 1.4 was chosen because of its intermediate position compared to sets 1.1 and 1.5 (Table s1). The concerning parameter values ($S_{generation}$ *= 1.0*, G_{limit}*=1.0*) have been selected and reported in table 4.

33

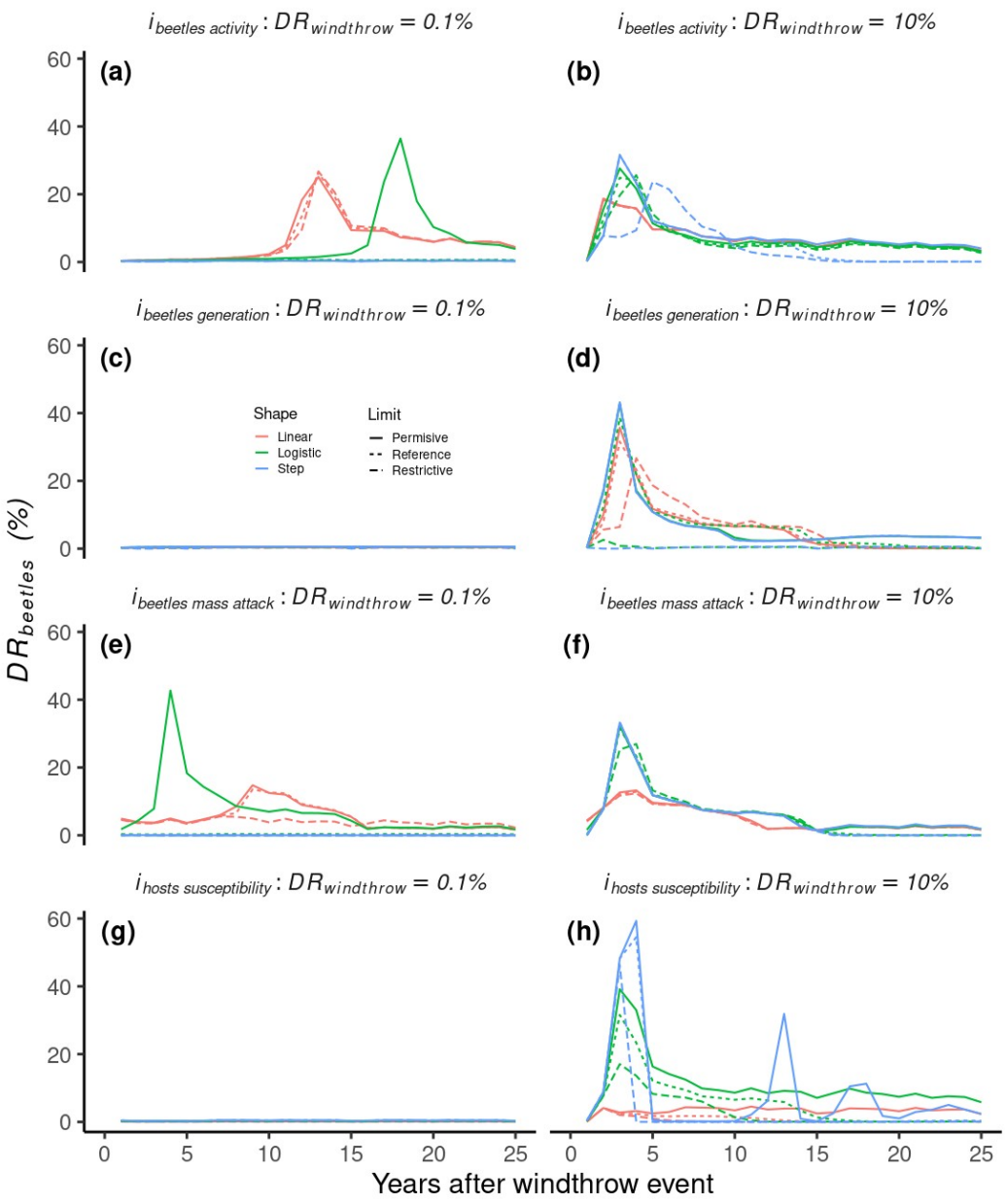
$i_{beetles\ activity} : DR_{windthrow} = 0.1\%$
$i_{beetles\ activity} : DR_{windthrow} = 10\%$
(a)
(b)
$i_{beetles\ generation} : DR_{windthrow} = 0.1\%$
$i_{beetles\ generation} : DR_{windthrow} = 10\%$
(c)
(d)
Shape
Linear
Logistic
Step
Limit
Permisive
Reference
Restrictive
$i_{beetles\ mass\ attack} : DR_{windthrow} = 0.1\%$
$i_{beetles\ mass\ attack} : DR_{windthrow} = 10\%$
(e)
(f)
$i_{hosts\ susceptibility} : DR_{windthrow} = 0.1\%$
$i_{hosts\ susceptibility} : DR_{windthrow} = 10\%$
(g)
(h)
$DR_{beetles}$ (%)
0
20
40
60
0
5
10
15
20
25
Years after windthrow event

34

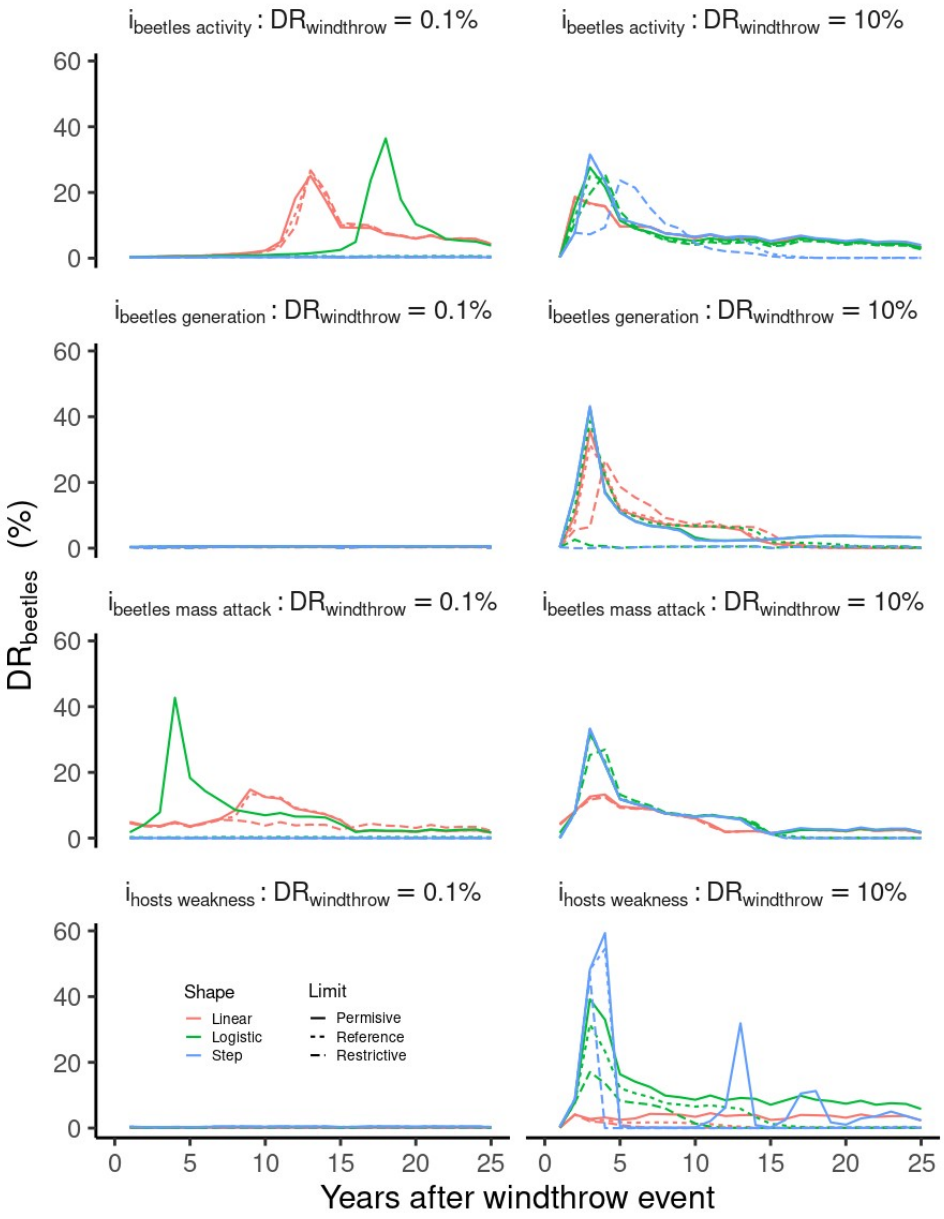

Figure 5: Simulation results from the sensitivity experiment at the THA site. Eight parameters from four equations were evaluated. Each equation represents an index from the bark beetle outbreak ~~module~~model (*$i_{hosts\ ~~weakness~~susceptibility}$* *$i_{hosts\ mass\ attack}$*, *$i_{beetles\ activity}$*, *$i_{beetles\ generation}$*). Each index is represented by a logistic function defined by a shape parameter (~~S~~*Shape*) and a limit parameter (~~L~~*Limit)*. Three values were chosen for each parameter resulting in 9 pairs of parameters for each index. Colored lines represent the shape parameter varying from linear : ~~S~~*Shape* = ~~-1, logistic -1< S < -100, to step function where S < -100~~1.0 (red), logistic -5.0 < *Shape* < -30.0 (green), to step function where *Shape* = -500.0 (blue). Line type represents three different values for ~~L~~*Limit* parameters where references (dashed line) are values of ~~RDi~~$_{~~weakness~~}$*$i_{rd\ susceptibility}$*, *BP_{limt}*, *act_{limit}* and *G_{limit}* (given in ~~Table~~table 4), whereas permissive ~~and restrictive représent~~(full line) and restrictive (dashed dotted) represent a 50% decrease or increase respectively.

35

4.2. Model tuning

By comparing the outcomes of the sensitivity tests (section 4.1) to a ~~summary~~compilation of observations (Table 3), a first estimate ~~of the values of~~for several parameters was proposed (Table 4).

~~**Table 4: Parameters values from the bark beetle module tested in the sensitivity analysis. Values labeled with (*) correspond to the parameters adjusted following the sensitivity analysis results.**~~

~~Parameter~~	~~Source~~	~~Value~~
~~$S_{generation}$~~	~~This study: from SA (see 3.1.4)~~	~~-1.0 (*)~~
~~G_{limit}~~	~~Adapted from Temperli et al. 2013~~	~~1.0 (*)~~
~~DD_{ref}~~	~~Adapted from Temperli et al. 2013~~	~~547.0~~
~~$S_{drought}$~~	~~Adapted from Temperli et al. 2013~~	~~-9.5~~
~~PWS_{limit}~~	~~Adapted from Temperli et al. 2013~~	~~0.4~~
~~max_{Nwood}~~	~~This study: scale dependent (see 2.4.2)~~	~~0.2~~
~~$S_{activity}$~~	~~This study: from SA (see 3.1.3)~~	~~-500 (*)~~
~~act_{limit}~~	~~This study: from SA (see 3.1.3)~~	~~0.06 (*)~~
~~$S_{weakness}$~~	~~This study: from SA (see 3.1.1)~~	~~-5.0 (*)~~
~~$RDi_{weakness}$~~	~~This study: from SA (see 3.1.1)~~	~~0.55 (*)~~
~~RDi_{limit}~~	~~This study: scale dependent (see 2.4.1)~~	~~0.4~~
~~$S_{mass\ attack}$~~	~~This study: From SA (see 3.1.2)~~	~~-30.0 (*)~~
~~BP_{limit}~~	~~This study: scale dependent (see 3.1.2)~~	~~0.12 (*)~~
~~S_{share}~~	~~This study: not used (see 2.5)~~	~~15.5~~
~~SH_{limit}~~	~~This study: not used (see 2.5)~~	~~0.6~~

Table 4: Parameter values from the bark beetle model based on the score obtained in the sensitivity analysis. (*) parameter values deliberately fixed and excluded from the sensitivity analysis (section 3.3 for justification).

Parameter	Source	Chosen parameters
$S_{generation}$	This study: from SA (see 3.1.4)	-1.0
G_{limit}	Adapted from Temperli et al. 2013	1.0
DD_{ref}	Adapted from Temperli et al. 2013	547.0 (*)
$S_{drought}$	Adapted from Temperli et al. 2013	-9.5 (*)
PWS_{limit}	Adapted from Temperli et al. 2013	0.4 (*)
max_{Nwood}	This study: scale dependent (see 2.4.2)	0.2 (*)
$S_{activity}$	This study: from SA (see 3.1.3)	-500.0
act_{limit}	This study: from SA (see 3.1.3)	0.06
$S_{susceptibility}$	This study: from SA (see 3.1.1)	-20.0
$i_{rd\ susceptibility}$	This study: from SA (see 3.1.1)	0.55
$S_{competition}$	This study: from SA (see 3.1.1)	-5.0 (*)
$i_{rd\ limit}$	This study: scale dependent (see 2.4.1)	0.4 (*)
$S_{mass\ attack}$	This study: From SA (see 3.1.2)	-30.0
BP_{limit}	This study: scale dependent (see 3.1.2)	0.12
S_{share}	This study: not used (see 2.5)	15.5 (*)
SH_{limit}	This study: not used (see 2.5)	0.6 (*)

4.3. Impact of climate and windthrow on bark beetle damage

In ORCHIDEE, the ~~hottest~~warmest sites, HES and WET, experienced significant bark beetle outbreaks across a wide spectrum of windthrow mortality rates, whereas colder sites like REN and THA saw outbreaks only in response to the most severe windthrow events (Fig. 6, panel b, c). A greater average number of bark beetle generations in the years following windthrow events led to higher bark beetle damage rates at the peak of outbreaks. For instance, at a 35% windthrow mortality rate, HES reached a maximum bark beetle damage rate of 50%, whereas REN's maximum was 22% (Fig. 6 panel a, b).

Interestingly, high ~~windthrow~~tree mortality rates from windthrow could also lead to delays and lower maximum $DR_{beetles}$ (Fig. 6). For instance, at the HES site, 10%, 20%, and 35% windthrow damage rates triggered maximum $DR_{beetles}$ of 50%, 43%, and 37%, respectively (Fig. 6 panel a). Conversely, low $DR_{windthrow}$, like 5% at WET, delayed the peak of bark beetle outbreaks by 9 years (Fig. 6, panel d). Additionally, the model simulated a post-epidemic stage during which the outbreak damage rate remained relatively low (<10%) and lasted between 3 to 10 years (Fig. 6). Overall, the simulated outbreaks lasted between 11 to 20 years, consistent with field observations (Table 3).

37

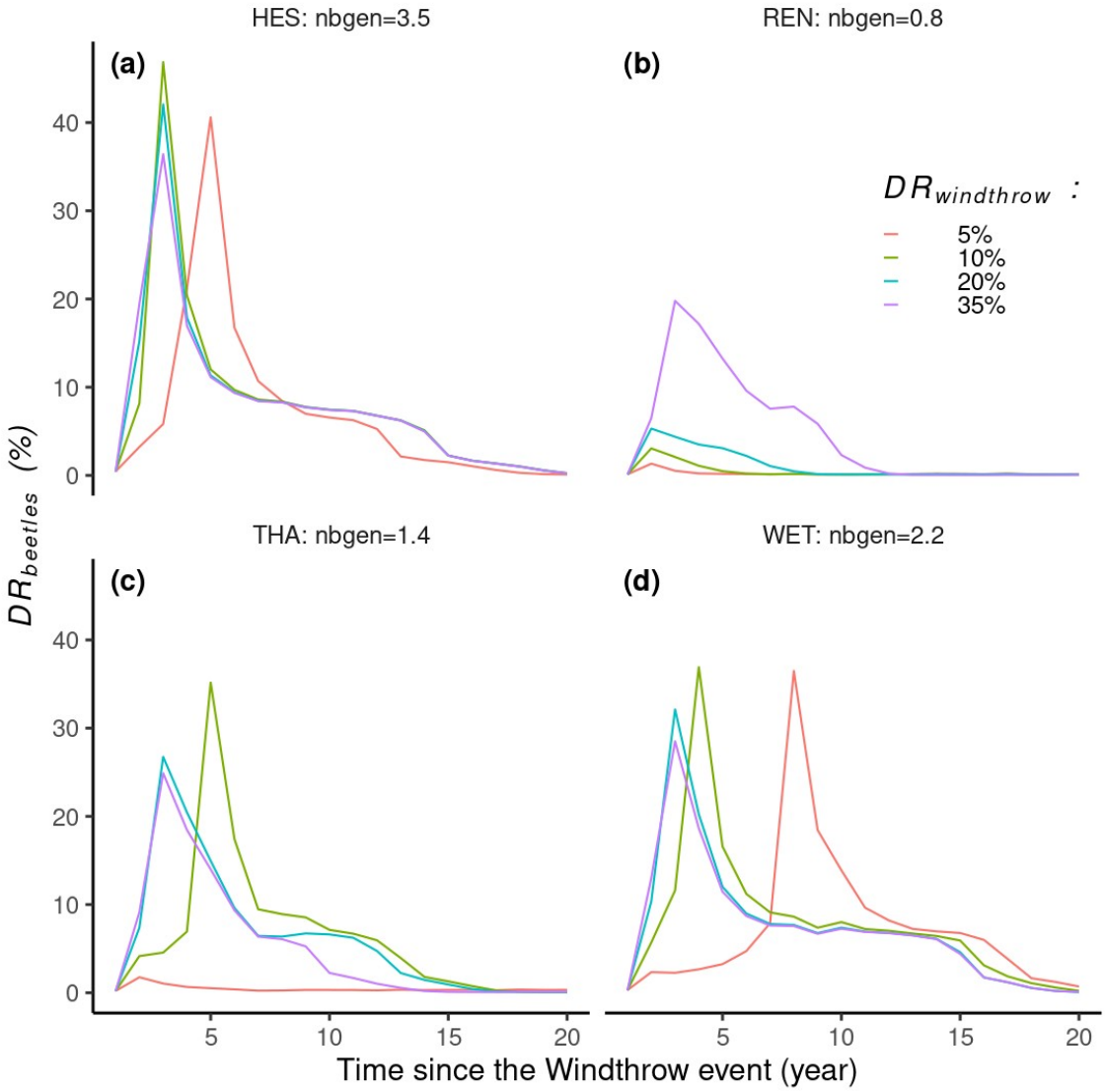
HES: nbgen=3.5
REN: nbgen=0.8
THA: nbgen=1.4
WET: nbgen=2.2
(a)
(b)
(c)
(d)
$DR_{windthrow}$:
5%
10%
20%
35%
$DR_{beetles}$ (%)
0
10
20
30
40
5
10
15
20
Time since the Windthrow event (year)

38

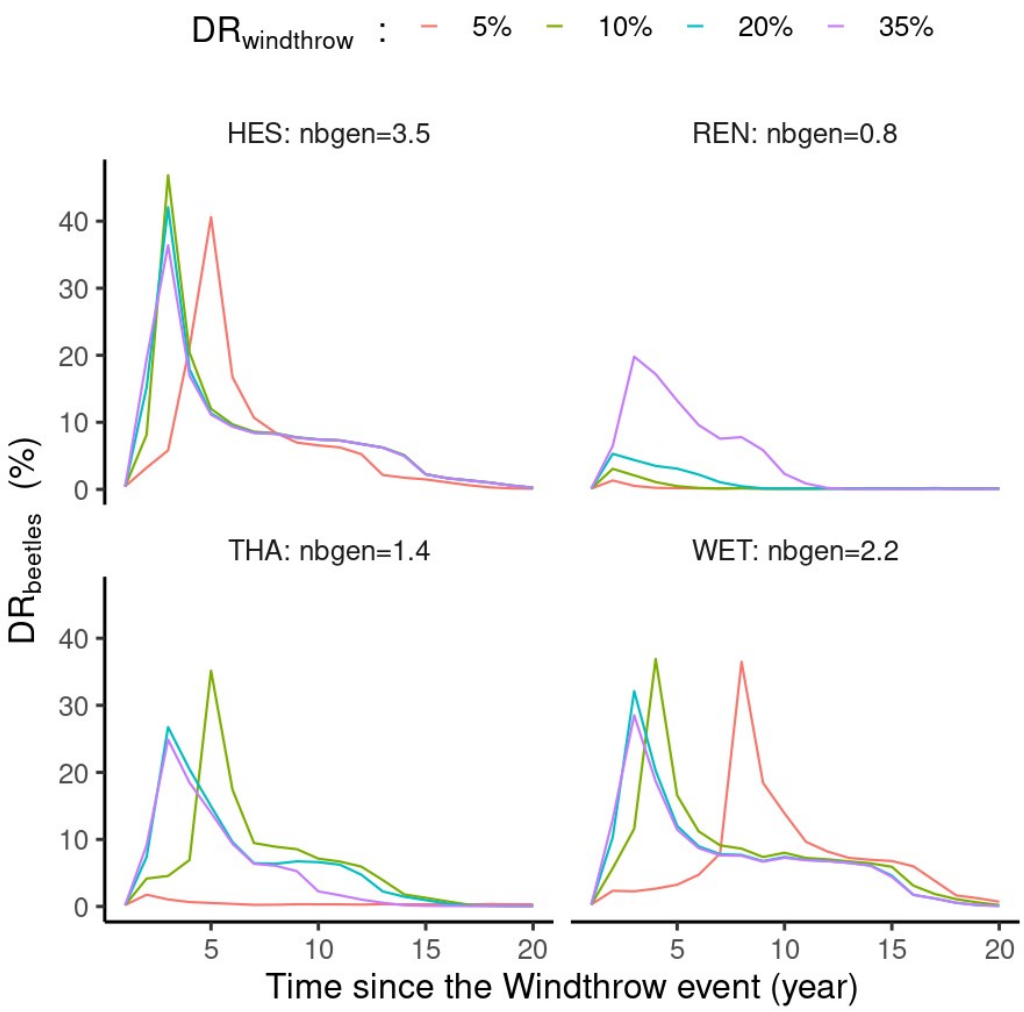

Figure 6: Simulation results of ~~24~~16 simulations (4 ~~sites~~locations x 4 windthrow damage ~~rate~~rates $DR_{windthrow}$). Lines represent the annual bark beetle damage rate as a fraction of the total biomass ($DR_{beetles}$). *Nbgen* is the average number of bark beetle generations during five years after the windthrow event. $DR_{windthrow}$ represents the percentage of biomass loss by a windthrow event at the start of the simulation.

At the coldest site, HYY, ORCHIDEE ~~predicted~~simulated only a small number of bark beetle generations, preventing outbreaks from occurring. This observation validates the initial parameter tuning (Table 4), indicating that it is robust enough to prevent ~~false positives~~improbable outbreaks, such as the model triggering outbreaks in sites where bark beetles cannot reproduce.

4.4. Impact of climate and windthrow on stand biomass and Net Primary Production

~~With the exception of REN, all sites experience a decrease in total biomass until around 9.000 gC.m^{-2} by the end of the outbreak, which typically lasted 10 to 20 years (Fig. 7). It is noteworthy that regardless of the severity of maximum damage inflicted by bark beetles, the overall cumulative damage consistently results in the same amount of biomass loss (Fig. 7). This characteristic is a key objective of the bark beetle module. Essentially, the model can~~

39

~~simulate significant epidemic events even if the initial trigger, such as the windthrow event in our study, is not particularly intense. Once a tipping point is reached, at~~All locations experienced a 10 to 20 years decrease in total biomass until at most 9 $kgC.m^{-2}$ at which time the outbreak ended (Fig. 7, panel a, b, c, d). The model can simulate significant epidemic events even if the initial trigger, such as the windthrow event in our study, is not particularly intense. Once the bark beetles can mass attack living trees, the bark beetle population ($i_{beetles\ pressure}$) will increase and kill more and more trees until so many trees are killed that the stand density of the remaining living trees drops below the threshold of $i_{rd\ spruce} = i_{rd\ limit} = 0.4$. In ORCHIDEE, an $i_{rd\ limit} = 0.4$ for spruce forest corresponds to a biomass ~~level~~ of ~~9.000 $gC.m^{-2}$ or $RDi_{limit} = 0.4$, there's no turning back until that threshold is passed. Interestingly, at the REN site where the number of generations is approximately one, the outbreak only reaches the tipping point with a high windthrow damage rate (35%)~~around 9 $kgC.m^{-2}$ which in ORCHIDEE is too low to maintain an epidemic population of bark beetles at the 2500 km2 grid cell. Interestingly, for the climate observed at REN where the number of generations is approximately one, the bark beetle population can only become epidemic t following an intense windthrow event with a 35% damage rate (Fig. 7).

Throughout the outbreak period, there was a notable decrease in ~~Net Primary Productivity (NPP), as illustrated in the second panel in Fig. 7, primarily attributed to a sharp decline in leaf area index, although not explicitly depicted. Subsequent to the epidemic phase, the forest undergoes recovery by regenerating its leaf area index. Consequently, individual leaf area indices tend to escalate to attain the overall stand leaf area index, concurrently boosting individual growth rates~~net primary production (*NPP*)(Fig. 7). This decrease is primarily attributed to a sharp decline in leaf area index (not shown). Following the epidemic phase, the leaf area recovers. Following the outbreak~~,~~; the reduction in stand tree density due to bark beetle damage ~~mitigates~~decreases autotrophic respiration~~, albeit not displayed, and fosters recruitment, also not depicted, thereby augmenting~~ (not shown) and the sparser canopy allows more light to reach the forest floor where it fosters recruitment (not shown), resulting a higher ***NPP*** or forest growth (Fig. 7). Consequently, carbon use efficiency tends to be higher in sparsely populated stands compared to densely populated ones.

40

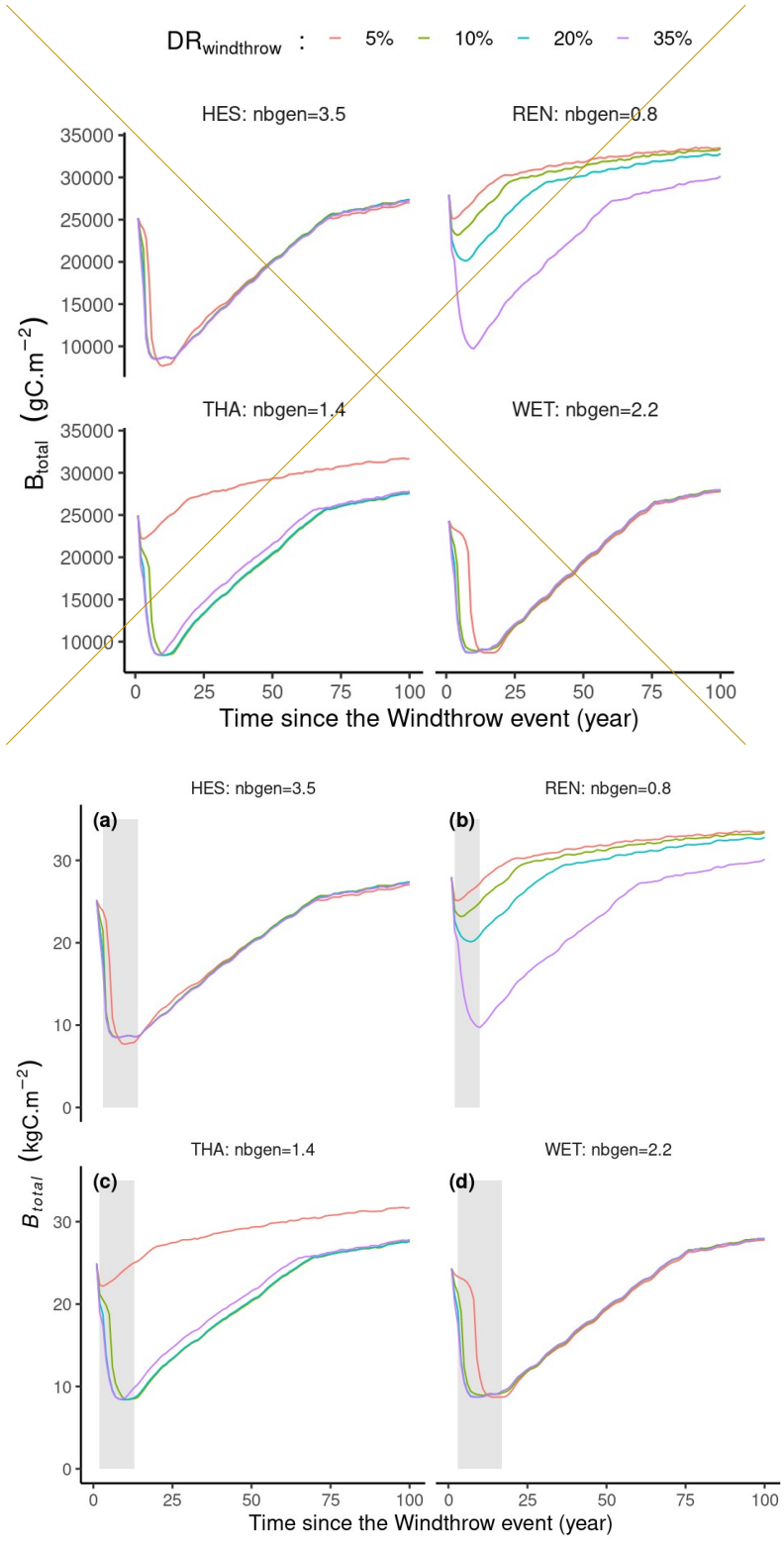
DR windthrow : 5% 10% 20% 35%
HES: nbgen=3.5
REN: nbgen=0.8
THA: nbgen=1.4
WET: nbgen=2.2
B total (gC.m−2)
Time since the Windthrow event (year)
(a)
(b)
(c)
(d)
B total (kgC.m−2)

41

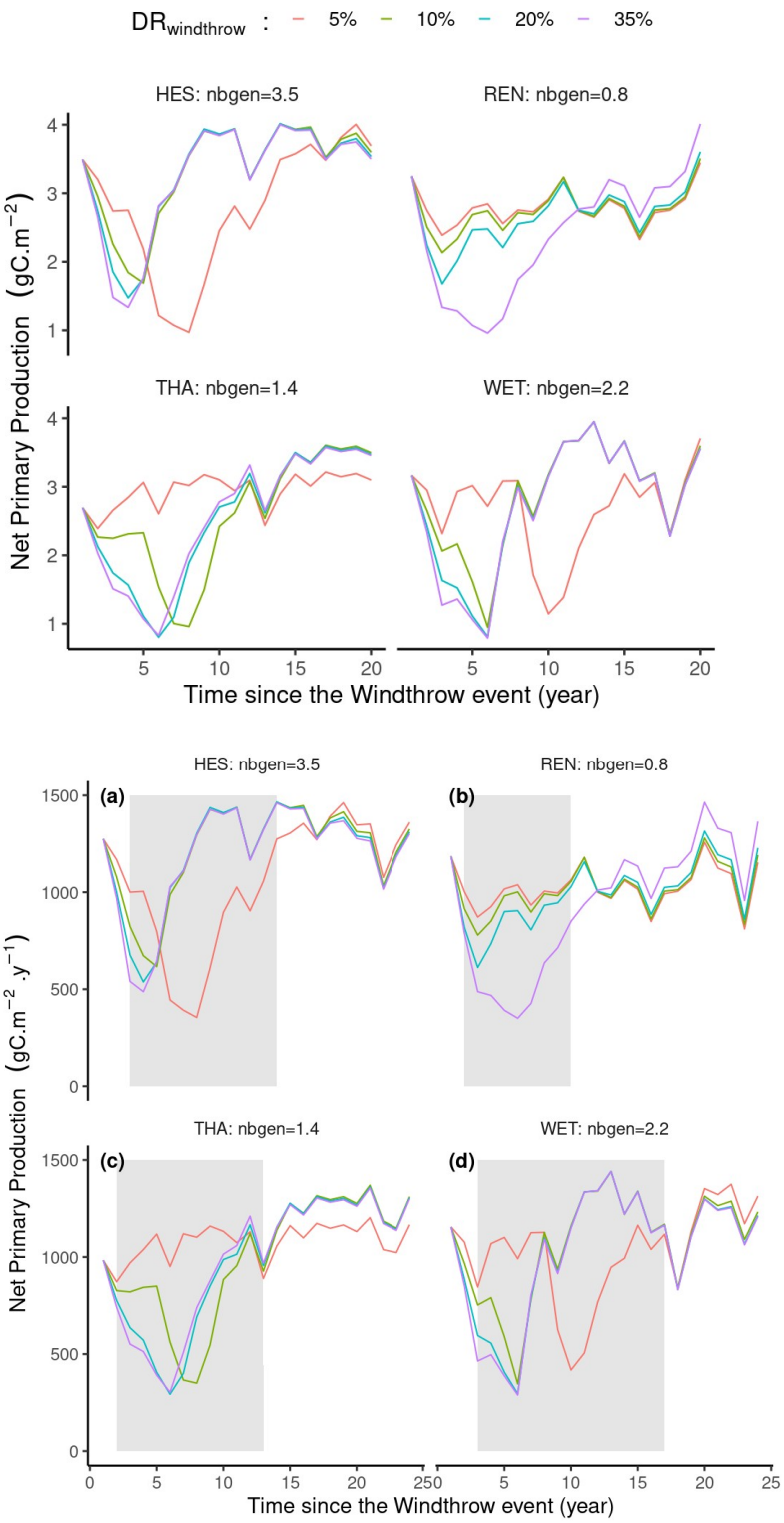

Figure 7: Simulation results of ~~24~~16 simulations (4 sites x 4 windthrow mortality rate). Lines represent the annual average net primary production (NPP) in gC.m^{-2}.y^{-1} or ~~Total~~total stand biomass (B_{total}) in ~~gC.m~~kgC.m^{-2}. *Nbgen* is the average number of ~~achieved~~ bark beetle generations during the five

42

years after the windthrow event. $DR_{windthrow}$ represents the percentage of biomass loss by a windthrow event at the start of the simulation. Grey areas represent the epidemic phase.

841

842 **4.5. Continuous vs. abrupt mortality**

843

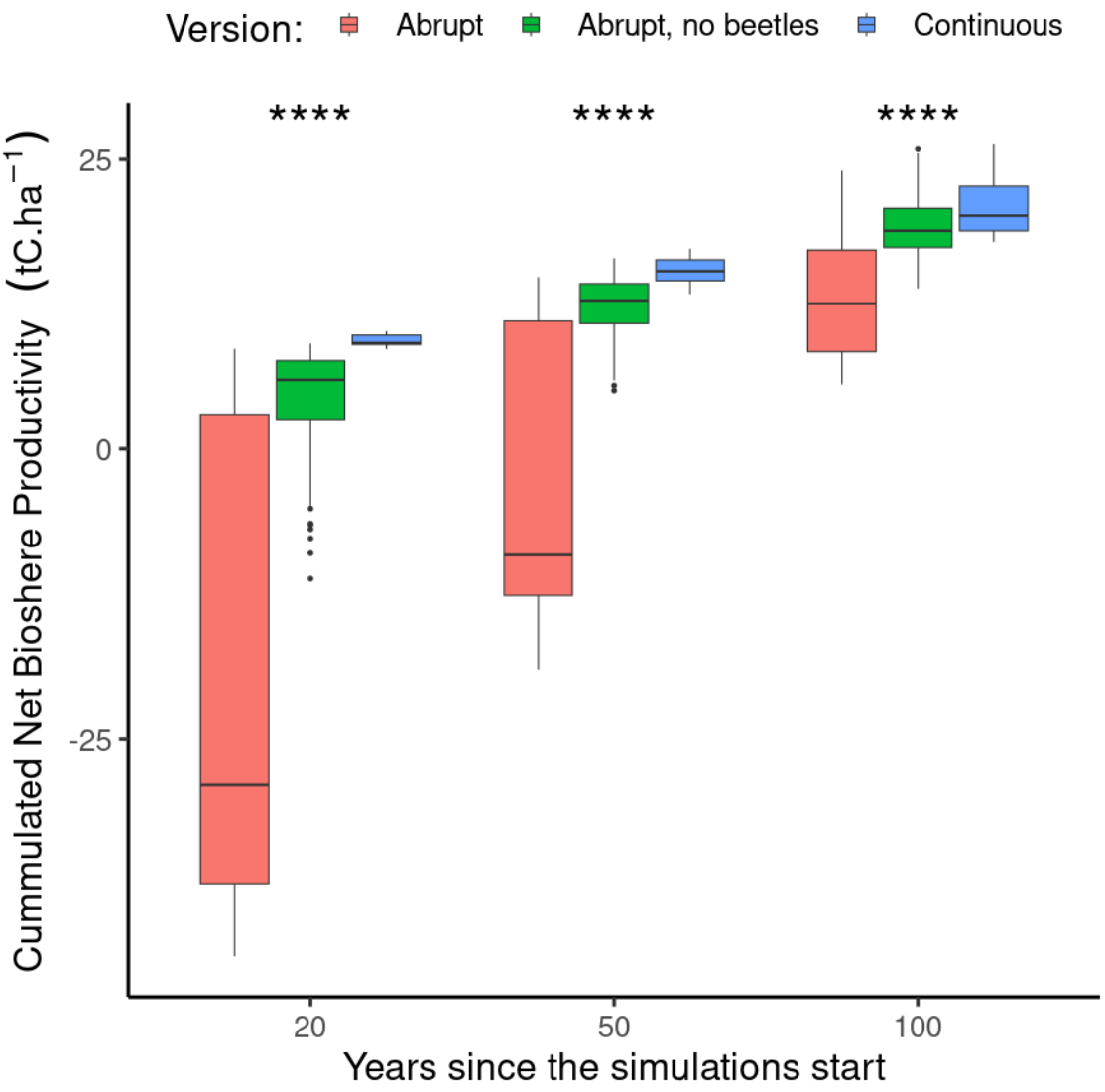

43

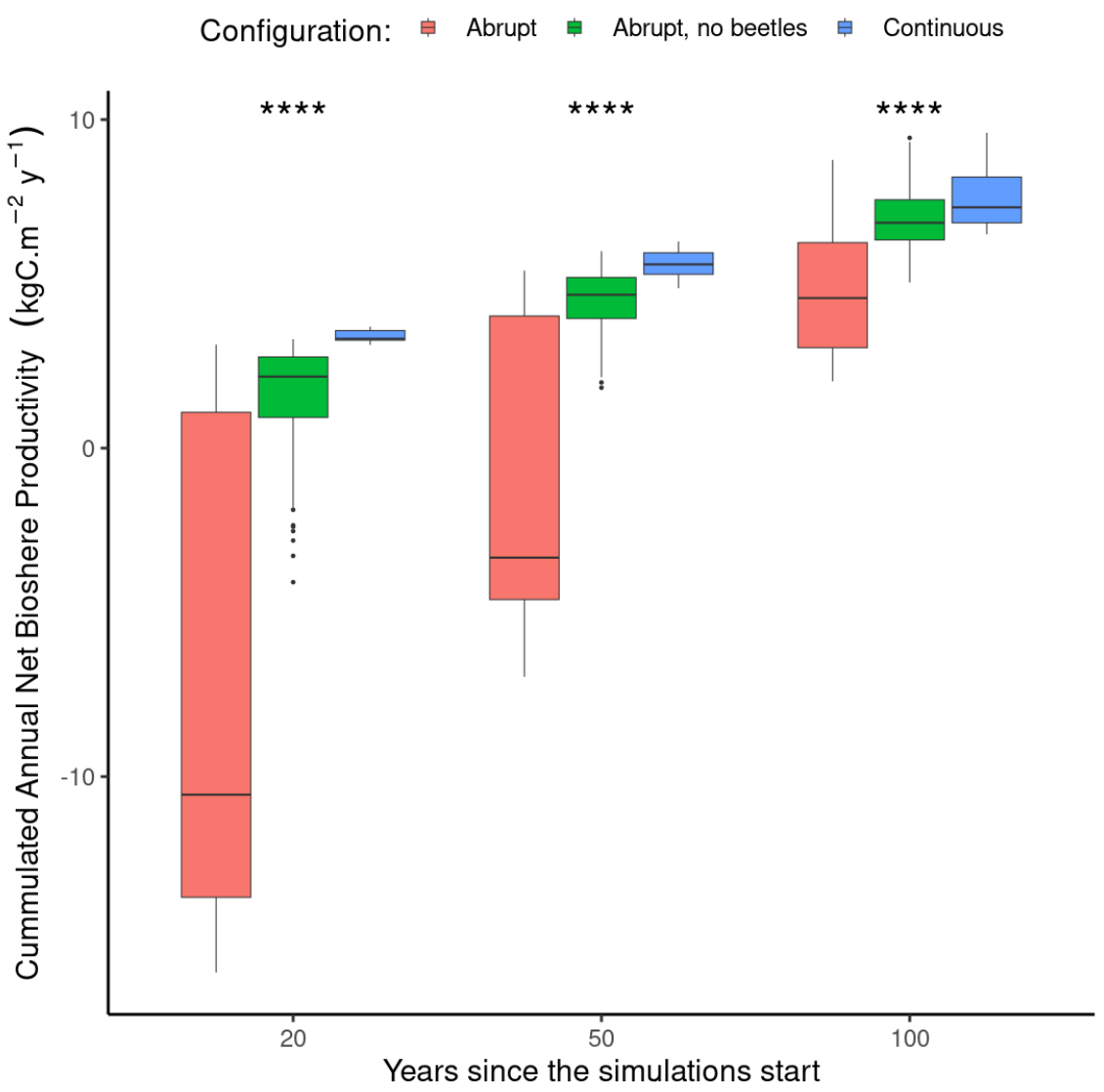

Figure 8: Difference in cumulative net biome production at three discrete time horizons (i.e. 20, 50 and 100 years) between a ~~continuous~~fixed continuous mortality rate (blue, n=8), abrupt ~~(red, n=56), abrupt with no~~tree mortality from a windstorm and the subsequent bark beetle outbreak (red, n=56), abrupt mortality from a windstorm not followed by a bark beetles outbreak (green, n=56) ~~mortality framework~~. Note that in the continuous mortality ~~framework~~configuration the mortality rate was adjusted to obtain a similar number of trees killed after 100 years as in the abrupt mortality ~~framework~~configuration. The variation of each boxplot arises due to different locations and prescribed storm intensities. Each boxplot displays the median value (thick horizontal line), the quartile range (box border), and the 95% confidence interval (vertical line). A Wilcoxon test between the three ~~versions~~configurations at each time horizon ~~has been carried out. When the p-value<0001 four stars are plotted above the boxes~~showed significant differences (p-value<0001) denoted by the four stars.

44

The total accumulated net biome production (***NBP***) was evaluated using the ORCHIDEE model across three different timeframes: 20, 50, and 100 years. At the 20-years mark, the average accumulated ***NBP*** notably differed between the ~~continuous, abrupt~~‘continuous’, ‘abrupt’ and the abrupt without bark beetles outbreak (~~abrupt, ~~‘no beetles’) mortality ~~frameworks: -19.5±2.7 tC.ha^{-1}, -3.7±0.7 tC.ha^{-1} and 9.3±0.2 tC.ha~~configurations: -7.12±0.97, -1.37±0.28 and 3.39±0.74 kgC.m^{-2}.y^{-1} for the ~~abrupt , abrupt~~‘abrupt’, ‘no beetles’ and ~~continuous~~‘continuous’ mortality ~~frameworks~~configurations, respectively. These differences were statistically significant (Wilcoxon, p-value<0001), indicating a substantial initial reduction in ***NBP*** with the ~~'Abrupt' models~~‘abrupt’ configurations, as ecosystems behaved as carbon sources, whereas under the ~~'Continuous' model~~‘continuous’ configuration, they acted as carbon sinks (Fig. 8). The variability in ***NBP*** demonstrated the broad temperature gradient in Europe and indicated that despite many locations potentially acting as sources under the '~~Abrupt' framework~~abrupt' configuration, some may transition to carbon sinks within the first 20 years following a disturbance.

Moving to the 50-years horizon, the difference between the three frameworks decreased, with net biome productions of ~~-3.8±1.6, 11.7±0.4 and 14.9±0.5 tC.ha~~0.81±0.60, 4.43±0.15 and 5.61±0.18 kgC.m^{-2}.y^{-1} for the ~~abrupt, abrupt,~~ ‘abrupt’, ‘no beetles’ and ~~continuous~~‘continuous’ mortality ~~frameworks~~configuration, respectively. The difference in sink strength ~~difference~~ remained statistically significant (Wilcoxon, p-value<0.001), with the ***NBP*** in the ~~'Abrupt' framework~~‘abrupt’ configuration approaching carbon neutrality while without the consecutive bark beetles outbreak the ecosystems already ~~become~~became a ~~sink of carbon. The variability of responses depending on climatic conditions persisted~~carbon sink. The climate conditions had a lasting effect on the responses, with the ~~'Abrupt' framework~~‘abrupt’ configuration showing a greater range in responses compared to the ~~'Continuous' one. Some locations transitioned from carbon sources to carbon sinks under the 'Continuous' framework, indicating a more resilient and gradual recovery in ecosystem productivity (Fig. 8)~~‘continuous’ one.

At the 100-years mark, the average ~~accumulated~~cumulative ***NBP*** for the '~~Abrupts~~abrupts' and '~~Continuous' frameworks became much closer (Wilcoxon, p-value<0.001), with values of 12.6±0.7, 18.9±0.5 and 19.9±1.2 tC.ha^{-1}, respectively (Fig. 8). The data showed a return to~~continuous' configurations approached each other with values of 4.85±0.26, 7.09±0.17 and 7.73±0.40 kgC.m^{-2}.y^{-1}, respectively (Fig. 8) but were still significantly different (Wilcoxon, p-value<0.001). ORCHIDEE simulated a return to a carbon sink (indicated by positive ~~Cumulative~~cumulative ***NBP*** values~~,~~) suggesting a long-term recovery and potential return to pre-disturbance productivity levels within ~~the~~a century following the windthrow ~~events~~and beetle outbreak event. The 'continuous' ~~model version~~configuration displayed a consistently higher median value, suggesting ~~a more resilient recovery over~~weaker impact of tree mortality dynamics on the long term carbon cycle.

5. Discussion

5.1. Simulating the dynamics of bark beetle outbreaks and their interaction with windthrow

Our ~~Bark beetle~~*Ips typographus* outbreak model ~~formulation~~ has demonstrated its capability to simulate a broad range of disturbance dynamics. The variation in the outbreak dynamics and the response of the outbreak to its main

45

drivers (Fig. 5 & 6) give confidence in the ability of ORCHIDEE to simulate various outbreak scenarios observed across the temperate and boreal zones under changing climate conditions.

Windthrow events have significant ecological ~~meaning~~impact because such disturbances offer fresh breeding substrates, which in turn increase bark beetle populations (Lausch et al., 2011). Our ~~modeling~~model results align with these findings, indicating that windthrows causing damage of 5% or more may trigger beetle outbreaks (Fig. 6). Additionally, ~~ Wermelinger (2004) reported~~ a strong increase in bark beetle populations ~~post-windthrow, a pattern that our ORCHIDEE simulations also reflect~~has been observed following a windthrow event (Wermelinger, 2004), a pattern reflected in the ORCHIDEE simulations. The model ~~pinpoints~~simulates a buildup stage~~—~~ spanning 1 to 9 years, where bark beetle numbers increase prior to peaking, with the duration influenced by the severity of the windthrow and the prevailing climate (Fig. 6).

Temperature is another critical factor affecting bark beetle life cycles. ~~Studies by Benz et al. (2005) have highlighted how intra~~Intra- and interannual variation in temperature impact bark beetles, with warmer conditions fostering multiple generations per year, whereas cooler, damp climates slow breeding and survival rates (Benz et al., 2005). In line with these findings, ~~ORCHIDEE's temperature-dependent simulations show variations in bark beetle impacts across different sites;~~the temperature dependence of the ORCHIDEE simulations show that cold winters at locations such as SOR and REN reduced bark beetle activity compared to warmer ~~sites~~locations like THA and WET (Fig. 6). Lieutier et al. (2004) documented that ~~significant bark beetle numbers can trigger mass attacks on~~if the population is large enough, bark beetles can mass attack healthy trees. Our model incorporates this dynamic, illustrated by epidemic stages where living trees become viable hosts, which then exacerbates the growth of the beetle population (Fig. 1).

The aftermath of a windthrow and subsequent bark beetle ~~infestations~~outbreak also affects the forest carbon and nitrogen cycles. This impact is observed in the form of snags~~—~~ which are standing dead trees that undergo decomposition. ~~As Rhoades, (2019) observed, this can~~Snags can temporarily disrupt the link between soil and ecosystem carbon and nitrogen dynamics~~, a point echoed by (~~ (Rhoades, 2019; ~~Custer et al., 2020)~~Custer et al., 2020). While ~~ORCHIDEE models~~in ORCHIDEE, the decay of fallen logs~~, it~~ does not account for snags~~. Nevertheless~~ yet, the model suggests a recovery period ranging from 5 to 15 years, contingent upon the intensity of the bark beetle outbreak (Fig. 7). As snags create gaps in the canopy, conditions favorable to natural forest regeneration emerge~~, corroborating the affirmation of Jonášová and Prach, 2004. The ORCHIDEE model forecasts an increase in tree recruitment due to the sharp reduction in stand density, allowing more sunlight to penetrate to the forest floor, thereby stimulating growth (Fig. 7)~~ (Jonášová and Prach, 2004) .

5.2. Emerging ~~property~~properties from interacting disturbances

While this study ~~hasn't provided a precise quantification of the impact of incorporating abrupt mortality versus a fixed continuous background mortality~~did not precisely quantified the impact of simulating abrupt mortality rather

than approaching mortality as a continuous process, it demonstrated that the impact of abrupt mortality ~~can vary across locations and over~~varies across location and time, i.e.~~,~~ ecosystem functions, such as carbon storage, are affected by natural ~~disasters like pest~~disturbances like *Ips typographus* outbreaks, having significant impacts on short~~-to-~~ to mid-term carbon balance estimates (Fig. 8). The simulation experiments also highlighted that the legacy effects of disturbances can endure for decades~~,~~; even for a simplified representation of forest ecosystems such as ORCHIDEE, where the recovery might be too fast due to the absence of snags (Senf et al., 2017).

The ability to simulate resistance (i.e., staying essentially unchanged despite the presence of disturbances; Grimm and Wissel, 1997) as an emerging property is evident from ~~Fig~~Figs. 6 and 7 for locations REN, where no bark beetle outbreaks were observed following a medium windthrow event (5%-20%). However, in all simulated locations that ~~couldn't~~could not resist a bark beetle outbreak, the forest was resilient ~~and ecosystem functions were restored to the level from before the windthrow. The elasticity of, e.g.,~~(i.e., returning to the reference state or dynamic after a temporary disturbance; Grimm and Wissel, 1997) and ecosystem functions were restored to the level from before the windthrow. The elasticity (the speed of return to the reference state or dynamic after a temporary disturbance; Grimm and Wissel, 1997) of the carbon sink capacity ranged from 7 to 14 years. This elasticity is in line with ~~current observational evidence from Millar and Stephenson, 2015 who found very little~~the little observational evidence of ecosystem shifts due to natural disturbances in forests~~,~~ (Millar and Stephenson, 2015). Finally, after the disturbance and the recovery of vegetation structure, the ecosystems simulated by ORCHIDEE showed persistence~~,~~ (i.e. ~~the ability to~~ continue along their initial developmental path~~. In this study we follow the definitions of Grimm and Wissel, 1997 for resistance, resilience, elasticity, and persistence~~; Grimm and Wissel, 1997).

5.3. Are cascading disturbances important for carbon balance estimates ?

The enhanced complexity introduced into the ORCHIDEE model by incorporating abrupt mortality events, as opposed to a ~~fixed-rate~~ continuous mortality, prompts the question: does this model refinement yield ~~significant~~ new insights into carbon balance estimates? Our century-long ~~timeframe~~ analysis ~~demonstrates~~demonstrated that the net biome production ~~(NBP; as defined in Chapin et al., 2006)~~, a the metric for carbon ~~balance ultimately aligns~~sequestration, ultimately converges between the continuous and abrupt mortality frameworks~~, thereby affirming the model's capacity for convergence~~ (Fig. 8). This suggests that irrespective of the nature of the mortality events, the forest ecosystem ~~exhibits~~goes through a recovery phase, marked by ~~a~~increased growth ~~boost~~ that compensates for the growth deficits ~~incurred~~ during the disturbance.

Yet, our experiment has not taken into account the frequency of disturbances. Given the profound influence of disturbance legacies on carbon dynamics, a recurrence interval shorter than the ~~forest's~~ recovery time of the forest might result in a tipping point. Such a scenario could diminish the ~~forest's~~ carbon sequestration potential ~~in the post-~~of the forest beyond 100-year ~~period~~timeframe, and in extreme cases, may even lead to ecosystem collapse~~—~~, outcomes not explored in the current simulations nor ~~reflected~~documented in ~~recent literature, such as the review by~~ the recent literature (Millar and Stephenson~~,~~ ~~(~~2015).

47

In the mid-term, spanning 20 to 50 years, the widely used continuous mortality model appears to inflate the carbon sink capabilities of forests when juxtaposed with abrupt mortality scenarios. Since policy frameworks, including the Green Deal for Europe (2023) and the Paris Agreement |~~ CCNUCC (2023), often hinged~~ (UNFCCC, 2023), upon these medium-term predictions, they would benefit from adopting model simulations that integrate abrupt mortality events to avoid an overestimation of ~~forests'~~ carbon sink capacities of forest. Furthermore, the accuracy of carbon balance estimates strongly depends upon the initial state of the forest in the model. Forest conditions markedly affect carbon uptake rates. Thus, incorporating an abrupt mortality framework into the ORCHIDEE model could substantially refine and ~~fortify~~strengthen the predictive power of our carbon balance assessments across short, medium, and long-term scales.

5.4. Shortcomings of the bark beetle outbreak model

The bark beetle outbreak ~~module~~model developed in this study builds upon the strengths of the previously established LandClim model, though it also inherited some of its limitations. One notable shortcoming is the ~~module~~model for bark beetle phenology, which is an empirical model making use of accumulated degrees-days. Since the ~~module's conception~~conception of the phenology model a decade ago, Europe's climate has undergone substantial changes, primarily manifested in warmer winters and springs (Copernicus, 2024). Because of these changes, chances have increased for two or even more bark beetle generations within a calendar year (Hlásny et al., 2021a). These changes call for an update of the beetle's phenology model to align with these more recent observations (Ogris et al., 2019).

A second limitation is that our study, ORCHIDEE, has been parameterized to simulate only ***Ips*** ~~Typographus~~*typographus* in Europe. In order to change the ~~Beetles/trees hosts ecosystem~~beetles and tree host interactions e.g. pine bark beetle in North America (***Dendroctonus monticolae Hopkins***), the sensitivity of indexes must be revised, for example, pine beetle is not breeding on the dead wood falling from withrow but very sensitive to drought ~~event~~events (Preisler et al., 2012). $i_{hosts\ defense}$, and $i_{hosts\ dead}$ as well as the phenology model will need to be revised.

Another issue is the model's consideration of drought. As outlined in the method section, drought is treated as an exacerbating factor, rather than a primary trigger as is the case for windthrow. This understanding was accurate for *Ips typographus* a decade ago (Temperli et al., 2013); however, emerging evidence increasingly suggests that drought events may indeed trigger bark beetle outbreaks across Europe (~~Netherer~~Nardi et al., ~~2015; Nardi~~2023; Netherer et al., ~~2023~~2015). Consequently, this extreme drought as a trigger should be incorporated in a future revision of ORCHIDEE's ~~bark beetle outbreak module~~*Ips typographus* outbreak model.

6. Outlook

48

This study simulated ~~how windthrow interacts with bark beetle infestations~~the one-way interaction between windthrow and *Ips typographus* outbreaks in unmanaged forests. Future research will incorporate additional interactions, such as: the interplay between droughts, storms, and bark beetles; storms, bark beetles, and fires; as well as forest management, storms, and bark beetles.

The bark beetle outbreak ~~module~~model could also be enhanced by simulating: (a) standing dead trees (or snags), which would help account for differences in wood decomposition between snags and logs (Angers et al., 2012; Storaunet et al., 2005), (b) the migration of bark beetles to neighboring locations, which becomes significant to account for in a model that operates at spatial resolutions below approximately 10 kilometers, and (c) an up-to-date beetle phenology ~~module~~model which accounts for the recent change in their behavior induced by climate change.

This research ~~provides~~provided an initial qualitative assessment of a new model feature. However, the application of the model necessitates an evaluation of the simulations against observations of cascading disturbances at the regional scale, which is the topic of an ongoing study.

7. Conclusion

Our approach enables improving the realism of the ~~bark beetle~~*Ips typographus* model in ORCHIDEE without reducing its generality (Levins, 1966). The integration of a bark beetle outbreak ~~module~~model in interaction with other natural disturbance such as windthrow into the ORCHIDEE land surface model has resulted in a broader range of disturbance dynamics and has demonstrated ~~ORCHIDEE's capacity~~the importance to simulate various disturbance interaction scenarios under different climatic conditions. Incorporating abrupt mortality events instead of a fixed continuous mortality calculation~~ ~~provided new insights into carbon balance estimates. The study showed that the continuous mortality framework, which is commonly used in the land-surface modeling community, tends to overestimate the carbon sink capacity of forests in the 20 to 50 year range in ecosystems under high disturbance pressure, compared to scenarios with abrupt mortality events.

Apart from these advances, the study revealed~~ ~~possible shortcomings in the bark beetle outbreak model including the need to update the beetle's phenology model to reflect recent climate changes, and the need to consider extreme drought as a trigger for bark beetle outbreaks in line with emerging evidence. Looking ahead, future work will further develop the capability of ORCHIDEE to simulate interacting disturbances such as the interplay between extreme droughts, storms, and bark beetles, and between storms, bark beetles, and fires.

The final step ~~would~~will be ~~to realize~~ a ~~complete~~ quantitative evaluation based on ~~observation~~observed data ~~such as produced by~~ (Marini et al., 2017) in order to assess the capability of ORCHIDEE to simulate complex interaction between multiple sources of tree mortality affecting the carbon balance at large scale.

8. Code availability

- R script and data are available at :

  https://doi.org/~~10.5281/zenodo.~~10.5281/zenodo.~~8004954 or DOI https://doi.org/10.5281/zenodo.8004954~~12806280

- ORCHIDEE rev 7791 code is also available from:

  ~~https://forge.ipsl.jussieu.fr/orchidee/browser/branches/publications/~~https://forge.ipsl.jussieu.fr/orchidee/browser/branches/publications/~~ORCHIDEE_gmd-2023-05~~ORCHIDEE_Bark_beetles_outbreak_gmd_2024

9. Data availability

- The Fluxnet climate forcing data are available at https://fluxnet.org/
- The simulation results use in this study are available at

  https://doi.org/~~10.5281/zenodo.~~10.5281/zenodo.~~8004954~~12806280

10. Author contribution

G. Marie, S. Luyssaert designed the experiments and G. Marie conducted them. Following discussions with H. Jactel, G. Petter and M. Cailleret, G. Marie developed the bark beetles model code and performed the simulations. J. Jeong integrated the wind damage and bark beetle ~~modules~~models with each other. G. Marie, J. Jeong, V. Bastrikov, J. Ghattas, B. Guenet, A.S. Lansø, M.J. McGrath, K. Naudts, A. Valade, C. Yue, and S. Luyssaert, contributed to the development, parameterization and evaluation of the ORCHIDEE revision used in this study. G. Marie, J. Jeong, and S. Luyssaert prepared the manuscript with contributions from all co-authors.

11. Competing interests

No competing interest

12. Acknowledgements

GM was funded by MSCF (CLIMPRO) and ADEME (DIPROG). SL and KN were funded by Horizon 2020, HoliSoils (SEP-210673589) and Horizon Europe INFORMA (101060309). JJ ~~was funded by Horizon 2020, HoliSoils (SEP-210673589). BG was~~and BG were funded by Horizon 2020, HoliSoils (SEP-210673589). GP acknowledges funding by the Swiss National Science Foundation (SNF 163250). ASL was funded by Horizon 2020, Crescendo (641816). C.Y. was funded by the National Science Foundation of China (U20A2090 and 41971132). MJM was supported by the European Commission, Horizon 2020 Framework Programme (VERIFY, grant no. 776810) and the European Union's Horizon 2020 research and innovation programme under Grant Agreement No. 958927 (CoCO2). AV acknowledges funding by Agropolis Fondation (2101-048). This work was performed using HPC resources from GENCI-TGCC (Grant 2022-06328). The Textual AI - Open AI GPT4 (https://chat.openai.com/) has been used for language editing at an early stage of manuscript preparation.

13. References

Abramowitz, G., Leuning, R., Clark, M., and Pitman, A.: Evaluating the Performance of Land Surface Models, J. Clim., 21, 5468–5481, https://doi.org/10.1175/2008JCLI2378.1, 2008.
Allen, C. D., Breshears, D. D., and McDowell, N. G.: On underestimation of global vulnerability to tree mortality and forest die-off from hotter drought in the Anthropocene, Ecosphere, 6, art129, https://doi.org/10.1890/ES15-00203.1, 2015.
Andrus, R. A., Hart, S. J., and Veblen, T. T.: Forest recovery following synchronous outbreaks of spruce and western balsam bark beetle is slowed by ungulate browsing, Ecology, 101, e02998, https://doi.org/10.1002/ecy.2998, 2020.
Angers, V. A., Drapeau, P., and Bergeron, Y.: Mineralization rates and factors influencing snag decay in four North American boreal tree species, Can. J. For. Res., 42, 157–166, https://doi.org/10.1139/x11-167, 2012.
European State of the Climate | Copernicus: https://climate.copernicus.eu/ESOTC, last access: 25 March 2024.
Bakke, A.: The recent Ips typographus outbreak in Norway - experiences from a control program, Ecography, 12, 515–519, https://doi.org/10.1111/j.1600-0587.1989.tb00930.x, 1989.
Ballard, R. G., Walsh, M. A., and Cole, W. E.: Blue-stain fungi in xylem of lodgepole pine: a light-microscope study on extent of hyphal distribution, Can. J. Bot., 60, 2334–2341, https://doi.org/10.1139/b82-285, 1982.
Bentz, B. J., Régnière, J., Fettig, C. J., Hansen, E. M., Hayes, J. L., Hicke, J. A., Kelsey, R. G., Negrón, J. F., and Seybold, S. J.: Climate Change and Bark Beetles of the Western United States and Canada: Direct and Indirect Effects, BioScience, 60, 602–613, https://doi.org/10.1525/bio.2010.60.8.6, 2010.
Berner, L. T., Law, B. E., Meddens, A. J. H., and Hicke, J. A.: Tree mortality from fires, bark beetles, and timber harvest during a hot and dry decade in the western United States (2003–2012), Environ. Res. Lett., 12, 065005, https://doi.org/10.1088/1748-9326/aa6f94, 2017.
Berryman, A. A.: Population Cycles: The Case for Trophic Interactions, Oxford University Press, 207 pp., 2002.
Biedermann, P. H. W., Müller, J., Grégoire, J.-C., Gruppe, A., Hagge, J., Hammerbacher, A., Hofstetter, R. W., Kandasamy, D., Kolarik, M., Kostovcik, M., Krokene, P., Sallé, A., Six, D. L., Turrini, T., Vanderpool, D., Wingfield, M. J., and Bässler, C.: Bark Beetle Population Dynamics in the Anthropocene: Challenges and Solutions, Trends Ecol. Evol., 34, 914–924, https://doi.org/10.1016/j.tree.2019.06.002, 2019.
Boucher, O., Servonnat, J., Albright, A. L., Aumont, O., Balkanski, Y., Bastrikov, V., Bekki, S., Bonnet, R., Bony, S., Bopp, L., Braconnot, P., Brockmann, P., Cadule, P., Caubel, A., Cheruy, F., Codron, F., Cozic, A., Cugnet, D., D'Andrea, F., Davini, P., Lavergne, C. de, Denvil, S., Deshayes, J., Devilliers, M., Ducharne, A., Dufresne, J.-L., Dupont, E., Éthé, C., Fairhead, L., Falletti, L., Flavoni, S., Foujols, M.-A., Gardoll, S., Gastineau, G., Ghattas, J., Grandpeix, J.-Y., Guenet, B., Guez, L., E., Guilyardi, E., Guimberteau, M., Hauglustaine, D., Hourdin, F., Idelkadi, A., Joussaume, S., Kageyama, M., Khodri, M., Krinner, G., Lebas, N., Levavasseur, G., Lévy, C., Li, L., Lott, F., Lurton, T., Luyssaert, S., Madec, G., Madeleine, J.-B., Maignan, F., Marchand, M., Marti, O., Mellul, L., Meurdesoif, Y., Mignot, J., Musat, I., Ottlé, C., Peylin, P., Planton, Y., Polcher, J., Rio, C., Rochetin, N., Rousset, C., Sepulchre, P., Sima, A., Swingedouw, D., Thiéblemont, R., Traore, A. K., Vancoppenolle, M., Vial, J., Vialard, J., Viovy, N., and Vuichard, N.: Presentation and Evaluation of the IPSL-CM6A-LR Climate Model, J. Adv. Model. Earth Syst., 12, e2019MS002010, https://doi.org/10.1029/2019MS002010, 2020.
Bugmann, H. K. M.: A Simplified Forest Model to Study Species Composition Along Climate Gradients, Ecology, 77, 2055–2074, https://doi.org/10.2307/2265700, 1996.
Buma, B.: Disturbance interactions: characterization, prediction, and the potential for cascading effects, Ecosphere, 6, art70, https://doi.org/10.1890/ES15-00058.1, 2015.
~~Chapin, F. S., Woodwell, G. M., Randerson, J. T., Rastetter, E. B., Lovett, G. M., Baldocchi, D. D., Clark, D. A., Harmon, M. E., Schimel, D. S., Valentini, R., Wirth, C., Aber, J. D., Cole, J. J., Goulden, M. L., Harden, J. W., Heimann, M., Howarth, R. W., Matson, P. A., McGuire, A. D., Melillo, J. M., Mooney, H. A., Neff, J. C., Houghton, R. A., Pace, M. L., Ryan, M. G., Running, S. W., Sala, O. E., Schlesinger, W. H., and Schulze, E.-D.: Reconciling Carbon-cycle Concepts, Terminology, and Methods, Ecosystems, 9, 1041–1050, https://doi.org/10.1007/s10021-005-0105-7, 2006.~~
Chen, Y., Ryder, J., Bastrikov, V., McGrath, M. J., Naudts, K., Otto, J., Ottlé, C., Peylin, P., Polcher, J., Valade, A., Black, A., Elbers, J. A., Moors, E., Foken, T., van Gorsel, E., Haverd, V., Heinesch, B., Tiedemann, F., Knohl, A., Launiainen, S., Loustau, D., Ogée, J., Vessala, T., and Luyssaert, S.: Evaluating the performance of land surface model ORCHIDEE-CAN v1.0 on water and energy flux estimation with a single- and multi-layer energy budget scheme, Geosci. Model Dev., 9, 2951–2972, https://doi.org/10.5194/gmd-9-2951-2016, 2016.
Chen, Y.-Y., Gardiner, B., Pasztor, F., Blennow, K., Ryder, J., Valade, A., Naudts, K., Otto, J., McGrath, M. J., Planque, C., and Luyssaert, S.: Simulating damage for wind storms in the land surface model ORCHIDEE-CAN (revision 4262), Geosci. Model Dev., 11, 771–791, https://doi.org/10.5194/gmd-11-771-2018, 2018.
Ciais, P., Reichstein, M., Viovy, N., Granier, A., Ogée, J., Allard, V., Aubinet, M., Buchmann, N., Bernhofer, C.,

Carrara, A., Chevallier, F., De Noblet, N., Friend, A. D., Friedlingstein, P., Grünwald, T., Heinesch, B., Keronen, P., Knohl, A., Krinner, G., Loustau, D., Manca, G., Matteucci, G., Miglietta, F., Ourcival, J. M., Papale, D., Pilegaard, K., Rambal, S., Seufert, G., Soussana, J. F., Sanz, M. J., Schulze, E. D., Vesala, T., and Valentini, R.: Europe-wide reduction in primary productivity caused by the heat and drought in 2003, Nature, 437, 529–533, https://doi.org/10.1038/nature03972, 2005.
Cox, P. M., Betts, R. A., Jones, C. D., Spall, S. A., and Totterdell, I. J.: Acceleration of global warming due to carbon-cycle feedbacks in a coupled climate model, Nature, 408, 184–187, https://doi.org/10.1038/35041539, 2000.
Custer, G. F., van Diepen, L. T. A., and Stump, W. L.: Structural and Functional Dynamics of Soil Microbes following Spruce Beetle Infestation, Appl. Environ. Microbiol., 86, e01984-19, https://doi.org/10.1128/AEM.01984-19, 2020.
Das, A. J., Stephenson, N. L., and Davis, K. P.: Why do trees die? Characterizing the drivers of background tree mortality, Ecology, 97, 2616–2627, https://doi.org/10.1002/ecy.1497, 2016.
Deleuze, C., Pain, O., Dhôte, J.-F., and Hervé, J.-C.: A flexible radial increment model for individual trees in pure even-aged stands, Ann. For. Sci., 61, 327–335, https://doi.org/10.1051/forest:2004026, 2004.
Edburg, S. L., Hicke, J. A., Brooks, P. D., Pendall, E. G., Ewers, B. E., Norton, U., Gochis, D., Gutmann, E. D., and Meddens, A. J.: Cascading impacts of bark beetle-caused tree mortality on coupled biogeophysical and biogeochemical processes, Front. Ecol. Environ., 10, 416–424, https://doi.org/10.1890/110173, 2012.
Faccoli, M. and Stergulc, F.: A practical method for predicting the short-time trend of bivoltine populations of Ips typographus (L.) (Col., Scolytidae), J. Appl. Entomol., 130, 61–66, https://doi.org/10.1111/j.1439-0418.2005.01019.x, 2006.
Friedlingstein, P., Cox, P., Betts, R., Bopp, L., Bloh, W. von, Brovkin, V., Cadule, P., Doney, S., Eby, M., Fung, I., Bala, G., John, J., Jones, C., Joos, F., Kato, T., Kawamiya, M., Knorr, W., Lindsay, K., Matthews, H. D., Raddatz, T., Rayner, P., Reick, C., Roeckner, E., Schnitzler, K.-G., Schnur, R., Strassmann, K., Weaver, A. J., Yoshikawa, C., and Zeng, N.: Climate–Carbon Cycle Feedback Analysis: Results from the C4MIP Model Intercomparison, J. Clim., 19, 3337–3353, https://doi.org/10.1175/JCLI3800.1, 2006.
Grimm, V. and Wissel, C.: Babel, or the ecological stability discussions: an inventory and analysis of terminology and a guide for avoiding confusion, Oecologia, 109, 323–334, https://doi.org/10.1007/s004420050090, 1997.
Havašová, M., Ferenčík, J., and Jakuš, R.: Interactions between windthrow, bark beetles and forest management in the Tatra national parks, For. Ecol. Manag., 391, 349–361, https://doi.org/10.1016/j.foreco.2017.01.009, 2017.
Haverd, V., Lovell, J. L., Cuntz, M., Jupp, D. L. B., Newnham, G. J., and Sea, W.: The Canopy Semi-analytic Pgap And Radiative Transfer (CanSPART) model: Formulation and application, Agric. For. Meteorol., 160, 14–35, https://doi.org/10.1016/j.agrformet.2012.01.018, 2012.
Hicke, J. A., Allen, C. D., Desai, A. R., Dietze, M. C., Hall, R. J., Hogg, E. H., Kashian, D. M., Moore, D., Raffa, K. F., Sturrock, R. N., and Vogelmann, J.: Effects of biotic disturbances on forest carbon cycling in the United States and Canada., https://doi.org/10.1111/j.1365-2486.2011.02543.x, 2012.
Hlásny, T., König, L., Krokene, P., Lindner, M., Montagné-Huck, C., Müller, J., Qin, H., Raffa, K. F., Schelhaas, M.-J., Svoboda, M., Viiri, H., and Seidl, R.: Bark Beetle Outbreaks in Europe: State of Knowledge and Ways Forward for Management, Curr. For. Rep., 7, 138–165, https://doi.org/10.1007/s40725-021-00142-x, 2021a.
Hlásny, T., Zimová, S., Merganičová, K., Štěpánek, P., Modlinger, R., and Turčáni, M.: Devastating outbreak of bark beetles in the Czech Republic: Drivers, impacts, and management implications, For. Ecol. Manag., 490, 119075, https://doi.org/10.1016/j.foreco.2021.119075, 2021b.
Huang, J., Kautz, M., Trowbridge, A. M., Hammerbacher, A., Raffa, K. F., Adams, H. D., Goodsman, D. W., Xu, C., Meddens, A. J. H., Kandasamy, D., Gershenzon, J., Seidl, R., and Hartmann, H.: Tree defence and bark beetles in a drying world: carbon partitioning, functioning and modelling, New Phytol., 225, 26–36, https://doi.org/10.1111/nph.16173, 2020.
JonášováJönsson, M. and Prach, K.: Central-European mountain spruce (*Picea abies* (L.) Karst.) forests: regeneration of tree species after a bark beetle outbreak, Ecol. Eng., 23, 15–27, https://doi.org/10.1016/j.ecoleng.2004.06.010, 2004A. M., Appelberg, G., Harding, S., and Bärring, L.: Spatio-temporal impact of climate change on the activity and voltinism of the spruce bark beetle, Ips typographus, Glob. Change Biol., 15, 486–499, https://doi.org/10.1111/j.1365-2486.2008.01742.x, 2009.
Jönsson, A. M., Harding, S., Krokene, P., Lange, H., Lindelöw, Å., Økland, B., Ravn, H. P., and Schroeder, L. M.: Modelling the potential impact of global warming on Ips typographus voltinism and reproductive diapause, Clim. Change, 109, 695–718, https://doi.org/10.1007/s10584-011-0038-4, 2011.
Jönsson, A. M., Schroeder, L. M., Lagergren, F., Anderbrant, O., and Smith, B.: Guess the impact of *Ips typographus*—An ecosystem modelling approach for simulating spruce bark beetle outbreaks, Agric. For. Meteorol., 166–167, 188–200, https://doi.org/10.1016/j.agrformet.2012.07.012, 2012.

Kärvemo, S. and Schroeder, L. M.: A comparison of outbreak dynamics of the spruce bark beetle in Sweden and the mountain pine beetle in Canada (Curculionidae: Scolytinae), 2010.
Kautz, M., Anthoni, P., Meddens, A. J. H., Pugh, T. A. M., and Arneth, A.: Simulating the recent impacts of multiple biotic disturbances on forest carbon cycling across the United States, Glob. Change Biol., 24, 2079–2092, https://doi.org/10.1111/gcb.13974, 2018.
Komonen, A., Schroeder, L. M., and Weslien, J.: Ips typographus population development after a severe storm in a nature reserve in southern Sweden, J. Appl. Entomol., 135, 132–141, https://doi.org/10.1111/j.1439-0418.2010.01520.x, 2011.
Krinner, G., Viovy, N., de Noblet-Ducoudré, N., Ogée, J., Polcher, J., Friedlingstein, P., Ciais, P., Sitch, S., and Prentice, I. C.: A dynamic global vegetation model for studies of the coupled atmosphere-biosphere system: DVGM FOR COUPLED CLIMATE STUDIES, Glob. Biogeochem. Cycles, 19, https://doi.org/10.1029/2003GB002199, 2005.
Kurz, W. A., Dymond, C. C., Stinson, G., Rampley, G. J., Neilson, E. T., Carroll, A. L., Ebata, T., and Safranyik, L.: Mountain pine beetle and forest carbon feedback to climate change, Nature, 452, 987–990, https://doi.org/10.1038/nature06777, 2008a.
Kurz, W. A., Dymond, C. C., Stinson, G., Rampley, G. J., Neilson, E. T., Carroll, A. L., Ebata, T., and Safranyik, L.: Mountain pine beetle and forest carbon feedback to climate change, Nature, 452, 987–990, https://doi.org/10.1038/nature06777, 2008b.
Kurz, W. A., Stinson, G., Rampley, G. J., Dymond, C. C., and Neilson, E. T.: Risk of natural disturbances makes future contribution of Canada's forests to the global carbon cycle highly uncertain, Proc. Natl. Acad. Sci., 105, 1551–1555, https://doi.org/10.1073/pnas.0708133105, 2008c.
Lasslop, G., Thonicke, K., and Kloster, S.: SPITFIRE within the MPI Earth system model: Model development and evaluation, J. Adv. Model. Earth Syst., 6, 740–755, https://doi.org/10.1002/2013MS000284, 2014.
Lausch, A., Fahse, L., and Heurich, M.: Factors affecting the spatio-temporal dispersion of *Ips typographus* (L.) in Bavarian Forest National Park: A long-term quantitative landscape-level analysis, For. Ecol. Manag., 261, 233–245, https://doi.org/10.1016/j.foreco.2010.10.012, 2011.
Levins, R.: The Strategy of Model Building in Population Biology, Am. Sci., 54, 421–431, 1966.
Lieutier, F.: Mechanisms of Resistance in Conifers and Bark beetle Attack Strategies, in: Mechanisms and Deployment of Resistance in Trees to Insects, edited by: Wagner, M. R., Clancy, K. M., Lieutier, F., and Paine, T. D., Springer Netherlands, Dordrecht, 31–77, https://doi.org/10.1007/0-306-47596-0_2, 2002.
Lombardero, M. J., Ayres, M. P., Ayres, B. D., and Reeve, J. D.: Cold Tolerance of Four Species of Bark Beetle (Coleoptera: Scolytidae) in North America, Environ. Entomol., 29, 421–432, https://doi.org/10.1603/0046-225X-29.3.421, 2000.
Luyssaert, S., Marie, G., Valade, A., Chen, Y.-Y., Njakou Djomo, S., Ryder, J., Otto, J., Naudts, K., Lansø, A. S., Ghattas, J., and McGrath, M. J.: Trade-offs in using European forests to meet climate objectives, Nature, 562, 259–262, https://doi.org/10.1038/s41586-018-0577-1, 2018.
Marini, L., Økland, B., Jönsson, A. M., Bentz, B., Carroll, A., Forster, B., Grégoire, J.-C., Hurling, R., Nageleisen, L. M., Netherer, S., Ravn, H. P., Weed, A., and Schroeder, M.: Climate drivers of bark beetle outbreak dynamics in Norway spruce forests, Ecography, 40, 1426–1435, https://doi.org/10.1111/ecog.02769, 2017.
Mezei, P., Grodzki, W., Blaženec, M., and Jakuš, R.: Factors influencing the *wind–bark beetles*' disturbance system in the course of an *Ips typographus* outbreak in the Tatra Mountains, For. Ecol. Manag., 312, 67–77, https://doi.org/10.1016/j.foreco.2013.10.020, 2014.
Mezei, P., Jakuš, R., Pennerstorfer, J., Havašová, M., Škvarenina, J., Ferenčík, J., Slivinský, J., Bičárová, S., Bilčík, D., Blaženec, M., and Netherer, S.: Storms, temperature maxima and the Eurasian spruce bark beetle *Ips typographus*—An infernal trio in Norway spruce forests of the Central European High Tatra Mountains, Agric. For. Meteorol., 242, 85–95, https://doi.org/10.1016/j.agrformet.2017.04.004, 2017.
Migliavacca, M., Dosio, A., Kloster, S., Ward, D. S., Camia, A., Houborg, R., Houston Durrant, T., Khabarov, N., Krasovskii, A. A., San Miguel-Ayanz, J., and Cescatti, A.: Modeling burned area in Europe with the Community Land Model, J. Geophys. Res. Biogeosciences, 118, 265–279, https://doi.org/10.1002/jgrg.20026, 2013.
Migliavacca, M., Musavi, T., Mahecha, M. D., Nelson, J. A., Knauer, J., Baldocchi, D. D., Perez-Priego, O., Christiansen, R., Peters, J., Anderson, K., Bahn, M., Black, T. A., Blanken, P. D., Bonal, D., Buchmann, N., Caldararu, S., Carrara, A., Carvalhais, N., Cescatti, A., Chen, J., Cleverly, J., Cremonese, E., Desai, A. R., El-Madany, T. S., Farella, M. M., Fernández-Martínez, M., Filippa, G., Forkel, M., Galvagno, M., Gomarasca, U., Gough, C. M., Göckede, M., Ibrom, A., Ikawa, H., Janssens, I. A., Jung, M., Kattge, J., Keenan, T. F., Knohl, A., Kobayashi, H., Kraemer, G., Law, B. E., Liddell, M. J., Ma, X., Mammarella, I., Martini, D., Macfarlane, C., Matteucci, G., Montagnani, L., Pabon-Moreno, D. E., Panigada, C., Papale, D., Pendall, E., Penuelas, J., Phillips, R.

P., Reich, P. B., Rossini, M., Rotenberg, E., Scott, R. L., Stahl, C., Weber, U., Wohlfahrt, G., Wolf, S., Wright, I. J., Yakir, D., Zaehle, S., and Reichstein, M.: The three major axes of terrestrial ecosystem function, Nature, 598, 468–472, https://doi.org/10.1038/s41586-021-03939-9, 2021.
Millar, C. I. and Stephenson, N. L.: Temperate forest health in an era of emerging megadisturbance, Science, 349, 823–826, https://doi.org/10.1126/science.aaa9933, 2015.
Morehouse, K., Johns, T., Kaye, J., and Kaye, M.: Carbon and nitrogen cycling immediately following bark beetle outbreaks in southwestern ponderosa pine forests, For. Ecol. Manag., 255, 2698–2708, https://doi.org/10.1016/j.foreco.2008.01.050, 2008.
Nardi, D., Jactel, H., Pagot, E., Samalens, J.-C., and Marini, L.: Drought and stand susceptibility to attacks by the European spruce bark beetle: A remote sensing approach, Agric. For. Entomol., 25, 119–129, https://doi.org/10.1111/afe.12536, 2023.
Naudts, K., Ryder, J., McGrath, M. J., Otto, J., Chen, Y., Valade, A., Bellasen, V., Berhongaray, G., Bönisch, G., Campioli, M., and others: A vertically discretised canopy description for ORCHIDEE (SVN r2290) and the modifications to the energy, water and carbon fluxes, Geosci. Model Dev., 8, 2035–2065, 2015a.
Naudts, K., Ryder, J., McGrath, M. J., Otto, J., Chen, Y., Valade, A., Bellasen, V., Berhongaray, G., Bönisch, G., Campioli, M., Ghattas, J., De Groote, T., Haverd, V., Kattge, J., MacBean, N., Maignan, F., Merilä, P., Penuelas, J., Peylin, P., Pinty, B., Pretzsch, H., Schulze, E. D., Solyga, D., Vuichard, N., Yan, Y., and Luyssaert, S.: A vertically discretised canopy description for ORCHIDEE (SVN r2290) and the modifications to the energy, water and carbon fluxes, Geosci. Model Dev., 8, 2035–2065, https://doi.org/10.5194/gmd-8-2035-2015, 2015b.
Naudts, K., Chen, Y., McGrath, M. J., Ryder, J., Valade, A., Otto, J., and Luyssaert, S.: Europe's forest management did not mitigate climate warming, Science, 351, 597–600, https://doi.org/10.1126/science.aad7270, 2016.
Netherer, S., Matthews, B., Katzensteiner, K., Blackwell, E., Henschke, P., Hietz, P., Pennerstorfer, J., Rosner, S., Kikuta, S., Schume, H., and Schopf, A.: Do water-limiting conditions predispose Norway spruce to bark beetle attack?, New Phytol., 205, 1128–1141, https://doi.org/10.1111/nph.13166, 2015.
Ogris, N., Ferlan, M., Hauptman, T., Pavlin, R., Kavčič, A., Jurc, M., and de Groot, M.: RITY – A phenology model of *Ips typographus* as a tool for optimization of its monitoring, Ecol. Model., 410, 108775, https://doi.org/10.1016/j.ecolmodel.2019.108775, 2019.
Pastorello, G., Trotta, C., Canfora, E., Chu, H., Christianson, D., Cheah, Y.-W., Poindexter, C., Chen, J., Elbashandy, A., Humphrey, M., Isaac, P., Polidori, D., Reichstein, M., Ribeca, A., van Ingen, C., Vuichard, N., Zhang, L., Amiro, B., Ammann, C., Arain, M. A., Ardö, J., Arkebauer, T., Arndt, S. K., Arriga, N., Aubinet, M., Aurela, M., Baldocchi, D., Barr, A., Beamesderfer, E., Marchesini, L. B., Bergeron, O., Beringer, J., Bernhofer, C., Berveiller, D., Billesbach, D., Black, T. A., Blanken, P. D., Bohrer, G., Boike, J., Bolstad, P. V., Bonal, D., Bonnefond, J.-M., Bowling, D. R., Bracho, R., Brodeur, J., Brümmer, C., Buchmann, N., Burban, B., Burns, S. P., Buysse, P., Cale, P., Cavagna, M., Cellier, P., Chen, S., Chini, I., Christensen, T. R., Cleverly, J., Collalti, A., Consalvo, C., Cook, B. D., Cook, D., Coursolle, C., Cremonese, E., Curtis, P. S., D'Andrea, E., da Rocha, H., Dai, X., Davis, K. J., Cinti, B. D., Grandcourt, A. de, Ligne, A. D., De Oliveira, R. C., Delpierre, N., Desai, A. R., Di Bella, C. M., Tommasi, P. di, Dolman, H., Domingo, F., Dong, G., Dore, S., Duce, P., Dufrêne, E., Dunn, A., Dušek, J., Eamus, D., Eichelmann, U., ElKhidir, H. A. M., Eugster, W., Ewenz, C. M., Ewers, B., Famulari, D., Fares, S., Feigenwinter, I., Feitz, A., Fensholt, R., Filippa, G., Fischer, M., Frank, J., Galvagno, M., et al.: The FLUXNET2015 dataset and the ONEFlux processing pipeline for eddy covariance data, Sci. Data, 7, 225, https://doi.org/10.1038/s41597-020-0534-3, 2020.
Pasztor, F., Matulla, C., Rammer, W., and Lexer, M. J.: Drivers of the bark beetle disturbance regime in Alpine forests in Austria, For. Ecol. Manag., 318, 349–358, https://doi.org/10.1016/j.foreco.2014.01.044, 2014.
Pfeifer, E. M., Hicke, J. A., and Meddens, A. J. H.: Observations and modeling of aboveground tree carbon stocks and fluxes following a bark beetle outbreak in the western United States, Glob. Change Biol., 17, 339–350, https://doi.org/10.1111/j.1365-2486.2010.02226.x, 2011.
Pineau, X., David, G., Peter, Z., Sallé, A., Baude, M., Lieutier, F., and Jactel, H.: Effect of temperature on the reproductive success, developmental rate and brood characteristics of Ips sexdentatus (Boern.), Agric. For. Entomol., 19, 23–33, https://doi.org/10.1111/afe.12177, 2017.
Preisler, H. K., Hicke, J. A., Ager, A. A., and Hayes, J. L.: Climate and weather influences on spatial temporal patterns of mountain pine beetle populations in Washington and Oregon, Ecology, 93, 2421–2434, https://doi.org/10.1890/11-1412.1, 2012.
Pugh, T. A. M., Jones, C. D., Huntingford, C., Burton, C., Arneth, A., Brovkin, V., Ciais, P., Lomas, M., Robertson, E., and Piao, S. L.: A Large Committed Long-Term Sink of Carbon due to Vegetation Dynamics, Earths Future, 2017.
Quillet, A., Peng, C., and Garneau, M.: Toward dynamic global vegetation models for simulating vegetation–climate

interactions and feedbacks: recent developments, limitations, and future challenges, Environ. Rev., 18, 333–353, https://doi.org/10.1139/A10-016, 2010.
Raffa, K. F., Aukema, B. H., Bentz, B. J., Carroll, A. L., Hicke, J. A., Turner, M. G., and Romme, W. H.: Cross-scale Drivers of Natural Disturbances Prone to Anthropogenic Amplification: The Dynamics of Bark Beetle Eruptions, BioScience, 58, 501–517, https://doi.org/10.1641/B580607, 2008.
~~Rhoades, C. C.: Soil Nitrogen Leaching in Logged Beetle-Killed Forests and Implications for Riparian Fuel Reduction, J. Environ. Qual., 48, 305–313, https://doi.org/10.2134/jeq2018.04.0169, 2019.~~
Ryder, J., Polcher, J., Peylin, P., Ottlé, C., Chen, Y., van Gorsel, E., Haverd, V., McGrath, M. J., Naudts, K., Otto, J., Valade, A., and Luyssaert, S.: A multi-layer land surface energy budget model for implicit coupling with global atmospheric simulations, Geosci. Model Dev., 9, 223–245, https://doi.org/10.5194/gmd-9-223-2016, 2016.
Schumacher, S.: The role of large-scale disturbances and climate for the dynamics of forested landscapes in the European Alps, Doctoral Thesis, ETH Zurich, https://doi.org/10.3929/ethz-a-004818825, 2004.
Seidl, R. and Rammer, W.: Climate change amplifies the interactions between wind and bark beetle disturbances in forest landscapes, Landsc. Ecol., 1–14, https://doi.org/10.1007/s10980-016-0396-4, 2016.
Seidl, R., Fernandes, P. M., Fonseca, T. F., Gillet, F., Jönsson, A. M., Merganičová, K., Netherer, S., Arpaci, A., Bontemps, J.-D., Bugmann, H., González-Olabarria, J. R., Lasch, P., Meredieu, C., Moreira, F., Schelhaas, M.-J., and Mohren, F.: Modelling natural disturbances in forest ecosystems: a review, Ecol. Model., 222, 903–924, https://doi.org/10.1016/j.ecolmodel.2010.09.040, 2011.
Seidl, R., Schelhaas, M.-J., Rammer, W., and Verkerk, P. J.: Increasing forest disturbances in Europe and their impact on carbon storage, Nat. Clim. Change, 4, 806–810, https://doi.org/10.1038/nclimate2318, 2014.
Seidl, R., Thom, D., Kautz, M., Martin-Benito, D., Peltoniemi, M., Vacchiano, G., Wild, J., Ascoli, D., Petr, M., Honkaniemi, J., Lexer, M. J., Trotsiuk, V., Mairota, P., Svoboda, M., Fabrika, M., Nagel, T. A., and Reyer, C. P. O.: Forest disturbances under climate change, Nat. Clim. Change, 7, 395–402, https://doi.org/10.1038/nclimate3303, 2017.
Seidl, R., Klonner, G., Rammer, W., Essl, F., Moreno, A., Neumann, M., and Dullinger, S.: Invasive alien pests threaten the carbon stored in Europe's forests, Nat. Commun., 9, 1626, https://doi.org/10.1038/s41467-018-04096-w, 2018.
Senf, C., Pflugmacher, D., Hostert, P., and Seidl, R.: Using Landsat time series for characterizing forest disturbance dynamics in the coupled human and natural systems of Central Europe, ISPRS J. Photogramm. Remote Sens., 130, 453–463, https://doi.org/10.1016/j.isprsjprs.2017.07.004, 2017.
Storaunet, K. O., Rolstad, J., Gjerde, I., and Gundersen, V. S.: Historical logging, productivity, and structural characteristics of boreal coniferous forests in Norway, Silva Fenn., 39, 2005.
Temperli, C., Bugmann, H., and Elkin, C.: Cross-scale interactions among bark beetles, climate change, and wind disturbances: a landscape modeling approach, Ecol. Monogr., 83, 383–402, https://doi.org/10.1890/12-1503.1, 2013a.
Temperli, C., Bugmann, H., and Elkin, C.: Cross-scale interactions among bark beetles, climate change, and wind disturbances: a landscape modeling approach, Ecol. Monogr., 83, 383–402, https://doi.org/10.1890/12-1503.1, 2013b.
Thurner, M., Beer, C., Ciais, P., Friend, A. D., Ito, A., Kleidon, A., Lomas, M. R., Quegan, S., Rademacher, T. T., Schaphoff, S., Tum, M., Wiltshire, A., and Carvalhais, N.: Evaluation of climate-related carbon turnover processes in global vegetation models for boreal and temperate forests, Glob. Change Biol., 23, 3076–3091, https://doi.org/10.1111/gcb.13660, 2017.
Van Meerbeek, K., Jucker, T., and Svenning, J.-C.: Unifying the concepts of stability and resilience in ecology, J. Ecol., 109, 3114–3132, https://doi.org/10.1111/1365-2745.13651, 2021.
Vuichard, N., Messina, P., Luyssaert, S., Guenet, B., Zaehle, S., Ghattas, J., Bastrikov, V., and Peylin, P.: Accounting for carbon and nitrogen interactions in the global terrestrial ecosystem model ORCHIDEE (trunk version, rev 4999): multi-scale evaluation of gross primary production, Geosci. Model Dev., 12, 4751–4779, https://doi.org/10.5194/gmd-12-4751-2019, 2019.
Wermelinger, B.: Ecology and management of the spruce bark beetle Ips typographus—a review of recent research, For. Ecol. Manag., 202, 67–82, https://doi.org/10.1016/j.foreco.2004.07.018, 2004.
Wichmann, L. and Ravn, H. P.: The spread of *Ips typographus* (L.) (Coleoptera, Scolytidae) attacks following heavy windthrow in Denmark, analysed using GIS, For. Ecol. Manag., 148, 31–39, https://doi.org/10.1016/S0378-1127(00)00477-1, 2001.
Yao, Y., Joetzjer, E., Ciais, P., Viovy, N., Cresto Aleina, F., Chave, J., Sack, L., Bartlett, M., Meir, P., Fisher, R., and Luyssaert, S.: Forest fluxes and mortality response to drought: model description (ORCHIDEE-CAN-NHA r7236) and evaluation at the Caxiuanã drought experiment, Geosci. Model Dev., 15, 7809–7833,

https://doi.org/10.5194/gmd-15-7809-2022, 2022.
Yi-Ying, C., Gardiner, B., Pasztor, F., Blennow, K., Ryder, J., Valade, A., Naudts, K., Otto, J., McGrath, M. J., and Planque, C.: Simulating damage for wind storms in the land surface model ORCHIDEE-CAN (revision 4262), Geosci. Model Dev., 11, 771, 2018.
Yue, C., Ciais, P., Cadule, P., Thonicke, K., Archibald, S., Poulter, B., Hao, W. M., Hantson, S., Mouillot, F., Friedlingstein, P., Maignan, F., and Viovy, N.: Modelling the role of fires in the terrestrial carbon balance by incorporating SPITFIRE into the global vegetation model ORCHIDEE – Part 1: simulating historical global burned area and fire regimes, Geosci. Model Dev., 7, 2747–2767, https://doi.org/10.5194/gmd-7-2747-2014, 2014.
Zaehle, S. and Dalmonech, D.: Carbon–nitrogen interactions on land at global scales: current understanding in modelling climate biosphere feedbacks, Curr. Opin. Environ. Sustain., 3, 311–320, https://doi.org/10.1016/j.cosust.2011.08.008, 2011.
Zaehle, S. and Friend, A. D.: Carbon and nitrogen cycle dynamics in the O-CN land surface model: 1. Model description, site-scale evaluation, and sensitivity to parameter estimates, Glob. Biogeochem. Cycles, 24, https://doi.org/10.1029/2009GB003521, 2010.
Zhang, Q.-H. and Schlyter, F.: Olfactory recognition and behavioural avoidance of angiosperm nonhost volatiles by conifer-inhabiting bark beetles, Agric. For. Entomol., 6, 1–20, https://doi.org/10.1111/j.1461-9555.2004.00202.x, 2004.
Zscheischler, J., Westra, S., van den Hurk, B. J. J. M., Seneviratne, S. I., Ward, P. J., Pitman, A., AghaKouchak, A., Bresch, D. N., Leonard, M., Wahl, T., and Zhang, X.: Future climate risk from compound events, Nat. Clim. Change, 8, 469–477, https://doi.org/10.1038/s41558-018-0156-3, 2018.

Supplementary material:

Table s1: selection of 32 parameter sets used to access the sensitivity of four main equations driving the ips typographus outbreak model. Black values are reference values whereas red values correspond to the sensitivity analysis described in section 3.3. The parameter set in green corresponds to the chosen parameter values for which the credibility score =4 and the parameter set in green bold is the one chosen for this study.

$i_{beetles\ generation}$

	$S_{generation}$	G_{limit}	$S_{activity}$	act_{limit}	$S_{susceptibility}$	$i_{rd\ susceptibility}$	$S_{mass\ attack}$	BP_{limit}	Score
Set 1.1	1.0	0.5	-20.0	0.06	-5.0	0.55	-30.0	0.12	4
Set 1.2	5.0	0.5	-20.0	0.06	-5.0	0.55	-30.0	0.12	2
Set 1.3	500.0	0.5	-20.0	0.06	-5.0	0.55	-30.0	0.12	2
Set 1.4	**1.0**	**1.0**	-20.0	0.06	-5.0	0.55	-30.0	0.12	4
Set 1.5	5.0	1.0	-20.0	0.06	-5.0	0.55	-30.0	0.12	4
Set 1.6	500.0	1.0	-20.0	0.06	-5.0	0.55	-30.0	0.12	2
Set 1.7	1.0	1.5	-20.0	0.06	-5.0	0.55	-30.0	0.12	3
Set 1.8	5.0	1.5	-20.0	0.06	-5.0	0.55	-30.0	0.12	0
Set 1.9	500.0	1.5	-20.0	0.06	-5.0	0.55	-30.0	0.12	0

$i_{beetles\ activity}$

	$S_{generation}$	G_{limit}	$S_{activity}$	act_{limit}	$S_{susceptibility}$	$i_{rd\ susceptibility}$	$S_{mass\ attack}$	BP_{limit}	Score
Set 2.1	1.0	1.0	-1.0	0.03	-5.0	0.55	-30.0	0.12	0
Set 2.2	1.0	1.0	-20.0	0.03	-5.0	0.55	-30.0	0.12	0
Set 2.3	1.0	1.0	-500.0	0.03	-5.0	0.55	-30.0	0.12	3
Set 2.4	1.0	1.0	-1.0	0.06	-5.0	0.55	-30.0	0.12	0
Set 2.5	1.0	1.0	-20.0	0.06	-5.0	0.55	-30.0	0.12	2
Set 2.6	1.0	1.0	**-500.0**	**0.06**	-5.0	0.55	-30.0	0.12	4
Set 2.7	1.0	1.0	-1.0	0.09	-5.0	0.55	-30.0	0.12	0
Set 2.8	1.0	1.0	-20	0.09	-5.0	0.55	-30.0	0.12	0
Set 2.9	1.0	1.0	-500	0.09	-5.0	0.55	-30.0	0.12	2

$i_{hosts\ susceptibility}$

	$S_{generation}$	G_{limit}	$S_{activity}$	act_{limit}	$S_{susceptibility}$	$i_{rd\ susceptibility}$	$S_{mass\ attack}$	BP_{limit}	Score
Set 3.1	1.0	1.0	-20.0	0.06	-1.0	0.275	-30.0	0.12	0
Set 3.2	1.0	1.0	-20.0	0.06	-5.0	0.275	-30.0	0.12	1
Set 3.3	1.0	1.0	-20.0	0.06	-500.0	0.275	-30.0	0.12	1
Set 3.4	1.0	1.0	-20.0	0.06	-1.0	0.55	-30.0	0.12	0
Set 3.5	1.0	1.0	-20.0	0.06	**-5.0**	**0.55**	-30.0	0.12	4
Set 3.6	1.0	1.0	-20.0	0.06	-500.0	0.55	-30.0	0.12	2
Set 3.7	1.0	1.0	-20.0	0.06	-1.0	0.825	-30.0	0.12	0
Set 3.8	1.0	1.0	-20.0	0.06	-5.0	0.825	-30.0	0.12	2
Set 3.9	1.0	1.0	-20.0	0.06	-500.0	0.825	-30.0	0.12	2

$i_{beetles\ mass\ attack}$

	$S_{generation}$	G_{limit}	$S_{activity}$	act_{limit}	$S_{susceptibility}$	$i_{rd\ susceptibility}$	$S_{mass\ attack}$	BP_{limit}	Score
Set 4.1	1.0	1.0	-20.0	0.06	-5.0	0.55	-1.0	0.06	0
Set 4.2	1.0	1.0	-20.0	0.06	-5.0	0.55	-30.0	0.06	0
Set 4.3	1.0	1.0	-20.0	0.06	-5.0	0.55	-500.0	0.06	3
Set 4.4	1.0	1.0	-20.0	0.06	-5.0	0.55	-1.0	0.12	0
Set 4.5	1.0	1.0	-20.0	0.06	-5.0	0.55	-30.0	0.12	4
Set 4.6	1.0	1.0	-20.0	0.06	-5.0	0.55	**-500.0**	**0.12**	4
Set 4.7	1.0	1.0	-20.0	0.06	-5.0	0.55	-1.0	0.18	2
Set 4.8	1.0	1.0	-20.0	0.06	-5.0	0.55	-30.0	0.18	3

57

Set 4.9	1.0	1.0	-20.0	0.06	-5.0	0.55	-500.0	0.18	4

58

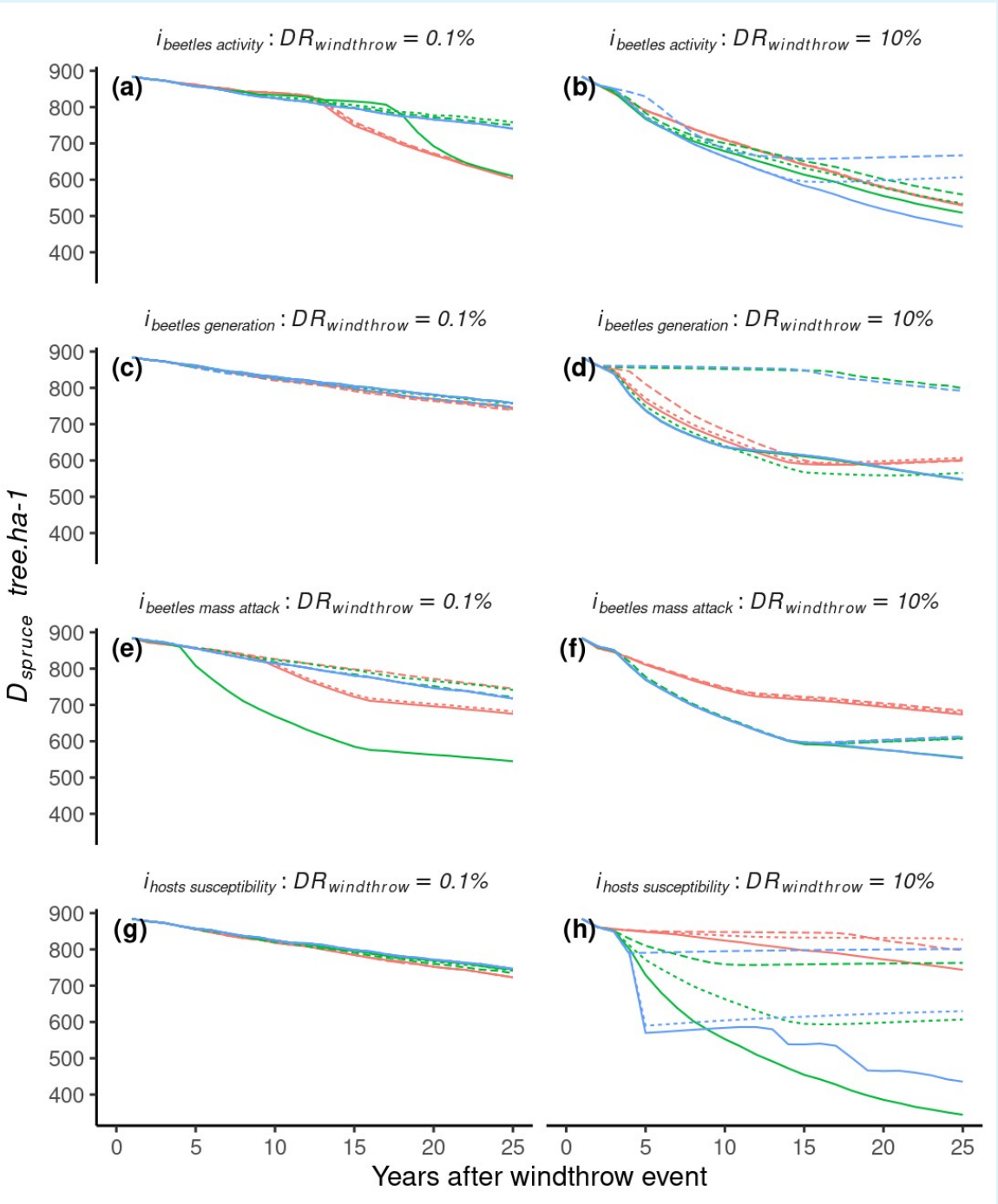

Figure s2: Simulation results from the sensitivity experiment at the THA site. Eight parameters from four equations were evaluated. Each equation represents an index from the bark beetle outbreak model ($i_{hosts\ susceptibility}$, $i_{hosts\ mass\ attack}$, $i_{beetles\ activity}$, $i_{beetles\ generation}$). Each index is represented by a logistic function defined by a shape parameter (*Shape*) and a limit parameter (*Limit*). Three values were chosen for each parameter resulting in 9 pairs of parameters for each index. Colored lines represent the shape parameter varying from linear : *Shape* = -1.0 (red), logistic -5.0 < *Shape* < -30.0 (green), to step function where *Shape* = -500.0 (blue). Line type represents three different values for *Limit* parameters where references (dashed line) are values of $i_{rd\ susceptibility}$, BP_{limit}, act_{limit} and G_{limit} (given in table 4), whereas permissive (full line) and restrictive (dashed dotted) represent a 50% decrease or increase respectively.

1387

59

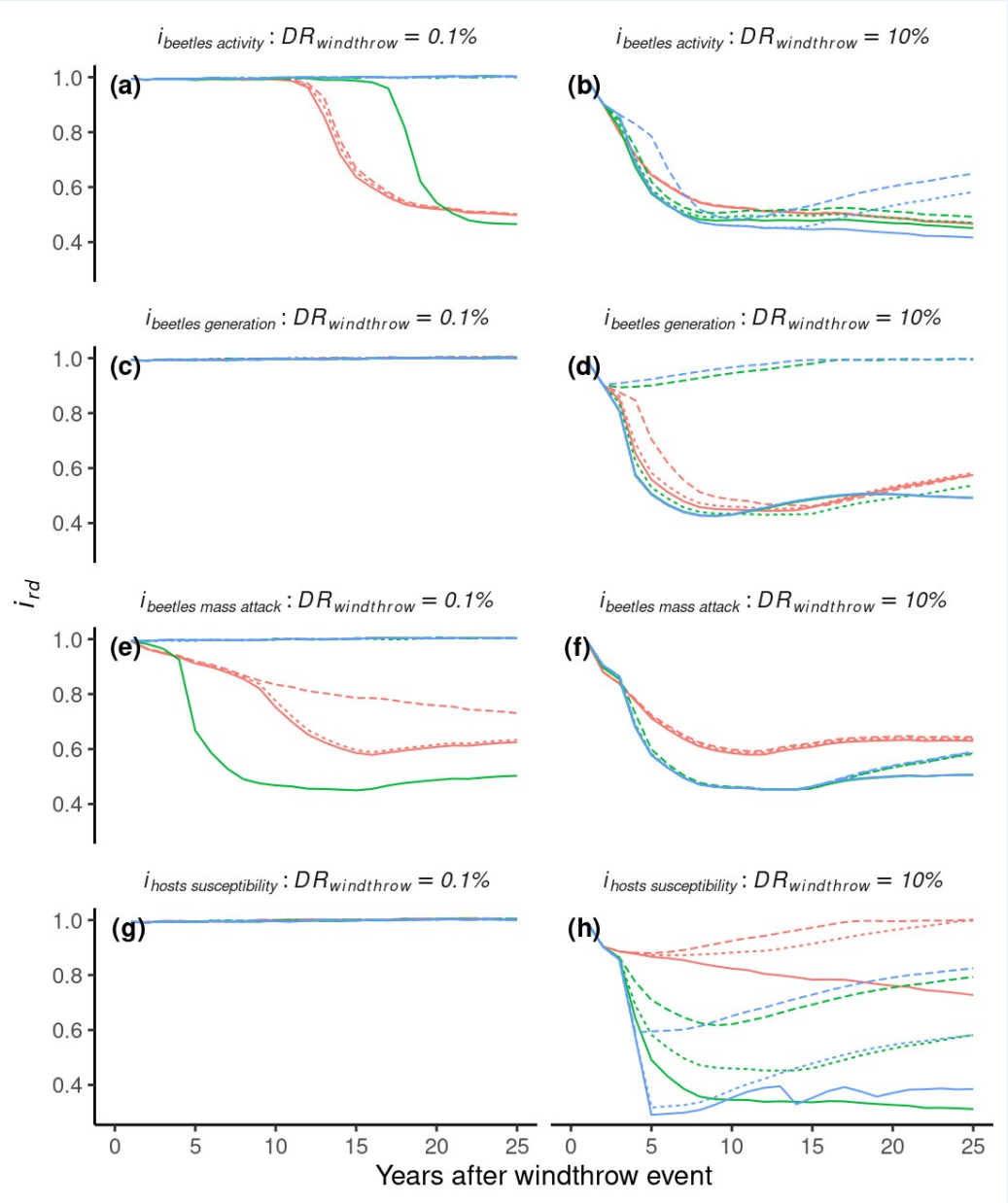

Figure s3: Simulation results from the sensitivity experiment at the THA site. Eight parameters from four equations were evaluated. Each equation represents an index from the bark beetle outbreak model ($i_{hosts\ susceptibility}$ $i_{hosts\ mass\ attack}$, $i_{beetles\ activity}$, $i_{beetles\ generation}$). Each index is represented by a logistic function defined by a shape parameter (*Shape*) and a limit parameter (*Limit)*. Three values were chosen for each parameter resulting in 9 pairs of parameters for each index. Colored lines represent the shape parameter varying from linear : *Shape* = -1.0 (red), logistic -5.0 < *Shape* < -30.0 (green), to step function where *Shape* = -500.0 (blue). Line type represents three different values for *Limit* parameters where references (dashed line) are values of $i_{rd\ susceptibility}$, BP_{limit}, act_{limit} and G_{limit} (given in table 4), whereas permissive (full line) and restrictive (dashed dotted) represent a 50% decrease or increase respectively.

60

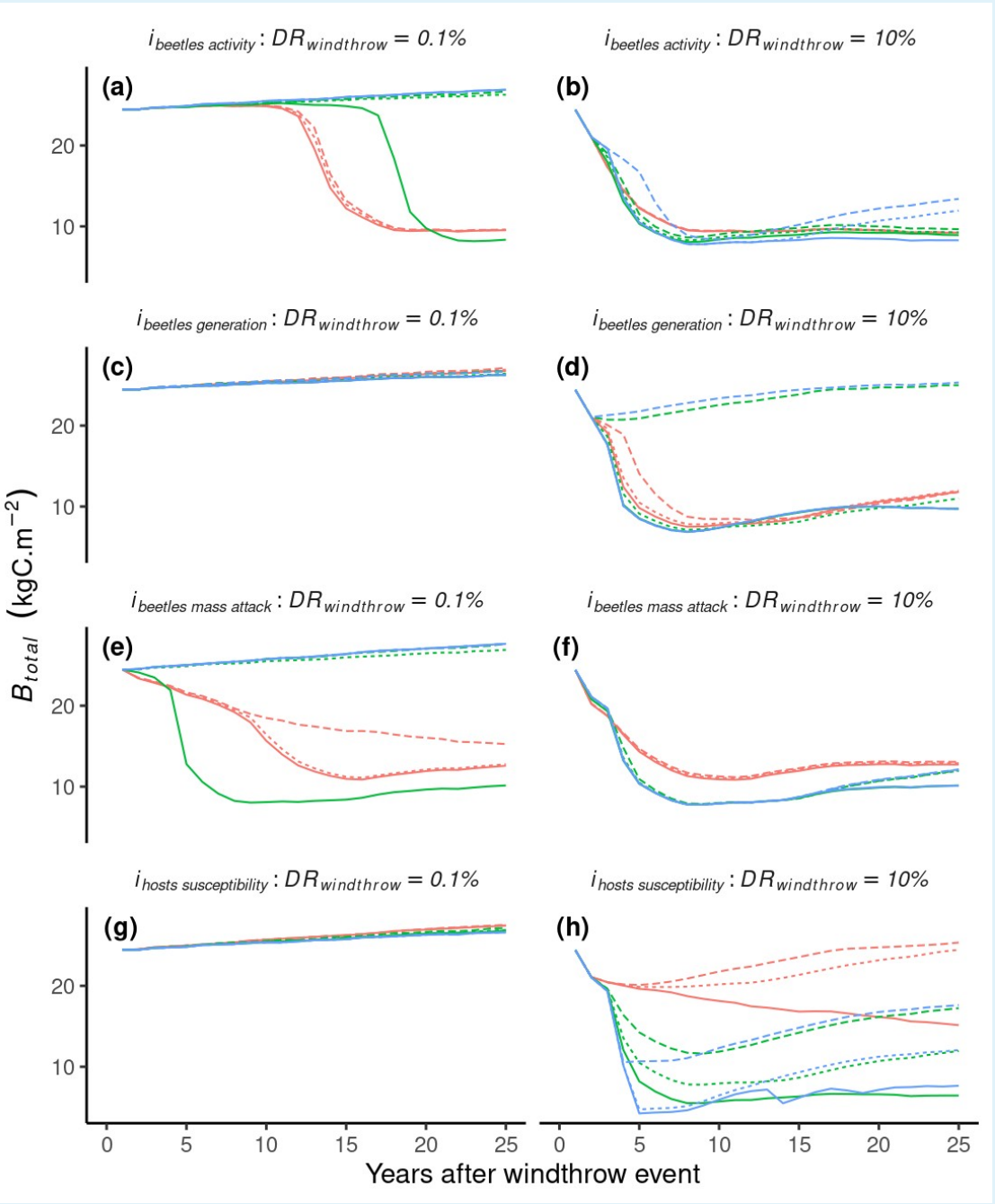

Figure s4: Simulation results from the sensitivity experiment at the THA site. Eight parameters from four equations were evaluated. Each equation represents an index from the bark beetle outbreak model ($i_{hosts\ susceptibility}$, $i_{hosts\ mass\ attack}$, $i_{beetles\ activity}$, $i_{beetles\ generation}$). Each index is represented by a logistic function defined by a shape parameter (*Shape*) and a limit parameter (*Limit*). Three values were chosen for each parameter resulting in 9 pairs of parameters for each index. Colored lines represent the shape parameter varying from linear : *Shape* = -1.0 (red), logistic -5.0 < *Shape* < -30.0 (green), to step function where *Shape* = -500.0 (blue). Line type represents three different values for *Limit* parameters where references (dashed line) are values of $i_{rd\ susceptibility}$, BP_{limit}, act_{limit} and G_{limit} (given in table 4), whereas permissive (full line) and restrictive (dashed dotted) represent a 50% decrease or increase respectively.